



The Nimbus Passenger Capsule

January 20th, 2016

SpaceX Hyperloop – Final Design Competition Package



**McMaster University Hyperloop
Design Team**

Executive Summary

The McMaster University Hyperloop Design Team is strong group of practising engineering students representing all streams of engineering at McMaster University. Together, our team has worked hard to compile our best ideas for Elon Musk's Hyperloop concept in to one efficient design, "The Nimbus".

The Nimbus is a new design that embodies the Hyperloop concept while introducing crucial elements that make this mode of transportation an experience on its own. Our team wants North America to feel safe, as our vision is to turn this mode of transport into a destination. The Nimbus is a unique design that optimizes the performance of the fragile vacuum environment by featuring a vacuum seal pressure lock system that isolates the low pressure environment in the tube. The Nimbus takes advantage of a built-in Photodetector and Diode dual system that can monitor the trajectory of the capsule throughout its flight without the use of a GPS communication device. To extrapolate, the design consists of a rotary gate system which allows for several secure passageways for the capsule. Our passenger capsule for the Nimbus not only communicates constantly with the station, the tube, and with satellites, but our internal safety mechanism as well. It communicates via sensors embedded in the seating system to ensure overall passenger safety, reliability, and product popularity to a larger group of passengers from across the world. Our team hopes to build and launch our design in to the near future.

Thank you to our Sponsors!



Bachelor of Technology
McMaster-Mohawk Partnership



Table of Contents

1 Introduction

 1.1 Final Design Package Purpose

 1.2 Our Vision

 1.3 Our Team

2 Nimbus

 2.1 Vehicle Overview

 2.1.0 Dimensions

 2.1.1 Mass by Sub-System

 2.1.2 Materials

 2.1.3 Structural Analysis of Materials

 2.1.3 Aerodynamic Coefficients

 2.1.4 Power Source & Consumptions

 2.1.5 Thermal Profile

 2.2 Sub-System Breakdown

 2.2.0 Propulsion

 2.2.1 Braking

 2.2.2 Levitation

 2.2.3 Navigation

 2.2.5 Sensor List & Location Map



3 Performance

3.0 System Trajectory

3.1 Predictive Velocity Profile

3.2 Predictive Acceleration Profile

3.3 Predictive Power Distribution Schematic

3.4 Predictive Power Profile

3.5 Predictive Energy Schematic

3.6 Payload Capability

1 Introduction

1.1 Final Design Package Purpose

The Final Design Package of McMaster Hyperloop is a further proposal document of the original Hyperloop Alpha published by Elon Musk outlining the primary visions for the concept of the Hyperloop.

This Design Package is intended for Judges and Sponsors alike in order to obtain a full understanding of McMaster Hyperloop's vision for the continuation of Elon's original proposal of the Hyperloop. Full details of McMaster Hyperloop's proposal are outlined in the sections to follow.

This Final Design Package is intended for submission for the Design Weekend on January 29th-30th of 2016. At Texas A&M University. McMaster Hyperloop has full intentions to update this document with further improvements and advancements to its Hyperloop design.

1.2 Our Vision

Our vision for Hyperloop is one where travel is made into an experience. The members of the McMaster Hyperloop Team (MHT) have a clear view in our minds of a fast and efficient transport technology establishing itself as a mainstream form of transport in North America in the upcoming decade.



For us all, it is the first time we are able to observe the birth of a new mode of transport. Many great individuals were a part of the revolution that brought cars, trains, planes and boats to the world, however by the time our generation came along, the foundations for these revolutionary ideas were already laid down and it was up to our generation to make those modes better and more efficient.

The introduction of this proposed form of transport sparked every member on this team's innovative drive to see this grow from concept to a fully functioning operating system. Fueled by the culture surrounding this idea, we are excited to be developing a design for a new mode of transport that will be faster, safer and cleaner than all other conventional modes of transport. It has become an innovative need for all of us here at McMaster Hyperloop to be a part of the developmental process of this "fifth mode of transport."

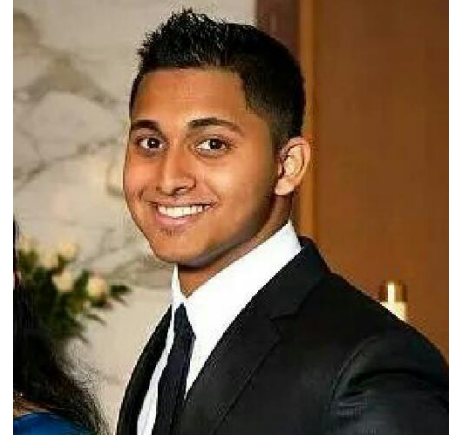
MHT hopes that through entering this competition, we are taking the first of many steps forward in order to see our vision come to life!

1.3 Our Team



Sree Sushmita

President



Vishal Kharker

Design Optimization
&
Finances

Prakhar Garg

Mechanical Design
Specialist

Ajith Josephs

Safety & UXD Engineering



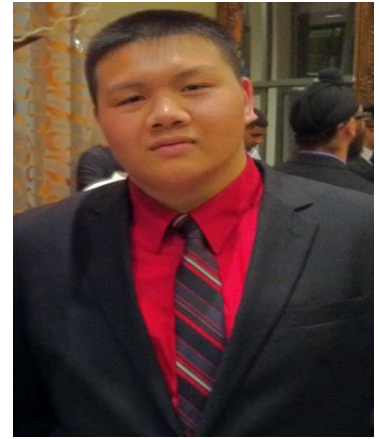
Jathuson Jeyakumar

Materials Engineering



Andy Chu

Mechanical Engineering



Peter Do

Power Systems Engineering



Abhijit Roy

Aerodynamics
&
External Design



Hossein Rejali

Electrical Engineering



Yash Gopal

Web/Graphic Design



David Finlay
Project Supervisor



Mayusanth Jeyakumar
Project Supervisor



2 Nimbus

2.1 Vehicle Overview

The Nimbus (Figure 2.0) is a capsule [Pod] that is intended to carry passengers and light cargo at near supersonic speeds inside a low pressure environment [Tube]. These high speeds are attained using a Linear Synchronous Motor for drive motion and a powerful Air Turbine compressor for levitation. The combination creates a movement unique enough to itself and the movement of the Pod in the Tube is referred to the Hyperloop.

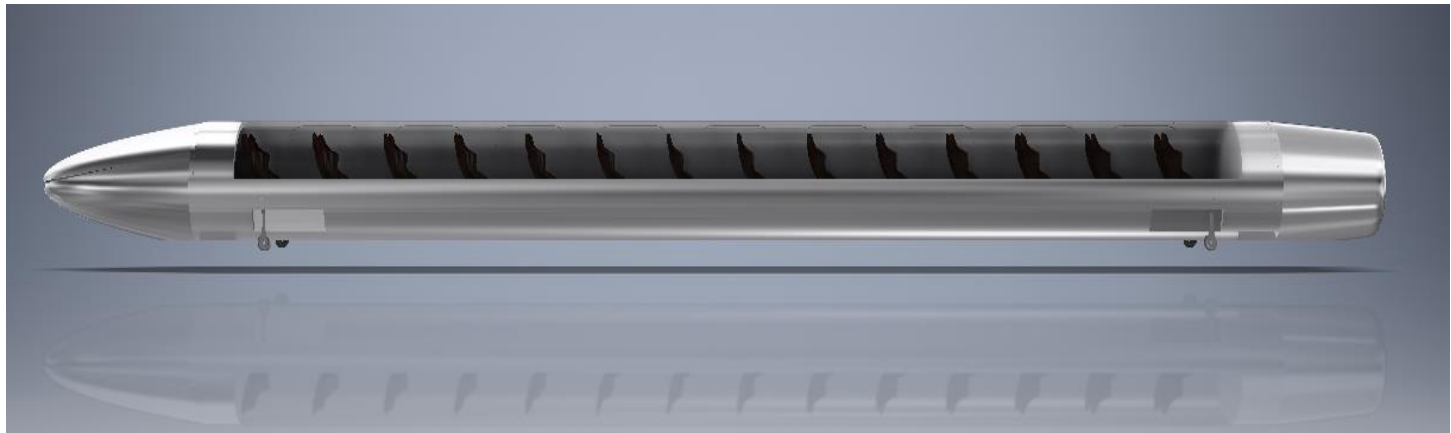
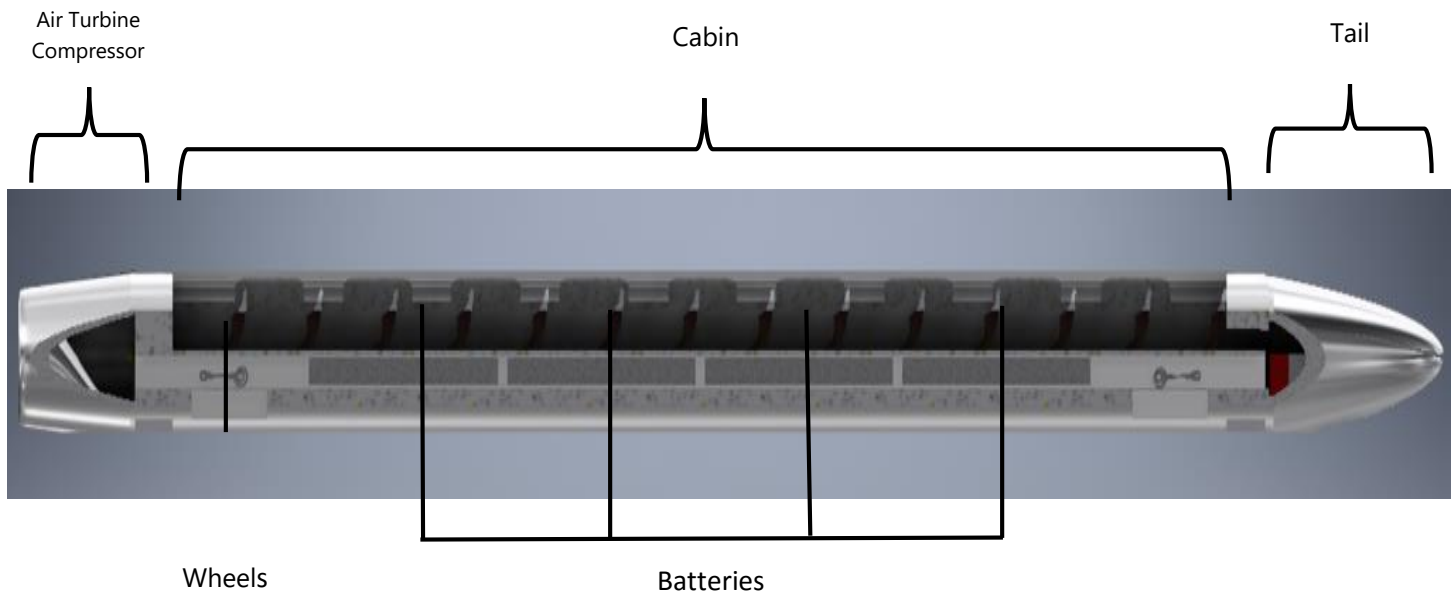


Figure 2.01 Shows an RHS view of the Nimbus with basic labelling of reference parts



With high speed being the primary focus of Nimbus, it was designed with heavy emphasis on the optimization of shape and mass to result in higher speed at a lower energy cost. Increased aerodynamic capability of the Pod is a direct result of the carefully chosen structural shape of the vehicle to minimize the effects of drag force on the exterior surface of the capsule. Inspiration for its design was drawn from power series nose cones which result in the least amount of relative drag force. In order to ensure stability, the Nimbus features a parabolic tail cone modelled for symmetry, stability, and speed all with the aid of multiple sensors including a gyroscope assist in assessing the condition of the Pod during flight.

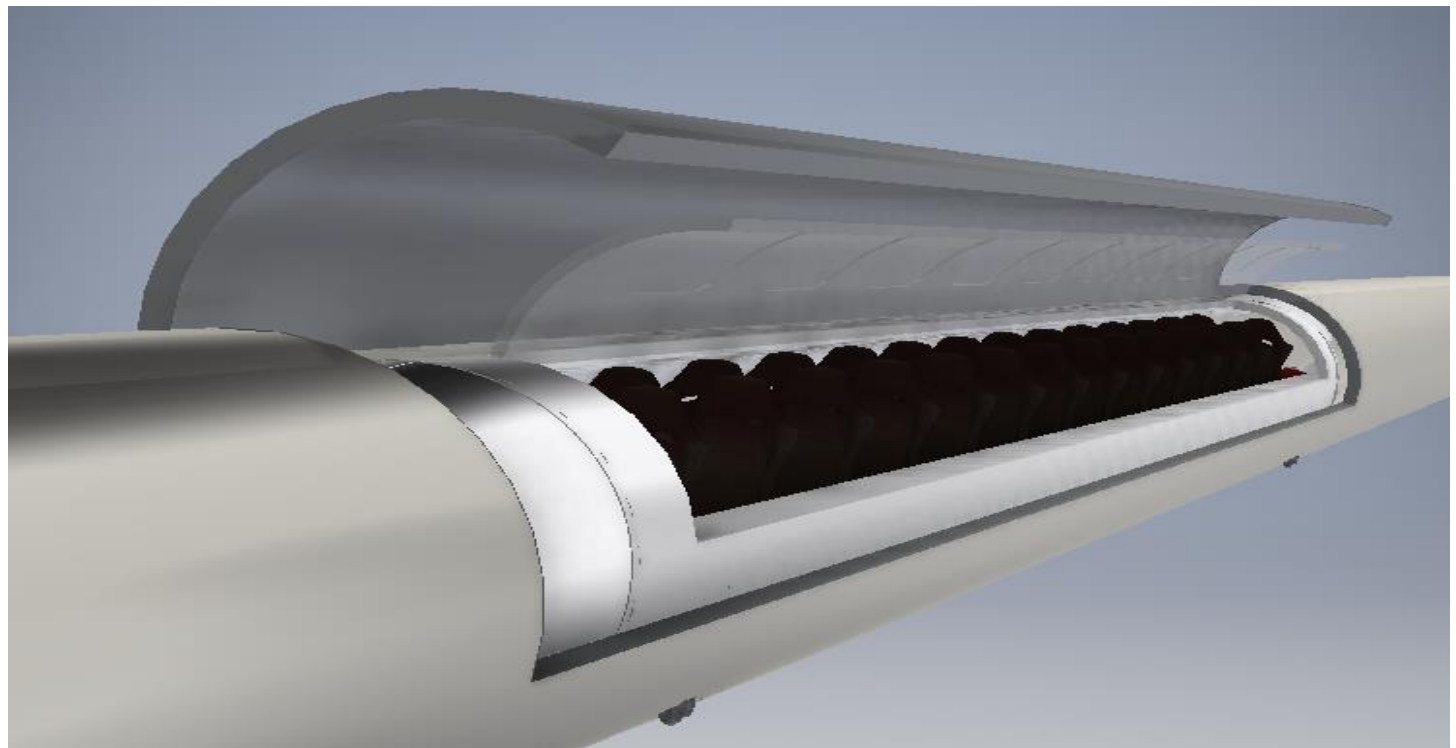


Figure 2.02 Shows a Cross sectional Isometric View along with The Hyperloop opening

As mentioned prior, the ability to move at high speeds at lower energy consumption was given equal importance when designing the Nimbus. Systems which increase power efficiency can be seen primarily through the regenerative braking mechanism. This type of braking allows for the system to re-absorb a portion of the energy back into the battery storage, therefore minimizing the loss of power during the deceleration phase. This energy may also be redirected for immediate use by the capsule.



Figure 2.03 Shows an Isometric and Top Cross Sectional View of Nimbus



Figure 2.04 Shows a Front View with the Turbine Air Compressor

2.1.0 Dimensions

Characteristic	Acceleration	Flight	Deceleration
Structure			
Length		757"	
Diameter		60"	
Shell Material		Aluminum	
Frame Material		Steel	
Average Velocity			
Propulsion			
Type	Linear Induction Motor	Linear Induction Motor	Eddy's Current
Manufacturer	N/A	N/A	N/A
Propellant	Electricity	Electricity	Electricity Regeneration
Max Acceleration	16.1 ft/s^2	0ft/s^2	-16.1m/s^2
Restart Capability	No	No	No
Levitation			
Type	Air Bearings Linear Induction Motor	Air Bearings	Air Bearings Linear Induction Motor
Power source	Electricity Compressed air	Electricity	Electricity Compressed Air
Manufacturer	N/A	N/A	N/A
Force			
Control	Solenoids	Solenoids	Solenoids
Landing Gear			
Type	Rubber wheel	Rubber wheel	Rubber wheel
Tire Specification	Diameter 6" Thickness 2"	Diameter 6" Thickness 2"	Diameter 6" Thickness 2"
Tire Material	rubber	rubber	rubber
Frame Material	steel	steel	steel
Position	Extended	Retracted	Extended
Door			
Material	Aluminum 6061-T6	Aluminum 6061-T6	Aluminum 6061-T6
Actuator	Hydraulic	Hydraulic	Hydraulic
Emergency	Emergency windows Rear gate	Rear gate	Emergency windows Rear gate
Staging			
Initiated By	Release from station	Threshold velocity	Location Faults
Acceleration Time	55.35 s	N/A	55.35 s
Gear Position Change Time			



*All units expressed in Inches

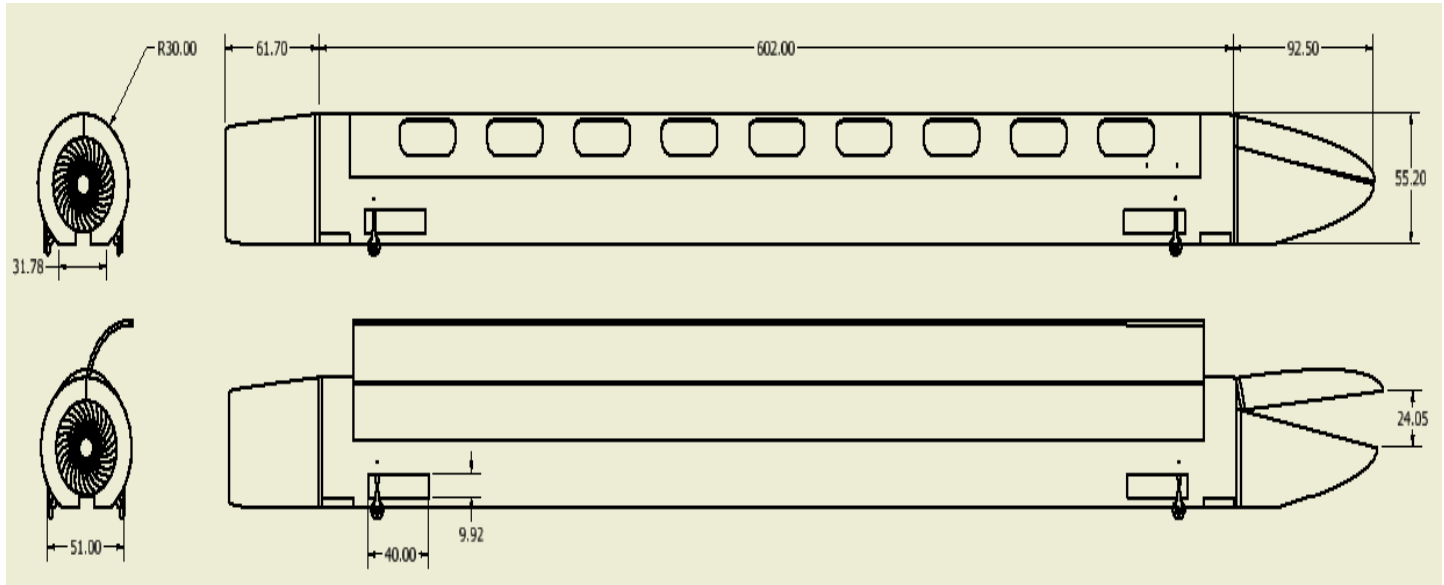


Figure 2.05 Show multiple views in a 2-D form with Dimension

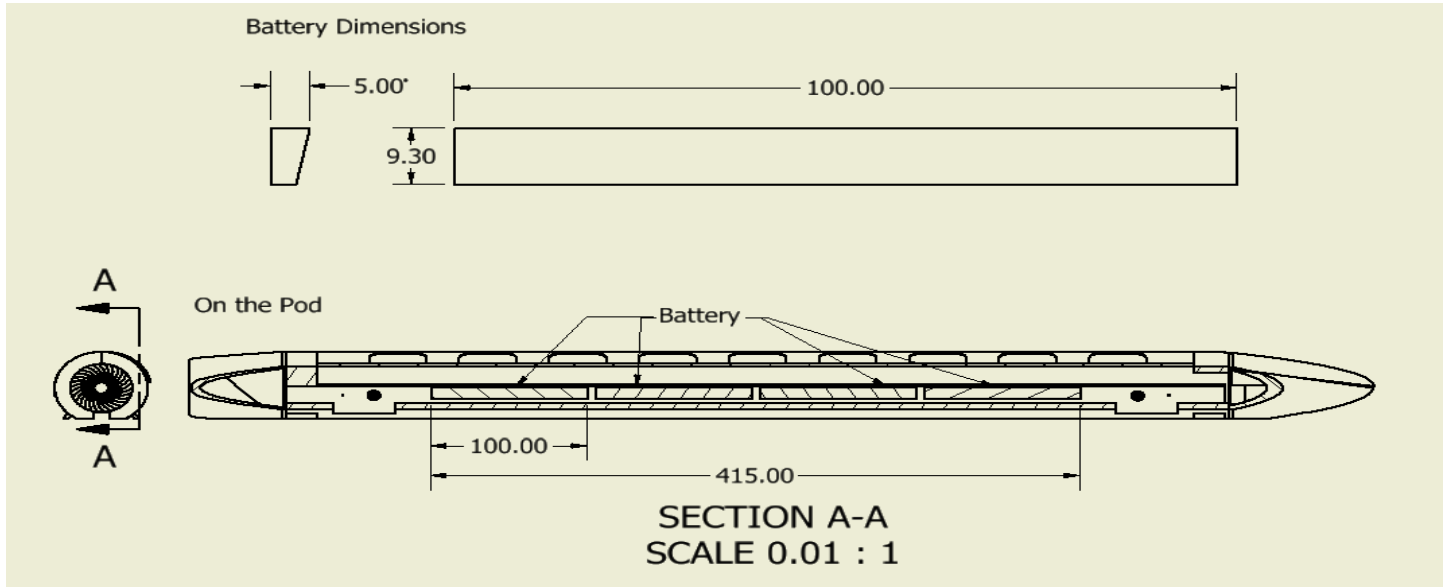


Figure 2.06 Show multiple views in a 2-D form with Dimension with Batteries included

2.1.1 Mass by Sub-System

Sub-System	Mass [kg]
Propulsion	
Levitation	
Braking	
Power	
Avionics	
Pod Structure	
Tube Structure	
Communications	

Mass of Pod Systems

Mass of Pod Systems + Passengers [Full]

Mass of Tube Systems

Mass of Hyperloop

[Pod + Passengers+Tube]

2.1.2 Materials

The selection of materials is determined by evaluating the environment that is created by the Tube and also by testing what conditions are experienced on the exterior of the capsule when the Pod moving through the environment. The areas of the capsule subject to relatively high amounts of pressure and heat, such as the nose and tail cone, must be built using a material with a relatively greater heat capacity. [1]

When selecting the materials that make up the exteriors of the Hyperloop capsule, the various states of the environment surrounding the capsule must be considered. Since the capsule is subjected to near vacuum conditions, it is important to not use materials in the construction of the Tube or Pod having high vapor pressures as it would result in vaporization of the material and increase the gas load in the Tube. [2] [3]

Research in the automotive industry suggests that carbon fibre would be the better choice compared to steel for exterior of the Pod. This is because there is a downward trend in the cost of producing fibre-reinforced polymers. Although steel is cheaper to make, carbon fibre-reinforced polymers offer greater mechanical properties along with lighter weight, but it may shatter when it reaches its yield strength. [4] [5]

Another choice for the body would be an aluminum alloy, which is cheaper and bends when it reaches its yield strength, but is heavier than carbon fibre reinforced polycarbonate.

Material	Density (kg/m ³)	Yield Strength (MPa)	Thermal Conductivity (W/(m°C))
Carbon Fibre Reinforced Polycarbonate	1750	2.5E02	60.5
Aluminum Alloy 6061 T6	2770	2.8E02	Varies from 150-155

Table 2.0 shows comparative properties of each material

*All values obtained from ANSYS

The nose cone and tail portion of the Pod require a material that would have higher resistance to the thermal and mechanical stresses of travel. The solution to this would be to use a ceramic material for the frontal compressor of the Pod or simply using a ceramic coating. The ceramic coating would be cheaper to use since it would be a thin layer. An alternative to the ceramic coating would be to use a ceramic or polyimide resin, which is used in the nacelles of commercial aircrafts. [6]

The walls of the Pod would be lined with R11 insulation and would be around 3.5" thick. The insulation is necessary to maintain constant temperature within the Pod, so that no heat enters or escapes. The values for the R11 insulation can be found at:

[Appendix] [7] <http://www.certainteed.com/resources/30-29-120.pdf>

The remaining unspecified material of the Pod would be in regards to windows. Windows of the Pod are suggested to be made of polycarbonate [Lexan] due to its light weight and durable properties. [8]

2.1.3 Structural Analysis of Materials

Stress analysis was conducted to determine the validity of the materials considered. Analysis was done independently for the nose cone, body, and the tail of the pod based on the difference in stresses and forces applicable to the component. The material most suitable for the stress experienced at the specific section was chosen, eliminating the need to consider stresses experienced at the other components.

Nose Cone

The nose cone is located at the front of the pod, experiencing the most aerodynamic stress. The nose cone also contains the axial air compressor, which creates higher pressure inside the compressor ducts. The air pressure inside the nose cone is the same as that of the tube at 100 Pa.

Assumptions:

- Axial compressor compression ratio is 30:1
- The area in contact with the rail as well as the nose cone's connection to the body are fixed structures
- Pressure from the compressor to the air bearing ducts is constant, at 94 times the inlet pressure
- Stress on the outer surfaces are based on pressures at the surface from computational fluid dynamics and isentropic flow assumptions [Refer to Figure 2. "Pressure Contour of Nose Cone" below]
- Acceleration due to gravity is considered
- Pod acceleration is at 0.5g, the maximum acceleration the pod is expecting to experience
- Stresses induced by vibrations are not considered and are assumed to fall within the assigned factor of safety

Pressure Contour of Nose Cone

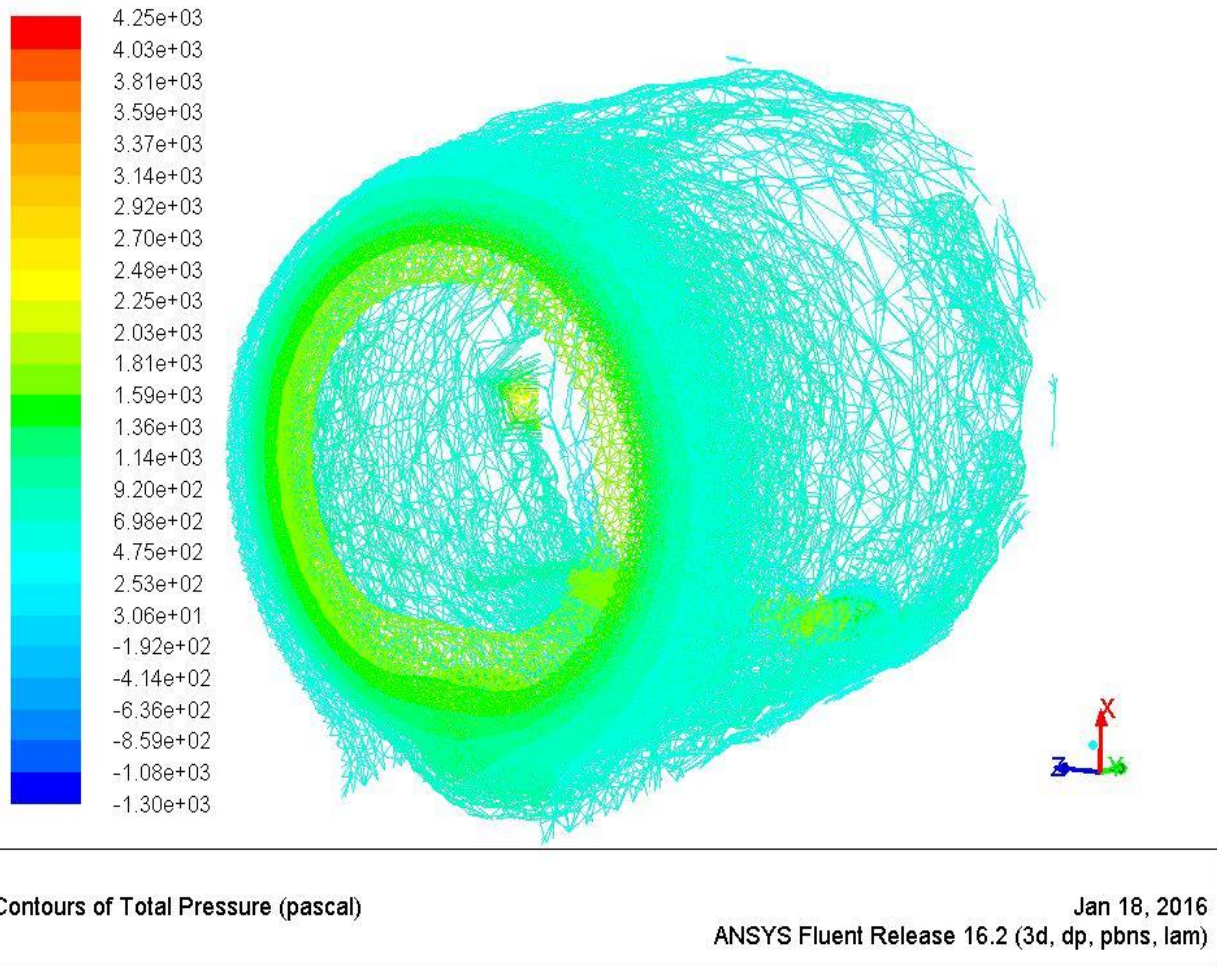
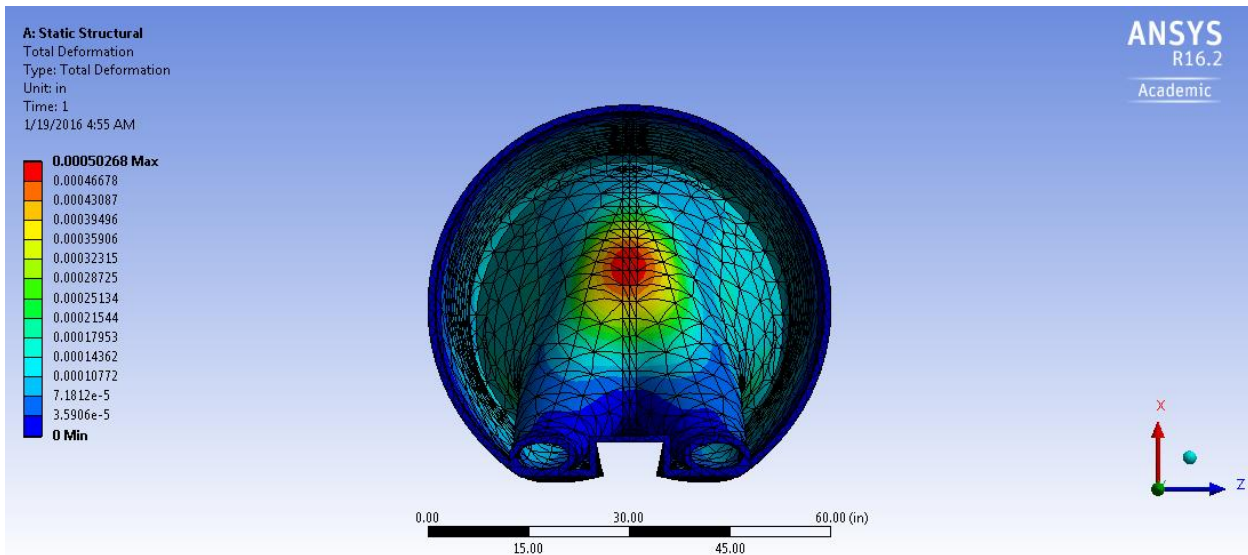
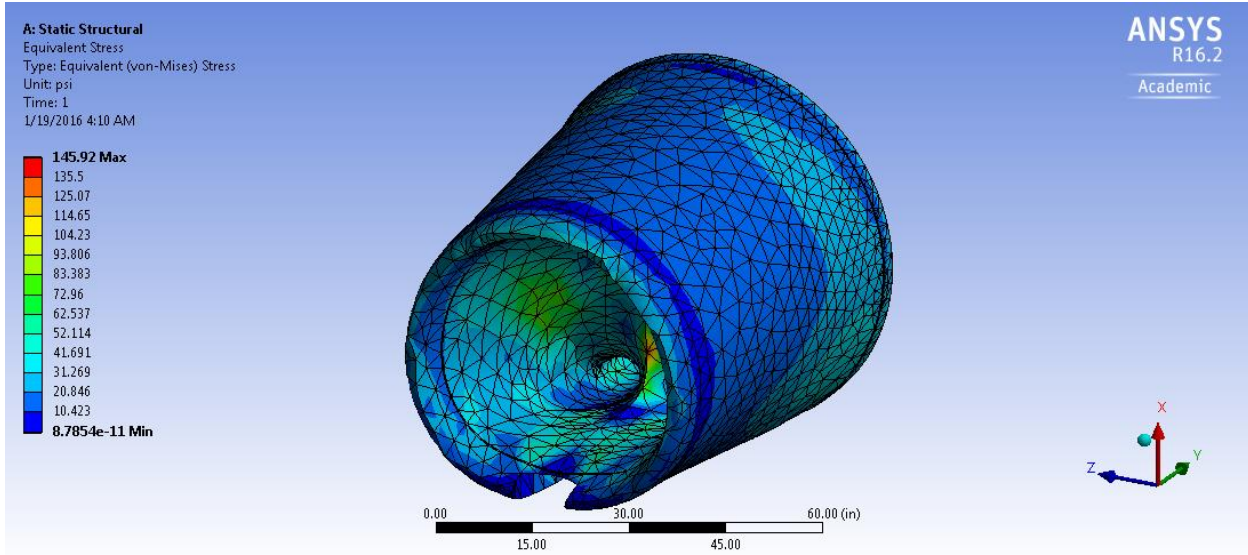


Figure 2.07 Shows the Pressure Contour of the Nose Cone Design

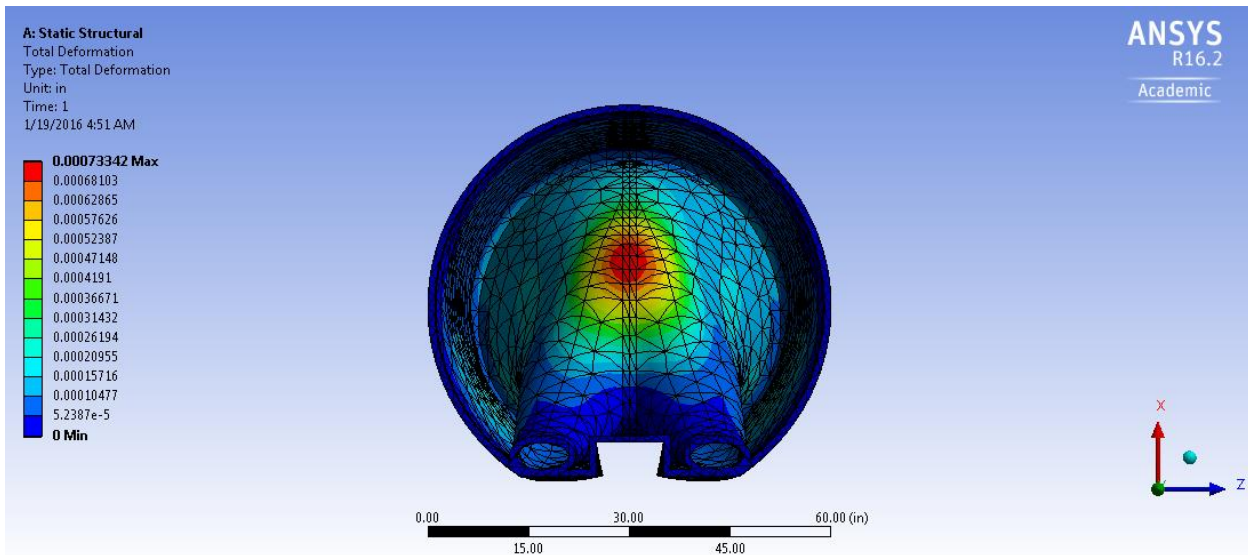
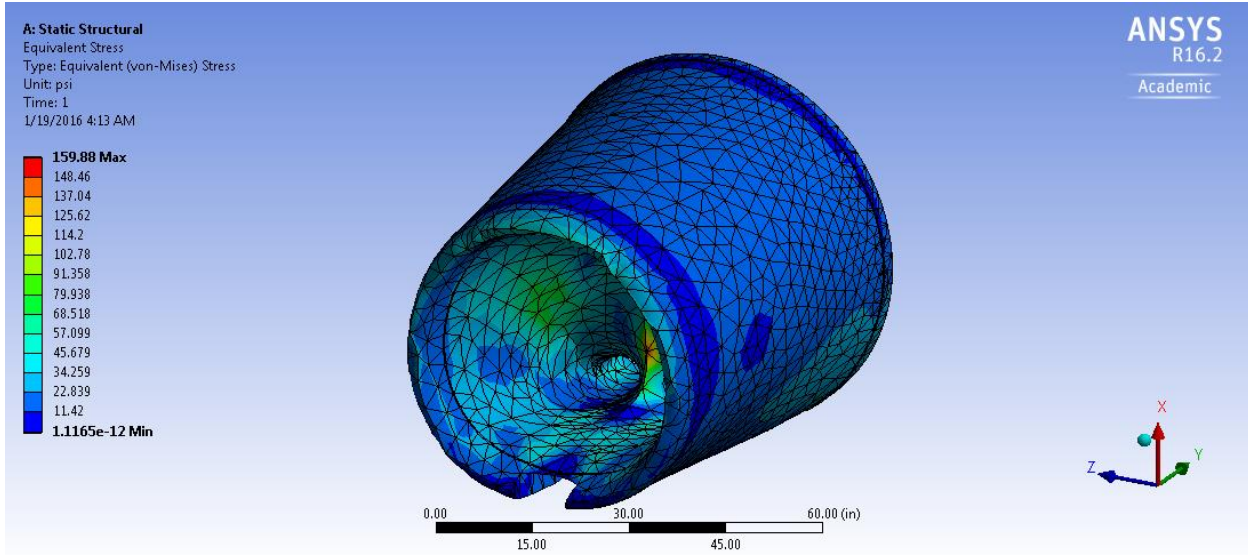
Material: Titanium Alloy



Maximum Equivalent Stress: 145.92 psi
Maximum Deformation: 0.00050268 in

Figure 2.08 Shows the Stress Analysis of a Nose Cone made of Titanium Alloy

Material: Aluminum 6061-T6

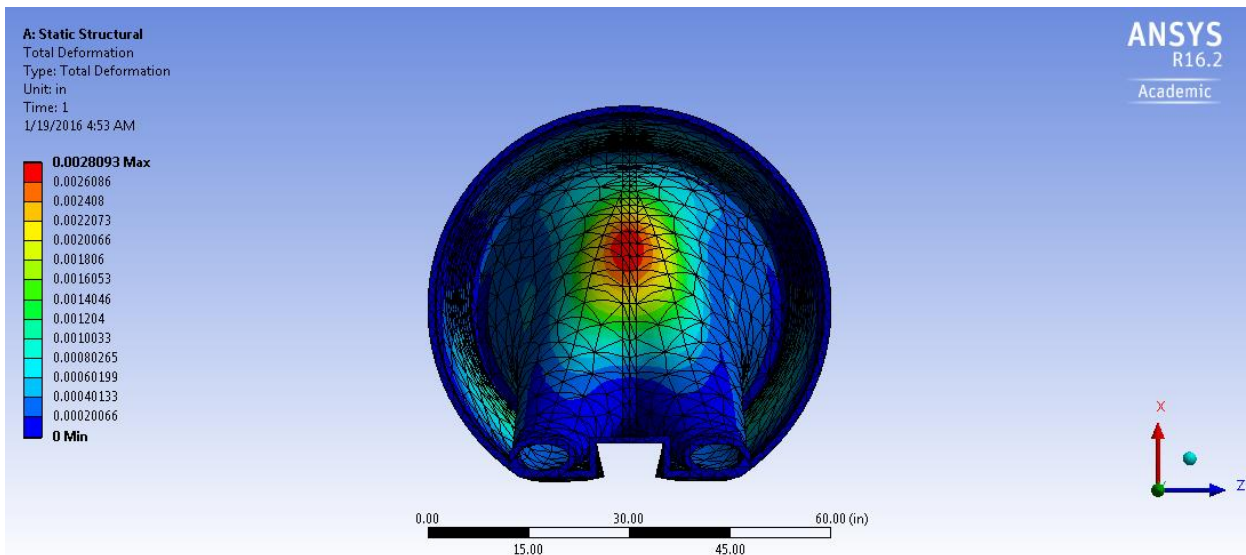
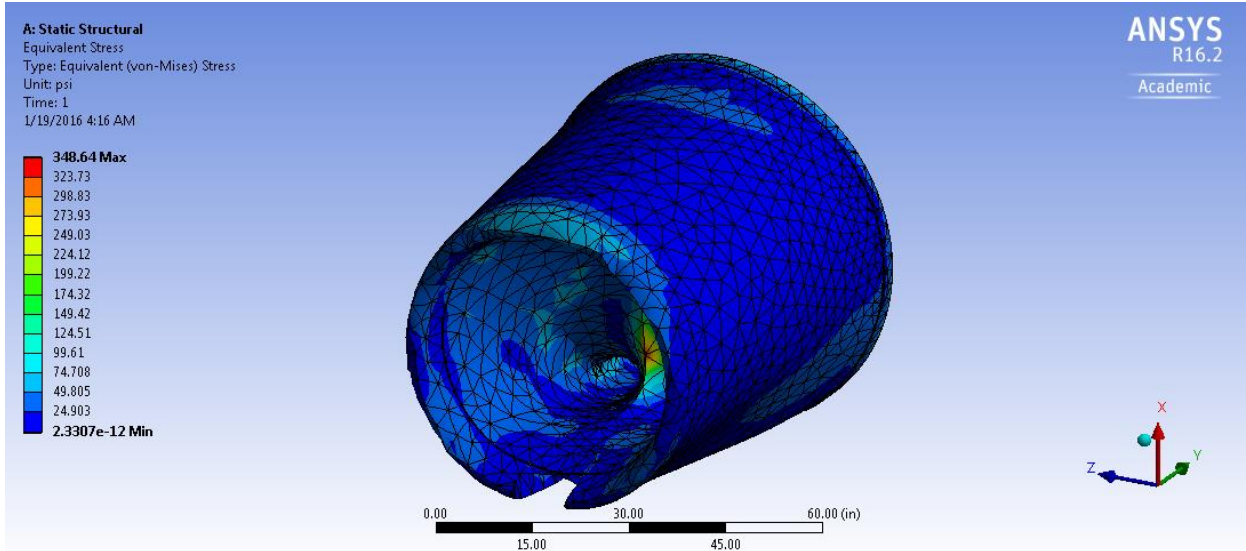


Maximum Equivalent Stress: 159.88 psi

Maximum Deformation: 0.00073342 in

Figure 2.09 Shows the Stress Analysis of a Nose Cone made of Aluminum 6061-T6

Material: Epoxy Carbon Woven (230 GPa)



Maximum Equivalent Stress: 159.88 psi

Maximum Deformation: 0.0028093 in

Figure 2.10 Shows the Stress Analysis of a Nose Cone made of Epoxy Carbon Woven (230 GPa)

Conclusion: Out of Aluminum, Epoxy Carbon, and Titanium alloy, **Titanium** alloy observed the lowest stress with the lowest deformation. However, all the materials analysed are capable of withstanding the stresses observed.

Passenger Cabin

The passenger cabin is pressurized and maintained at 101325 Pa which causes a pressure differential from the tube that is pressurized at 100 Pa. The primary source of stress. The stresses induced by the pressure difference are a result of hoop stress and axial stress, which are used to justify and validate the model. The analysis of the passenger cabin was sectioned into two parts due to software model size restraints.

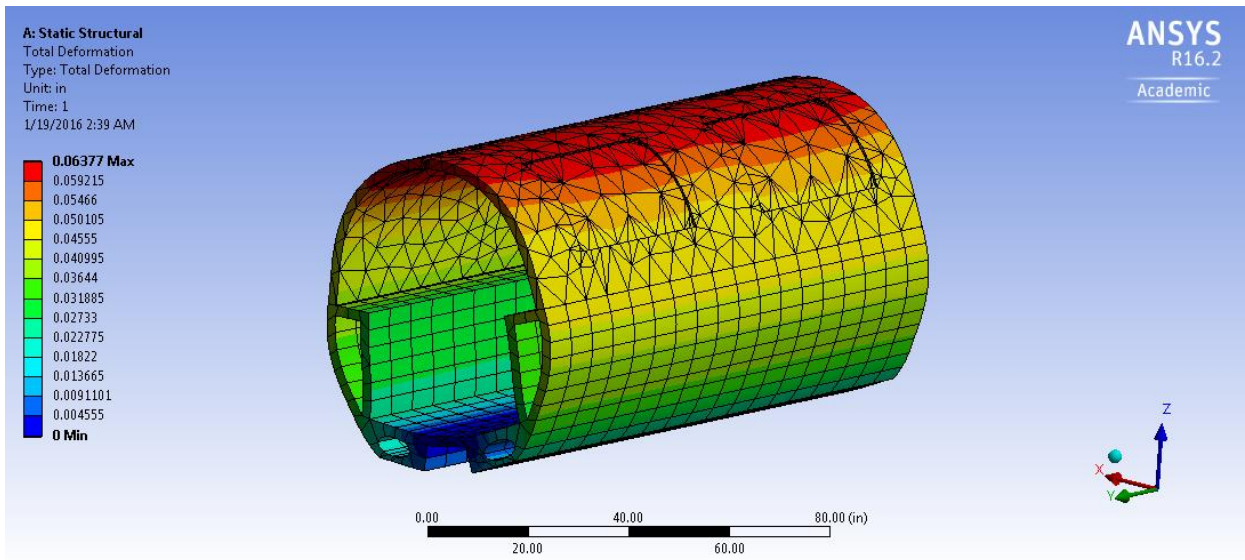
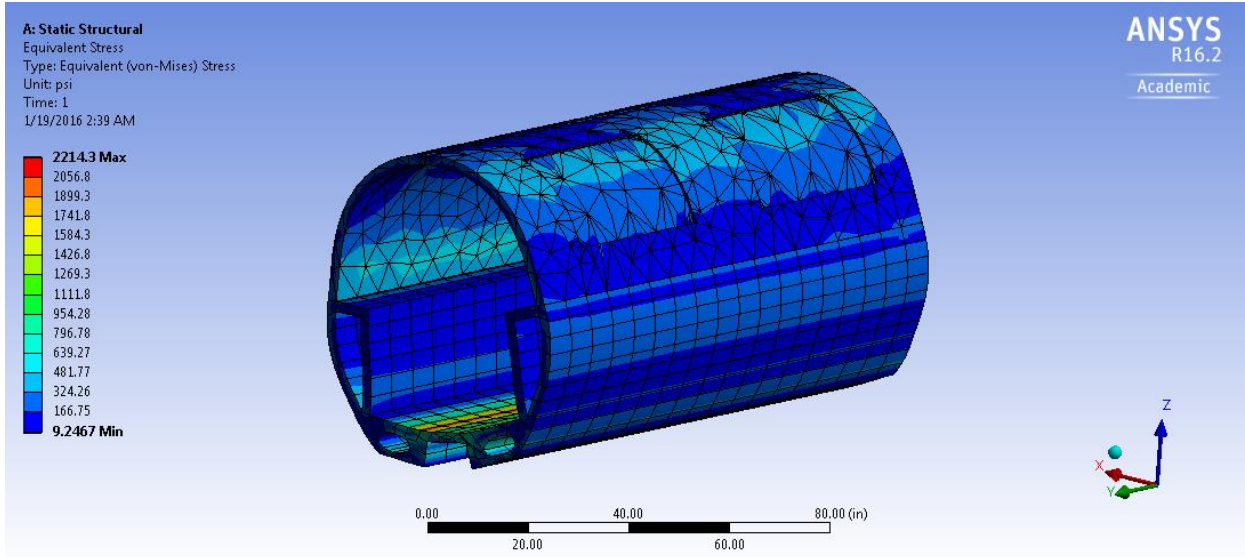
Center of Cabin

The main sources of stress considered for this component are from the pressure differential and the aerodynamic stress.

Assumptions:

- The section analysed is representative of the entire centre of the passenger cabin
- The windows are analysed as the same material as the body structure due to CAD limitations
- The aerodynamic stress is the same as that at the top of the nose cone, based on pressures at the surface from computational fluid dynamics and isentropic flow assumptions *Refer to Figure 2.13
- The rail is a fixed structure
- Acceleration due to gravity is considered
- Pod acceleration is at 0.5g, the maximum acceleration the pod is expecting to experience
- Stresses induced by vibrations are not considered and are assumed to fall within the assigned factor of safety
- Pressure in the air bearing duct is 11000 Pa

Material: Epoxy Carbon Woven (230 GPa)

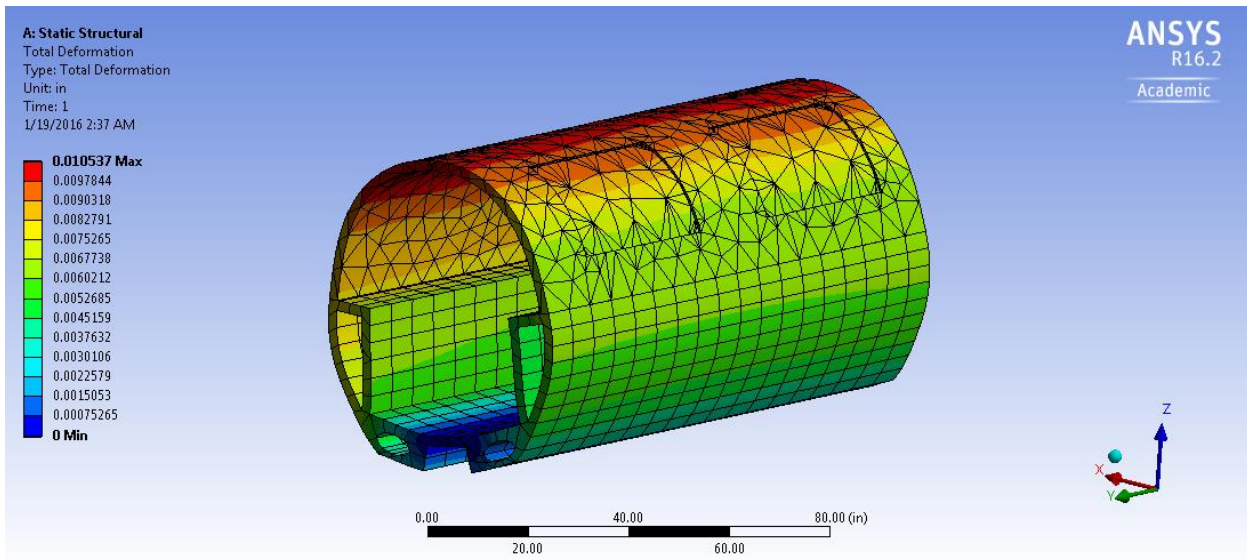
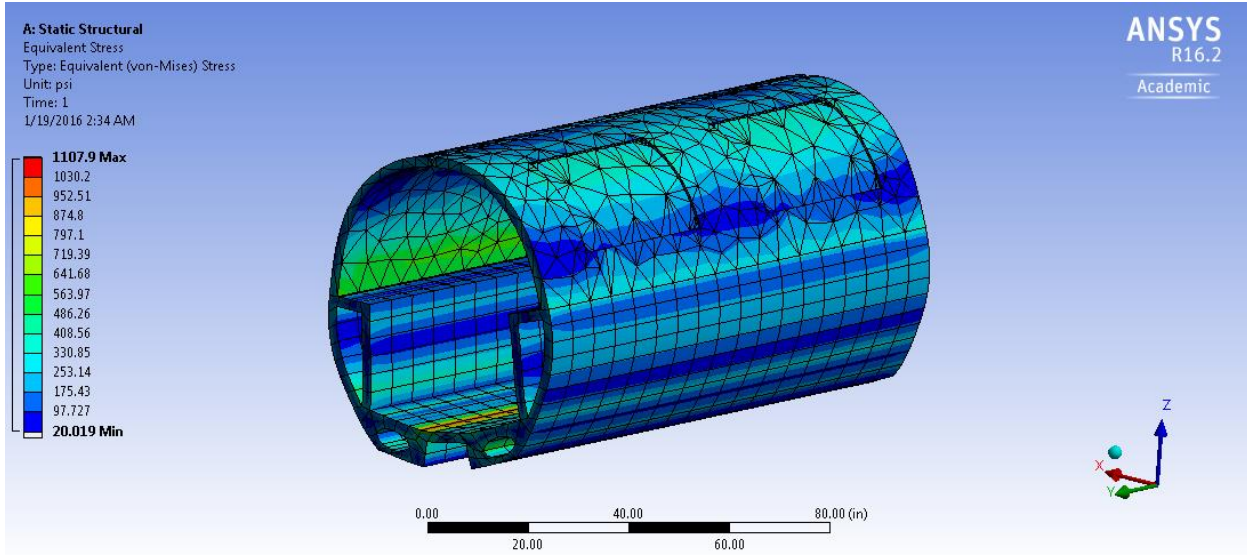


Maximum Equivalent Stress: 2214.3 psi

Maximum Deformation: 0.06377 in

Figure 2.11 Shows the Stress Analysis of a Cabin made of Epoxy Carbon Woven (230 GPa)

Material: Aluminum 6061-T6



Maximum Equivalent Stress: 1107.9 psi

Maximum Deformation: 0.010537 in

Figure 2.12 Shows the Stress Analysis of a Cabin made of Aluminum 6061-T6

Front and Rear of Cabin

This analysis applies to the front and rear ends, which are assumed to be identical in geometry. The walls are much thicker than the centre of the passenger cabin, however the stresses experienced are relatively the same. Based on the equations for hoop stress and axial stress, the overall stress on the component is less than that due to the inverse relation between thickness and stress. Thus, the stress is assumed to be lower than the centre and since the material is the same, it can be assumed that if the material is valid for the centre, it is also sufficient for the tail.

Assumptions:

- The pressure differential is relevant as the nose cone and the tail are assumed to be pressurized at 100 Pa
- The rail is a fixed structure
- Acceleration due to gravity is considered
- Pod acceleration is at 0.5g, the maximum acceleration the pod is expecting to experience
- Stresses induced by vibrations are not considered and are assumed to fall within the assigned factor of safety
- Pressure in the air bearing duct is 11000 Pa

Out of the Epoxy Carbon and Aluminum analysed, Aluminum 6061-T6 observed lower stresses and lower deformation. However, both materials are capable of withstanding the observed stresses.

Tail

Stress from form drag at the tail is relatively low since the tail has a decreasing cross sectional area, allowing for airflow to be redirected over from the larger cross sectional area of the passenger cabin. The main source of stress is from the pressure difference, which is relatively low compared to the cabin since the rounder geometry of the tail allows for greater stress distribution. [1]

Assumptions:

- The pressure differential between the tube is relevant as the tail is pressurized at 101325 Pa, the same as that of the passenger cabin
- The aerodynamic stress is based on pressures at the surface from computational fluid dynamics and isentropic flow assumptions *Refer to Figure 2.13
- The tail is fixed at the connection to the passenger cabin, as well as on the rail
- Acceleration due to gravity is considered
- Pod acceleration is at 0.5g, the maximum acceleration the pod is expecting to experience

Contour of Body and Tail

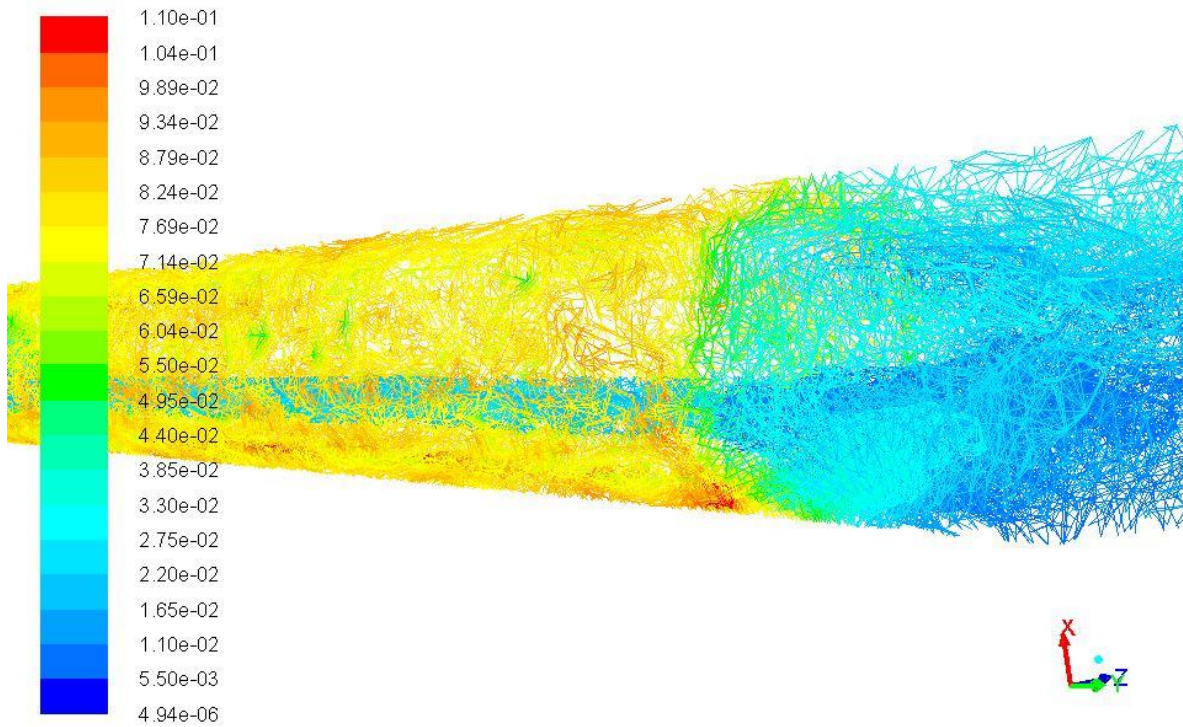
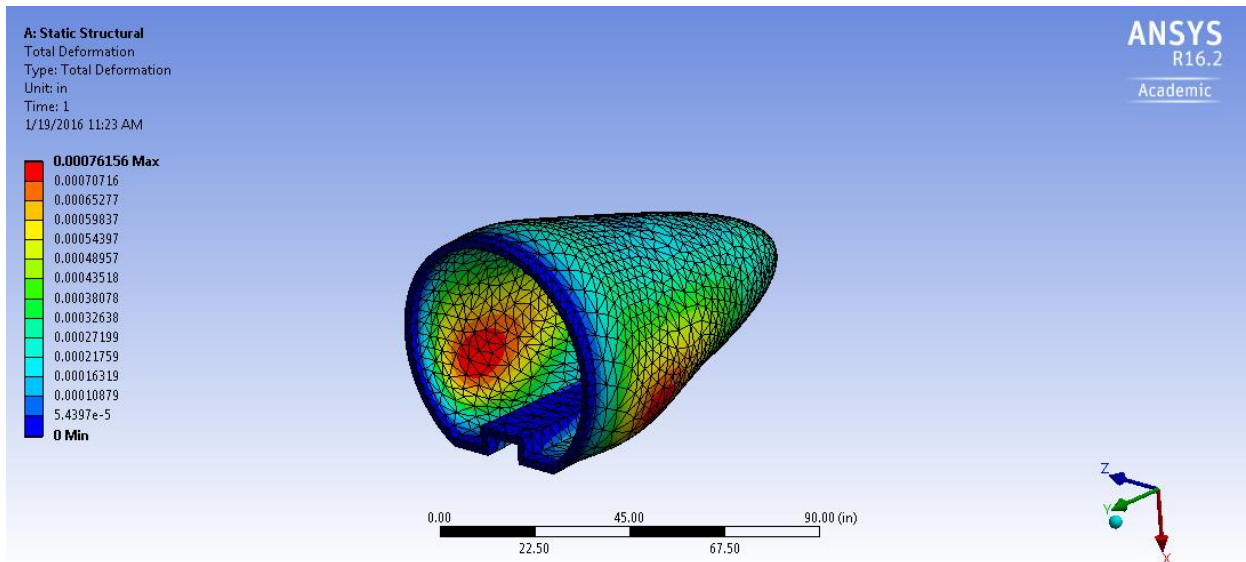
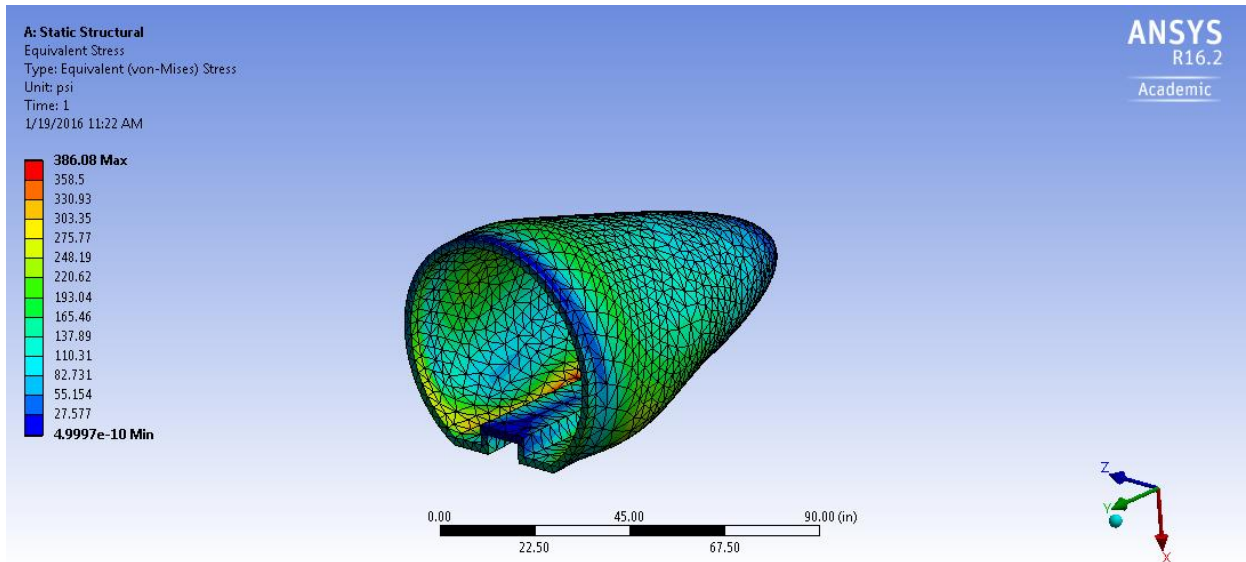


Figure 2.13 Shows the Contour of Body and Tail

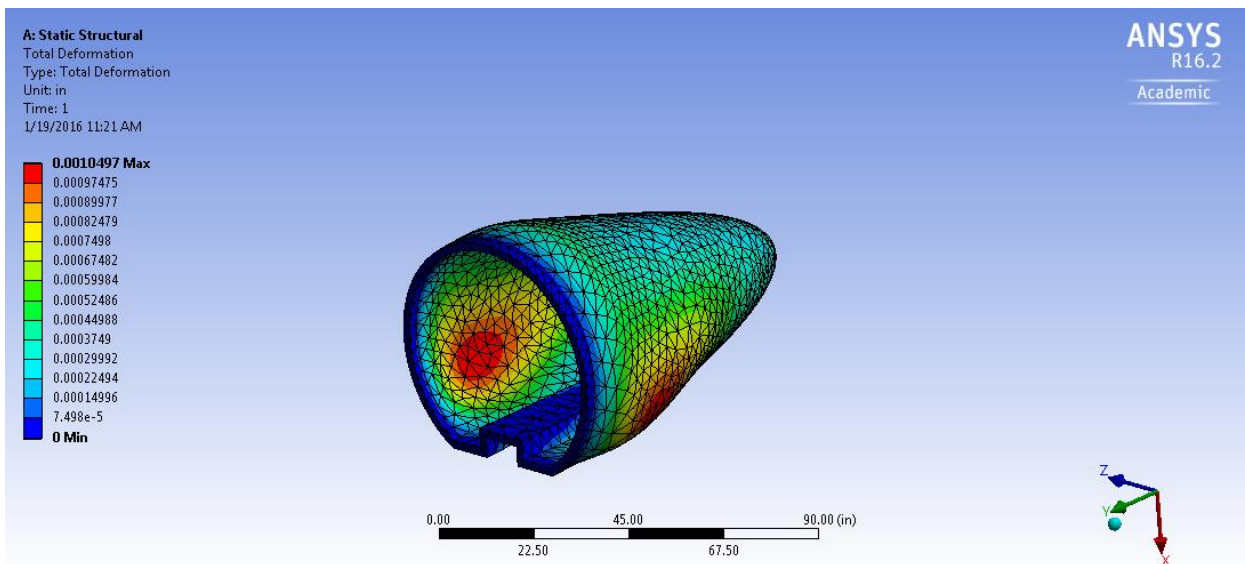
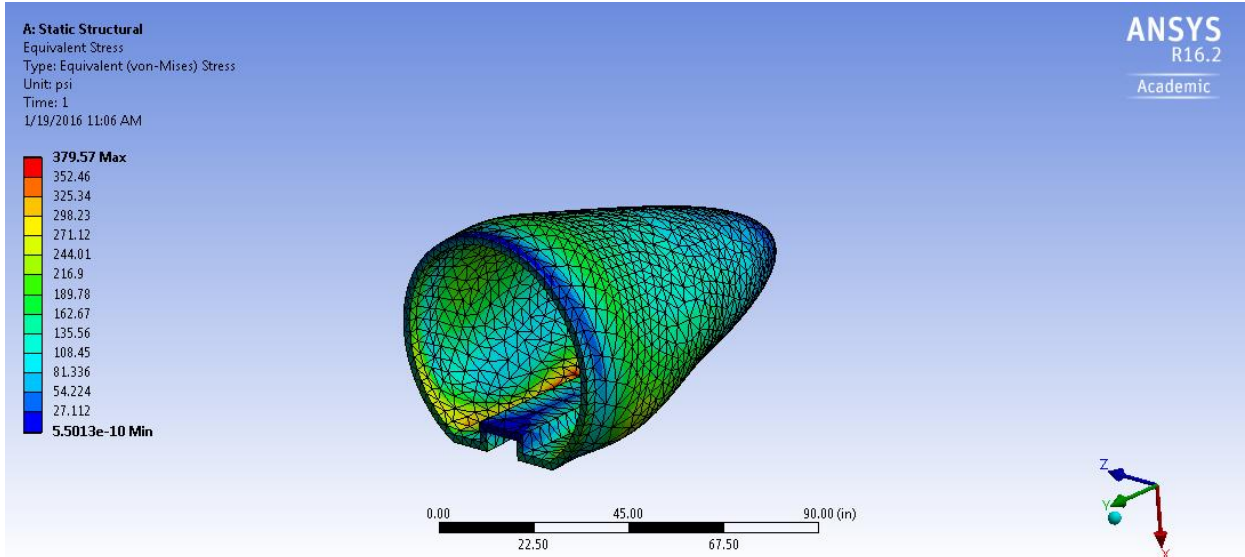
Material: Titanium Alloy



Maximum Equivalent Stress: 386.08 psi
Maximum Deformation: 0.00076157 in

Figure 2.14 Shows the Stress Analysis of a Tail made of Titanium Alloy

Material: Aluminum 6061-T6

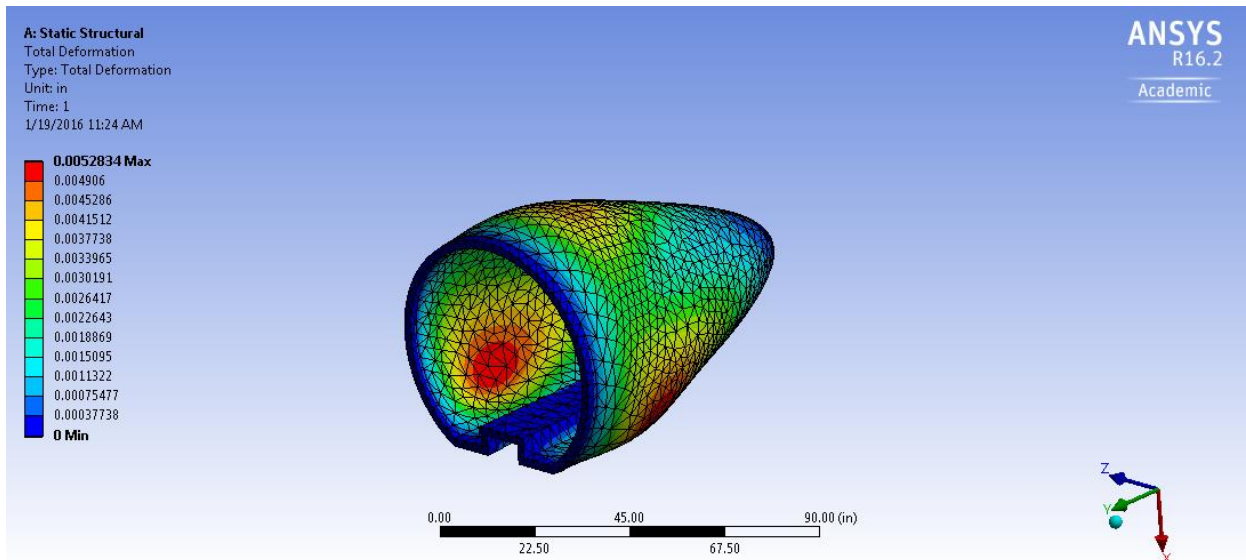
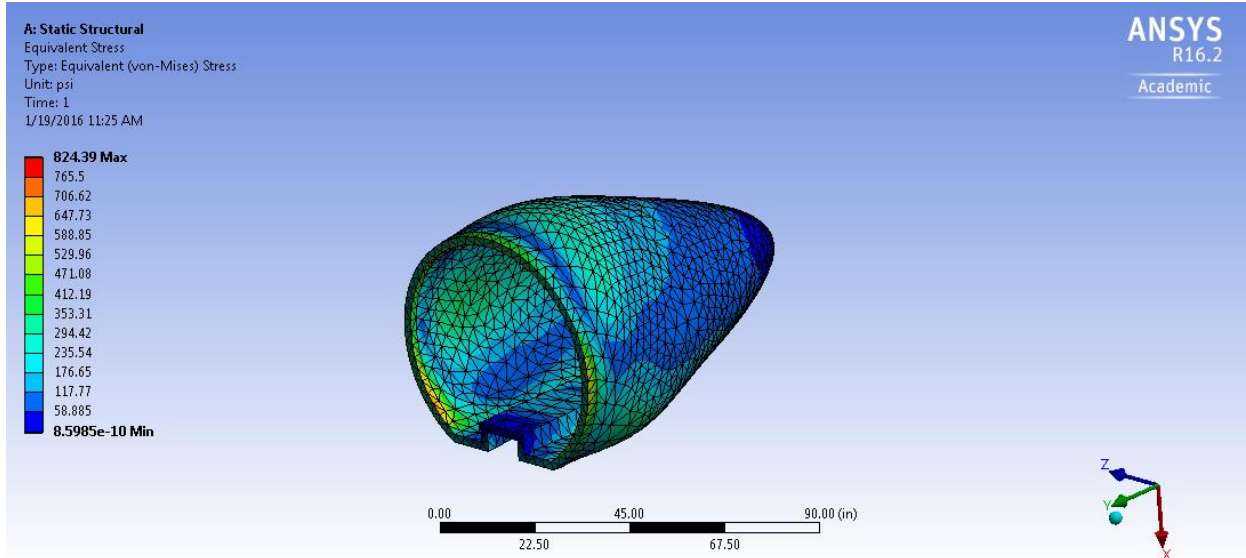


Maximum Equivalent Stress: 379.57 psi
 Maximum Deformation: 0.0010497 in

Figure 2.15 Shows the Stress Analysis of a Tail made of Material: Aluminum 6061-T6



Material: Epoxy Carbon Woven (230 GPa)



Maximum Equivalent Stress: 824.39 psi

Maximum Deformation: 0.0052834 in

Figure 2.16 Shows the Stress Analysis of a Tail made of Epoxy Carbon Woven (230 GPa)

The **Aluminum** and **Titanium** both exhibited similar stress and deformation behaviours, while the **Epoxy Carbon** resulted in higher stresses and greater deformation. All the materials are able to withstand the stresses.

Selection

Comparing results from the analysis of the nose, body, and tail, the materials tested were all capable of withstanding the observed stresses.

Based on the material's ability to withstand stress and deformation, Titanium Alloy should be used for the nose and tail, whereas Aluminum 6061-T6 should be used for the body. Although the observable stress and deformation is greater using the other materials, the safety of the capsule is not compromised as all the materials analysed were capable of withstanding the stresses. As a result, focusing on the cost and weight of the selected materials can help select the most appropriate material.

Material Costs retrieved from:

Material	Cost (\$US/kg)	Density (kg/m ³)
Aero-grade Aluminum Alloy	12	2703
Titanium Alloy	45	4620
Epoxy Carbon Resins	85	1420

Taking the cost and weight of the material into consideration, the most suitable material for use based on the mechanical stresses is Aluminum 6061-T6. It is the lowest cost out of the materials considered at roughly 25% of the cost of the next most cost effective material, the Titanium Alloy. Further, the weight of the material falls between the Titanium Alloy and the Epoxy Carbon Resin, saving approximately 41% of weight compared to the Titanium. The Aluminum is appropriate for the nose, body, and the tail. Note that this material selection has not considered thermal stresses and material thermal capabilities.

A more suitable material may be available depending on the priority of the cost, weight, and stress capabilities. Since the materials all are capable of handling the stress, materials with lower tensile strengths should be investigated. Depending on the material chosen, optimization can be done to the design of the components to minimize material wastage.

2.1.3 Aerodynamic Coefficients

In a high velocity mechanism such as the Hyperloop, the aerodynamics of the system become very important. For the Hyperloop system in particular, it is impractical to create a completely evacuated environment or a total vacuum, and as a result the tube is kept at a certain ambient pressure (albeit a very low pressure). The pressure chosen for the operation of the capsule is the lowest in the given range, which is 0.02psi. [1] Even at such a low ambient pressure in the artificial environment within the tube, the amount of air is enough to impede the motion of the capsule. As a result, the aerodynamic forces and coefficients must be seriously taken into consideration, especially during the acceleration phases of operation when the greatest amount of power output is required.

One of the most significant aerodynamic forces that must be taken into account is drag. There are many different forms of drag that affect such a design but several are more important than others for a design such as the Hyperloop; these include body drag, interference drag, ram drag and friction drag.

Nose Cone

Nose cone shaping is required in aerodynamic design because in most cases, the nose of the structure is the first part of the mechanism to make contact with the airflow boundary layer. This means that the surface of the nose cone furthest forward are the first surfaces to feel the pressure of the air as the structure moves through the fluid and this pressure over the reference area in contact with the boundary layer creates a drag force upon the structure.

Form drag is the most prominent of the aforementioned types of drag and it is influenced by the shape of the body traversing the fluid. This would not be a consideration in an absolute vacuum environment as previous similar concepts have suggested; however, the small amount of pressure present in the tube still exerts a force upon the capsule as it propagates forward through the medium. [2] This form drag can be minimized by optimizing the shape of the body to be more streamlined and aerodynamic as was tested analytically through MATLAB as described in Section [\(\)](#). Taking the results of this testing into account, a paraboloid-based nose cone profile was chosen for this capsule due to its low drag characteristics.

While historical testing [3] has resulted in a number of shapes and volumes of revolution that result in the lowest form drag (through a low coefficient of friction C_d) such as the Haack series or von Kármán ogives, the need for the absolute lowest coefficient of drag is mitigated by the effect of having a large inlet for the compressor at the front. Having the compressor at the front coupled with the lack of ambient air pressure diminishes the need for more complex shapes for the nose cone, and as a result it was decided that the paraboloid would be an excellent shape for the cone choice given the circumstances.

With form drag being the most commonly encountered form of drag, the general explanation of the effects of pressure upon the nose cone may be summarized in equation 1 as follows: [2]

Equation 1.0

$$F_D = \frac{1}{2} C_D \rho v^2 A_{ref}$$

The coefficient of drag C_D in the equation is not an absolute analytical evaluation of the design but is more of an empirical indicator of the aerodynamic "cleanness" of the design. This is because C_D depends on the choice of the arbitrary reference area, which is chosen as required for evaluation of the function desired; for example, the normal or pressure-based component of drag may depend on the frontal wetted area while the viscous component may use surface area as the chosen reference area. In this situation, the drag force must first be calculated experimentally and then be used to solve for C_D . Software simulation via ANSYS Fluent was used in order to obtain drag force values which were then used with Equation 1 in order to find the drag coefficient. The streamlines of velocity around the nose cone may be seen in Figure 2.0.

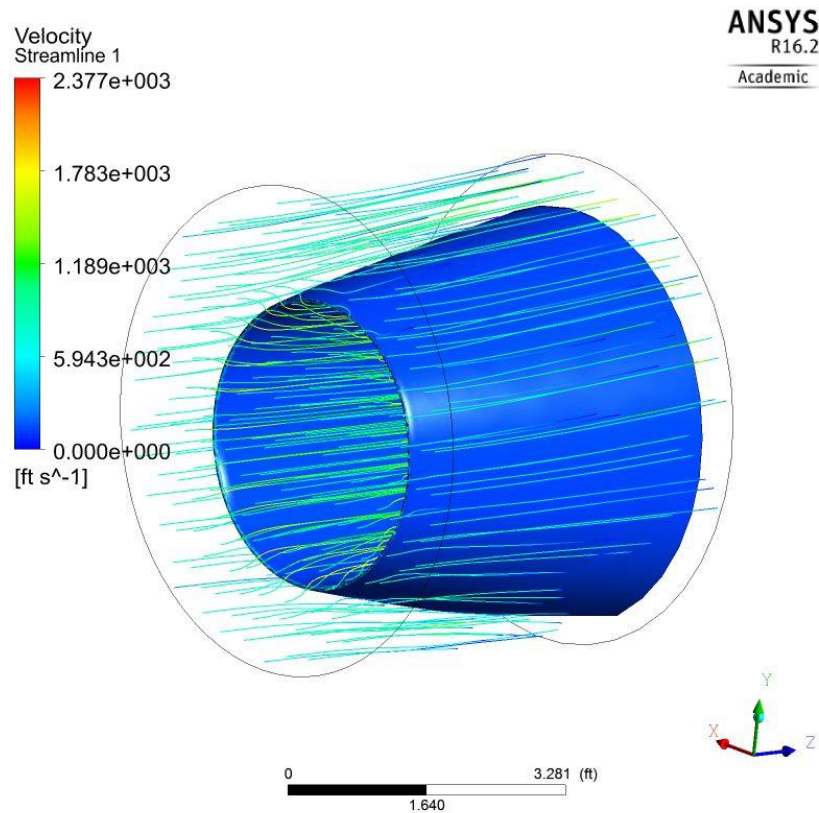


Figure 2.

The simulated pressure drag force output found for the nose cone is 26.3lbs. If this value is divided by the remaining parameters in the drag equation, then the coefficient of drag is found to be 0.44. While the value is not quite as low as that of a streamlined body or other shapes that have been optimized to experience low amounts of drag, this is somewhat due to the effect of the shape of the capsule. The capsule is an elongated cylinder with a blunted nose, and such a shape has a coefficient of drag that varies from around 0.2 to 0.4 depending on the fineness ratio [4]. The passenger capacity and tube diameter constraints require the pod to be stretched to create available space at the expense of aerodynamic performance as the blunted nose shape shows a minimum coefficient of drag at a fineness ratio (length divided by diameter) of around 4.

Interference Drag

Interference drag is generally defined as that caused by rapid changes in area causing the local velocities of air to speed up. This is regularly found on aircraft at wing roots, cockpit splits and other appendages where discontinuities in the streamlined designs occur [5]. However, the Hyperloop system is based on a tube and may be better modeled as a constriction within a stream tube in order to more accurately predict the effects of interference drag.

One of the issues that has been mentioned is that of the Kantrowitz limit [alpha] which can be explained as the air in front of the moving capsule acting as it would in a piston causing the entire air mass further forward in the tube to accelerate. While using Kantrowitz's area relations would yield the minimum area required to create supersonic flow past the constriction or "throat" after the normal shock due to the transonic behaviour of air occurs [6], these equations are more suited to model a supersonic diffuser or inlet. This is because the air still speeds up or slows down to Mach 1 at the throat, which would cause choked flow and thus cause the air mass in front of the capsule regardless; this is not a problem encountered by aircraft (for which the equations were developed) because in flight the air in front of the supersonic inlets of aircraft simply moves out of the way.

To gain a more accurate model of the air effects, a relative area and Mach number ratio based on isentropic nozzle flow equations developed by NASA [7] was adopted. This ratio depends primarily on the isentropic area relation as stated in **Equation 1.1** as follows:

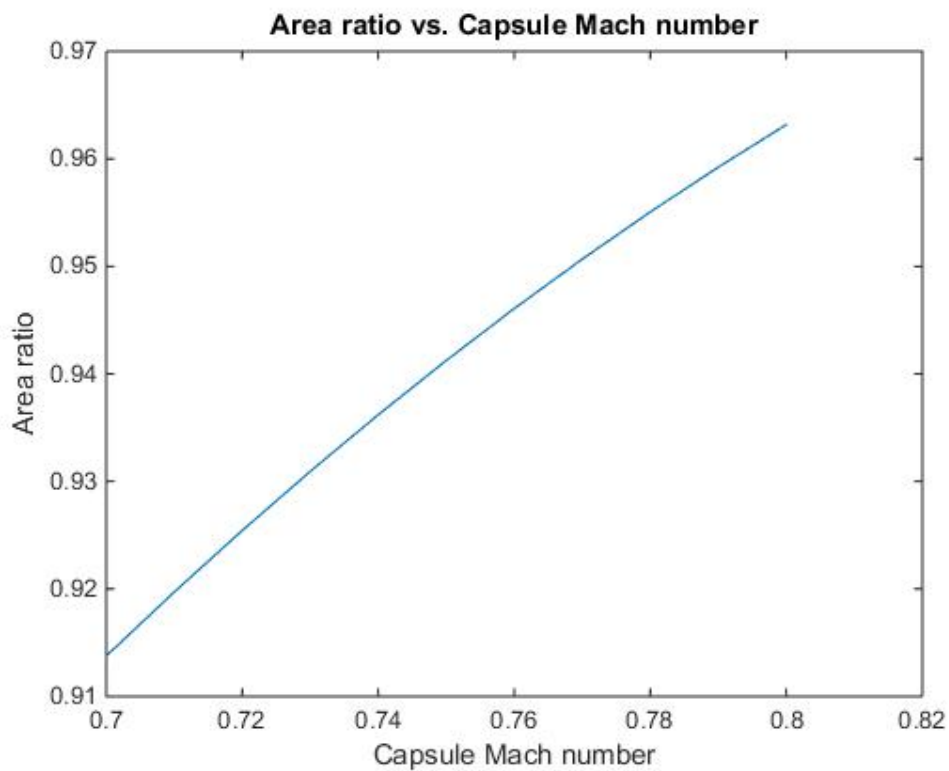
$$\frac{A}{A^*} = \left(\frac{\gamma+1}{2}\right)^{\frac{-\gamma+1}{2(\gamma+1)}} \frac{(1+\frac{\gamma-1}{2}M^2)^{\frac{\gamma+1}{2(\gamma-1)}}}{M}$$

This equation states the ratio of cross sectional area to the cross sectional area of the throat or constriction, which is a function of the ratio of specific heats (taken to be 1.4 with the assumption of air to be an ideal gas at lower pressures [8]) and the Mach number M. Exceeding this ratio results in choked flow with the flow at the throat reaching Mach 1 and with the mass flow rate reaching a limit. This equation is expressed as a ratio of the bypass area (as a function including the bypass Mach number) to the ratio of the tube area (with the corresponding Mach number being the capsule speed). This one is as follows [7]:

Equation 1.2

$$\frac{A_{bypass}}{A_{tube}} = \frac{M_{pod}}{M_{bypass}} \left(\frac{1 + \frac{\gamma-1}{2} M_{bypass}^2}{1 + \frac{\gamma-1}{2} M_{pod}^2} \right)^{\frac{\gamma+1}{2(\gamma-1)}}$$

The bypass Mach number can be assumed to be the constriction because the area of bypassed air that is smaller than the entire tube area can be visualized as the throat and thus a limit of Mach 1 may be applied to it. A small sample of how this affects the area ratio may be seen in the following graph by taking capsule Mach number as a parameter.



Graph 2.0

From this graph it may be seen that an ever-increasing area ratio is required in order to hit higher top speeds without accelerating the air mass in front of the capsule. While this renders the Hyperloop very unlikely to hit near transonic speeds in the tube dimensions specified, a design Mach number of 0.8 was chosen as it is still significantly in the high subsonic speed range.

Choosing Mach 0.8 (about 609mph) yielded an area ratio of 0.9632. In order to obtain that area ratio, a nominal inner diameter was chosen for the inlet where the air compressor would be situated and the following equation was used to calculate the outer diameter (which would effectively become the lip of the inlet).

Equation 1.3

$$A_{outer} - A_{inner} = A_{tube} \left(1 - \frac{A_{bypass}}{A_{tube}}\right)$$

By taking 20 inches as a nominal inner diameter and solving for outer area of the inlet at the compressor, an outer diameter of 21.06 inches was calculated, and a 1.06 inch wall thickness was applied at the maximum area prior to the air being ingested by the air compressor.

Body Drag

While nose cone design is important for the aerodynamic characteristics of the capsule, the length of the capsule makes skin friction drag a serious contribution to overall drag as well. Another major type of drag encountered was the ram drag which was induced due to the compressor taking in air and using it to power the air bearings instead of bypassing it.

Skin Friction Drag

The skin friction drag is caused by viscous effects as the air flows around the body of the capsule and the shear stress that it imparts on the capsule. The equation to find the skin friction coefficient is as follows where U_∞ is the freestream velocity and ρ_∞ is the freestream density of the fluid [9]:

Equation 1.4

$$C_f = \frac{\tau}{\frac{1}{2} \rho_\infty U_\infty^2}$$

In order to find the average shear stress, the drag experienced by the body of the capsule (which was found via simulation in ANSYS) was divided by the surface area of the body and applied to the equation. With a 140lb viscous force on the body divided by a 642ft² area (using the design speed 609mph as the freestream velocity of the air), a skin friction coefficient of 0.179 was obtained. This value was much higher than those measured on streamlined bodies such as aircraft or purpose-built vehicles [2], but this can be explained by the influence of the extremely low density of the fluid at 0.02psi of ambient pressure and the constraints that yield a design with such a low fineness ratio.

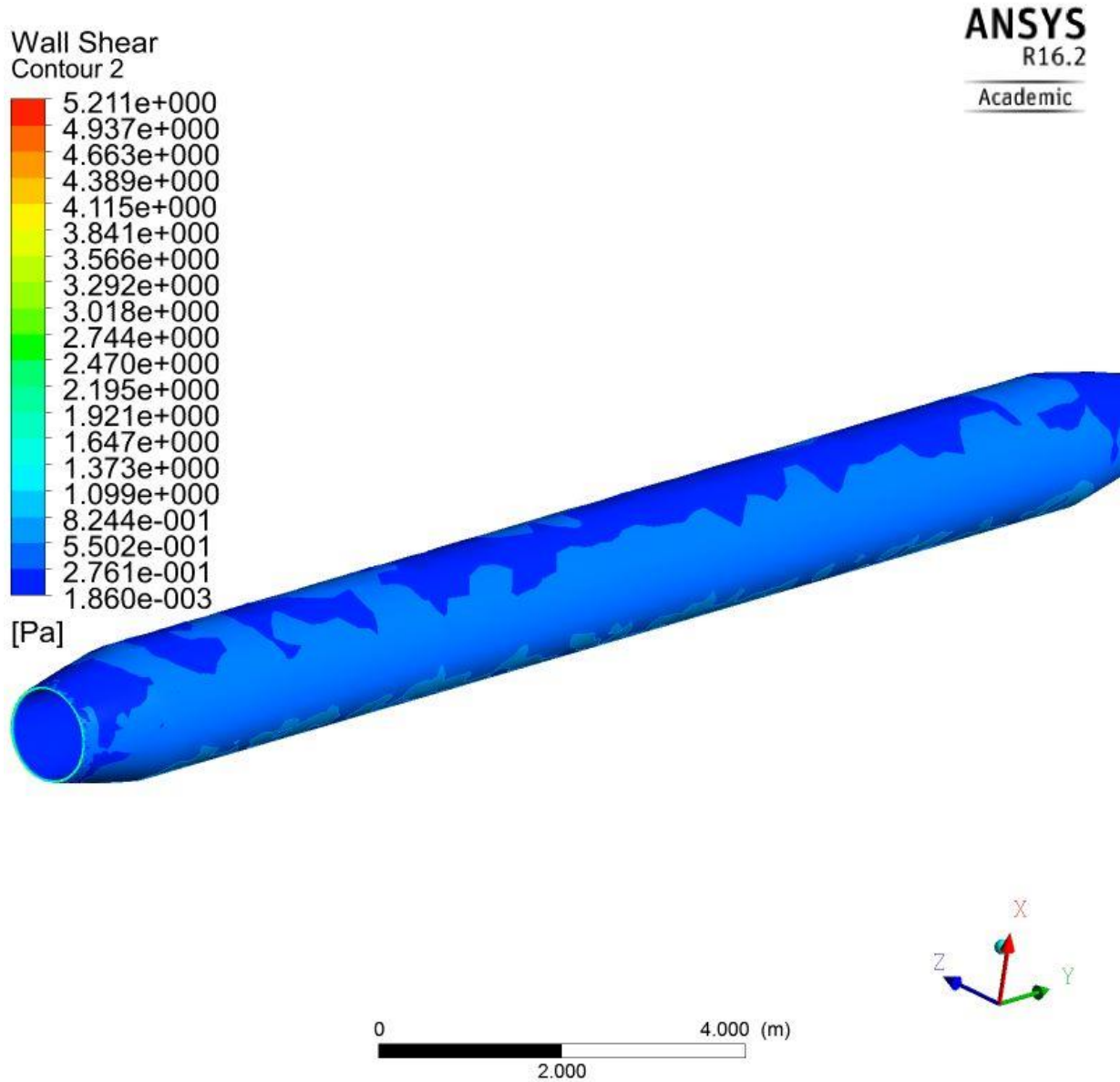


Figure 2.17 Shows a Wall Shear Contour of the Pod

Ram drag

When air from the freestream is ingested and taken into the body of the structure through mechanisms such as compressors or ducts, it has the ability to create ram drag. If this air is not completely bypassed or accelerated to a higher velocity during the propagation of the structure through the fluid, ram drag is likely created. This is because ram drag depends on the change in momentum of the air over time as expressed by the following equation [10]:

Equation 1.5

$$F_{ram} = \dot{m}\Delta v$$

With the entirety of the air being used for the purpose of the air bearings and other uses after being compressed, the change in velocity term may simply be represented by the inlet velocity. The mass flow rate may be expressed as such:

Equation 1.6

$$\dot{m} = \rho v A$$

By taking the velocity and area at the inlet, a mass flow rate of 0.0243 slug/s (equivalent to a 0.161lb weight per second) can be computed. Multiplying the mass flow rate by the inlet velocity of 893.2ft/s yields a total ram drag force of 21.3lb.

2.1.4 Power Source & Consumptions

A concern that is commonly raised by the community at large is the true sustainability of the Hyperloop. One of the ways to prove sustainability is by creating a Self-Powering system. In its initial proposal, Elon Musk truly believed that it is more than possible to and extremely feasible to have a completely self-powering system therefore making the Hyperloop the first self-powering mode of transport unlike other forms that are now trying to switch over to being self-sustaining in some form or another

Sources of Power

The Track

One of the most challenging problems encountered in designing Nimbus initially was the thought of the sheer amount of power simply required to accelerate the Pod or further keep it at a contents velocity.

This is mostly to overcome air resistance, as the aerodynamic resistance increases with square of speed, as seen from drag force:

Equation 1.7

$$F_D = \frac{1}{2} \rho u^2 C_D A$$

Drag force depends on both geometry of the design and the speeds at which it travels. In turn the power can be determined by:

Equation 1.8

$$P_d = \mathbf{F}_d \cdot \mathbf{v} = \frac{1}{2} \rho v^3 A C_d$$

As seen from the equation power required to overcome drag is proportional to the cube of speed. This becomes a problem because of the very high speeds the capsule must travel.

Fixing the problem of power consumption to the track simply requires an array of solar panels on top of the surface of the track through the entire distance from LA to San Francisco. Having this many solar panels running will be more than enough energy to supply the Tube. The stored excess energy can be used in cases when systems are not receiving sufficient energy and require more than that is being outputted. Amount of power at peak conditions can be seen in the below calculations:

Assumptions

- Typically at peak conditions one panel produces 120W/m^2
- Width of the cylindrical track is 14' (4.25m)
- Inverter from DC to AC is 80% efficient
- Total length of track is 354 miles (22440957 inches) long

Total Surface Area = $569708 \times 4.25 \text{ m}^2$

Total Surface Area = 2421259 m^2

∴ each panel produces 120W/m^2

$P_{\max} = 2421259 \text{ m}^2 \times 120\text{W/m}^2$

$P_{\max} = 290 \text{ MW}$

∴ at peak condition the maximum power produced is 290 MW, since Inverters are 80%

Thus there will be a 20% loss for any amount of power converted to AC [1]

Assuming that all 290 MW of power generated is stored, by using the same watt-to-kilogram ratio as the Tesla Roadster, the battery array is estimated to weigh approximately 2,396,695 kg. Therefore, using the known weight of a cell to be $449.0566831 = 0.06574 \text{ kg}$ cell, there would be a total 36,458,300 cells. Using the known dimensions of the 168A lithium-ion cell that is used, the total volume would be equal to $V = r^2 h$, producing a volume of $(0.01862)^2(0.0652)(36458300)650 \text{ m}^3$. The array is planned to be placed along the bottom of the track on the outside of the tube in order to conserve space and provide direct power to the linear stator motors. [2] [3]

The Pod

The primary concern of drawing power on the Pod itself was seen in the massive amount of power required to run the Air Turbine Compressor at the front of the Pod. As stated in the original proposal of the Hyperloop project, the compressor is estimated to use 325kW for a 45 minute trip. In order to store such a large payload, an array of 168A lithium-ion cells is used, similar to those that comprise the batteries of the Tesla Model S and Tesla Roadster.

Similar to the process used in determining the dimensions of the solar panel energy storage, the battery is determined to be around 2700kg in weight. To ensure there is sufficient energy, it was decided to increase this by a factor of 50% placing the final weight at 4000kg, just as proposed in the Hyperloop Alpha document. With this new increase in size, the overall onboard power capacity is increased to 485kW. With a new known weight and capacity, the battery array is determined to have a total volume of approximately 1.2 m^3 . The batteries are planned to be stored along the sides of the pod between the inner and outer capsule walls.

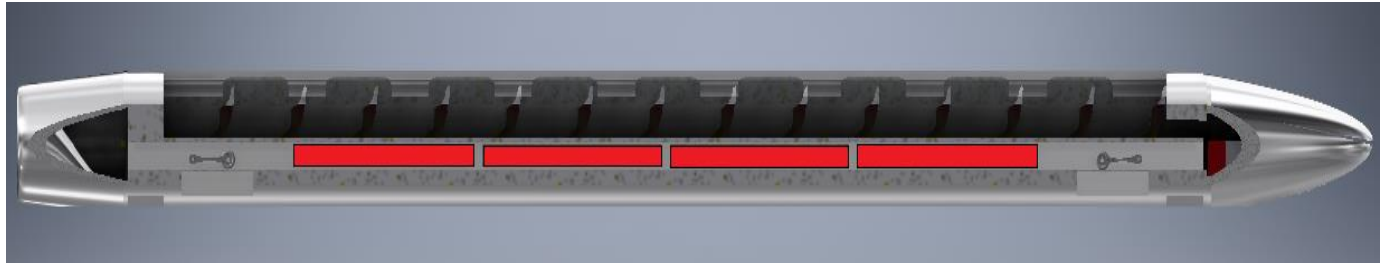


Figure 2.18 Shows onboard Battery Storage

Power Consumption

Track

The Hyperloop will be powered in two separate blocks, Pod and Track. Power to the track will be powering the both the Electric motor and Infrastructure power. The proposed Primary power source supplied to this block will be obtained from the stored solar energy from the top of the track, this will be. Secondary power source will also come from stored solar energy elsewhere. This power will be transferred when needed through a power grid when needed for consumption. A Power distribution schematic is shown Fig , which shows how power is distributed for the track. The average power consumption for an entire trip is $P_{ave}=0.3\text{MW}$, this was obtained by taking area under the Power Vs Time profile (Fig.) over the duration for the trip. The average power consumption can also be seen from Periodic Power consumption (Fig.) also showing the average power at the different stages of the trip.

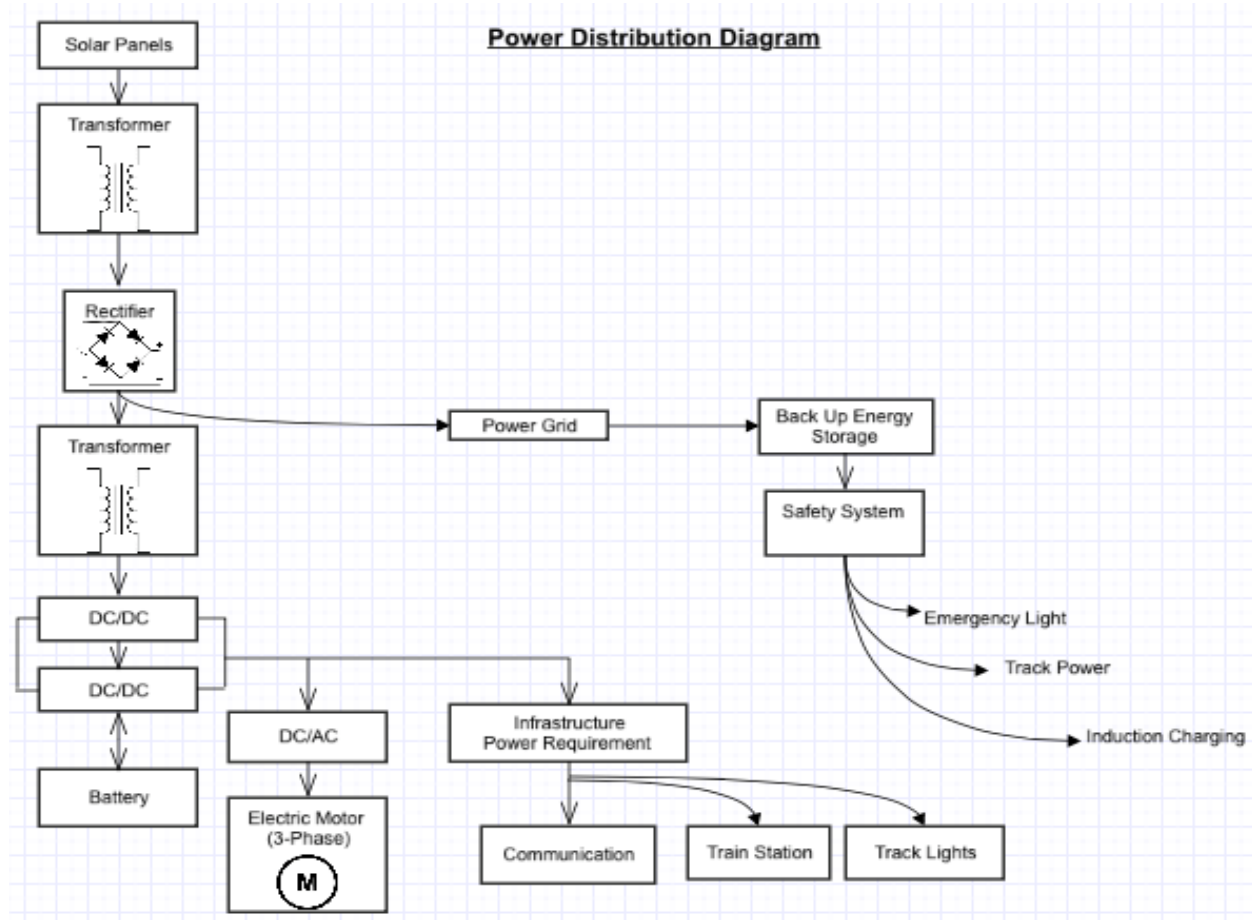


Figure 2.18 Shows The Power Distribution diagram for the Hyperloop

Other on Pod components requiring power such as the compressor, lighting, navigation, control, and other accessories will be powered via an on board battery (168A lithium-ion cells). The compressor itself requires 325KW to power, since the compressor is electric and will require high amounts of power consumption, the need for re-generative braking become more clear along with high frequency inductive charging, this will ensure that we have enough power for the pod throughout the duration of the trip and will also allow for the amount of batteries required on board to reduce as well. In total it is expected that collectively all battery cells will store 485 KW for both safety and to power other components of pod.

Periodic Power Consumption

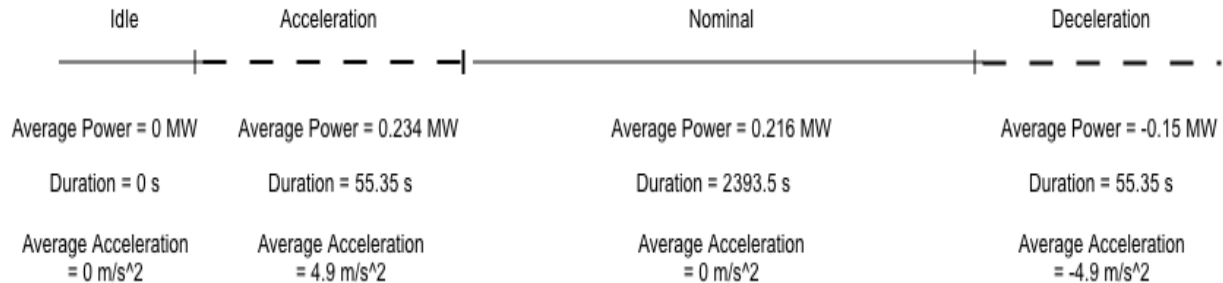


Figure 2.20 Shows Periodic Power Consumption [4]



2.1.5 Thermal Profile

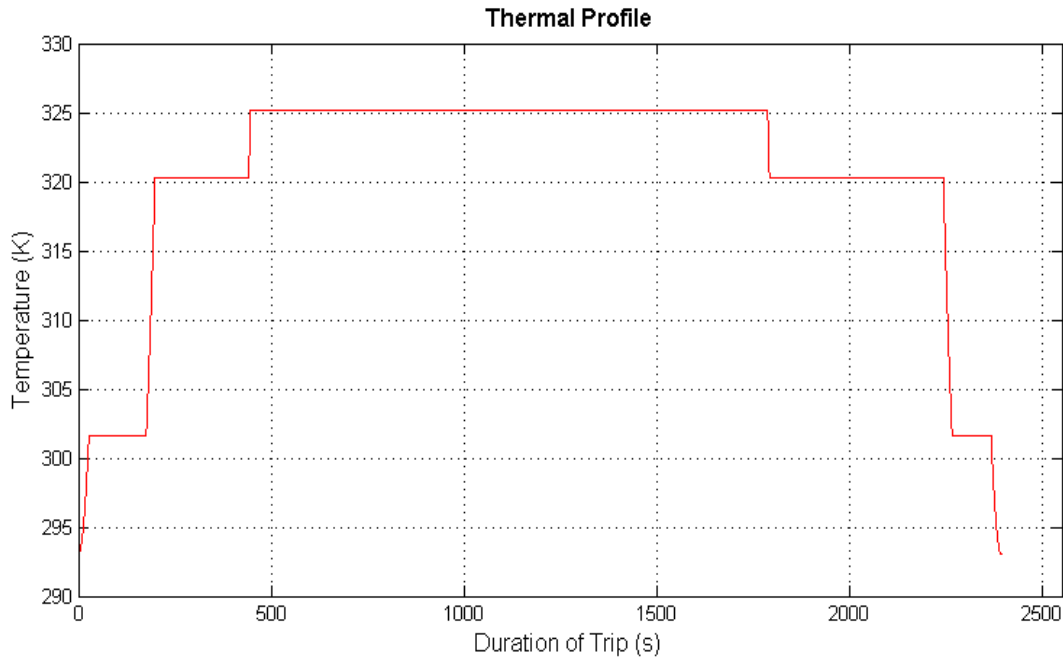


Figure 2.21 Shows the Thermal Profile of each Trip

The thermal profile plots the temperature the capsule experiences to the specific time of the trip. Based on the **assumption** of adiabatic compression in conjunction with the ideal gas law, a relation was derived using the velocity of the capsule as the input, holding all other variables constant.

$$T_2 = T_1 \cdot \left(1 + \frac{\rho v^2}{2P_1}\right)^{\frac{\gamma-1}{\gamma}}$$

$$T_1 = \text{Initial Temperature (K)} = 293K$$

$$T_2 = \text{Tempearture (K)}$$

$$\rho = \text{Density of air at specified pressure} \left(\frac{kg}{m^3}\right) = 0.00118 \frac{kg}{m^3}$$

$$P_1 = \text{Initial Pressure (Pa)} = 100 Pa$$

$$\gamma = \frac{C_p}{C_v} = \text{Specific heat ratio} = 1.4$$

$$\therefore T_2 = 293 \cdot \left(1 + \frac{0.00118v^2}{200}\right)^{0.2891}$$

From the derived relation, the temperature is proportional to the square of the velocity. Using the information from the velocity profile, the thermal profile was created. The maximum temperature reached based on this assumption and the provided velocity values is ~325K. [1][2]

See Appendix B for Thermal Profile Graph code

2.2 Sub-System Breakdown

2.2.0 Propulsion

The Nimbus' linear synchronous propulsion motor system is a one of its kind drive system. This method was selected due its wide support from the academic community and also backed up by extended research under unique conditions which assure that it would work under such conditions as that of the Hyperloop which has never been done before. One of the key features of the Nimbus system is the ability for it to travel at subsonic speeds. As safety is one of the constraints on the system a propulsion mechanism is required where it is cost and energy efficient.

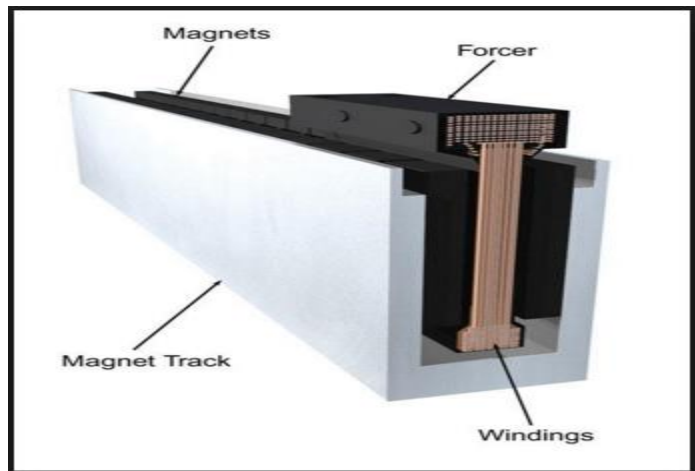
Referring back to the SpaceX Alpha document it is recommended that designers make use of Linear Synchronous Motors (LSM), a linear motor whose mechanical motion is in synchronous with the magnetic field [1]. The speciality about LSM is that the mechanical speed of the system is the same as the speed of the travelling magnetic field. To generate thrust for the system a rail is used at the bottom, this is to either lay a connected array of alternating magnetic poles N, S, N, S etc. or have reluctance Ferro magnet.

When using the LSM system, there are two options for one to produce magnetic fields using Permanent Magnets (PM)

- Sinusoidal waveform of the current, creating a form of moving (AC) current.
- Rectangular or trapezoidal waveform of the current, replicating DC source that is in sync with the speed and position of the moving part

The following highlights a few basic limitations set in place for the pod propulsion such as maintaining a relatively low speed of 300 mph in urban areas as well as ascents and descents around the mountains surrounding the LA to SF terrain. During the peak performance times, the pod should be able to travel up to speeds of 760 mph and this is planned for execution along the I-5 corridor area. Upon exiting the I-5 corridor area, the pod is expected to decelerate down to the speeds of 300 mph.

Below picture shows that the magnetic track will have to be built into the pre-existing track. The forcer is the part that is attached to the pod, the differentiating magnetic field causes the linear motion and moves the pod forward.



Linear Rotor -Stator Motor

Figure 2.21 Shows a Linear Synchronous Motors

2.2.1 Braking

Breaking Mechanism

With exponential increases in technological advancements of the transportation industry, the idea of travelling faster and safely is slowly becoming a reality. One of the biggest concerns with travelling faster is the ability of any mode of transportation to be able to come to a stop.

When looked at the Hyperloop pod which is expected to travel at subsonic speeds, it is crucial to design safe braking system. At such high speeds there is a significant loss in the adhesion coefficient and friction coefficient between the wheel and the rail as well as the brake shoe and the wheel, respectively. Thus operation of conventional braking systems is close to, if not, impossible in Hyperloop.

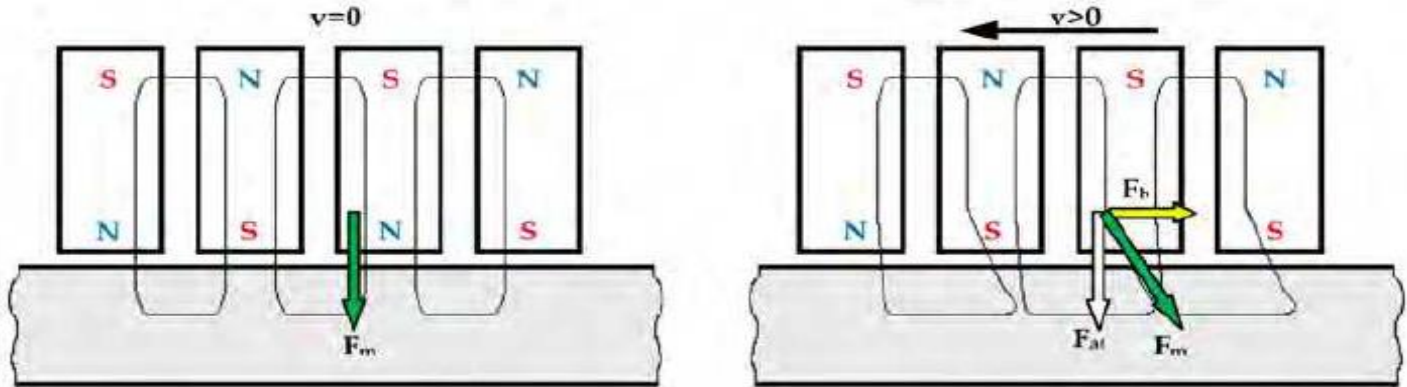
The following scenarios describe various braking mechanisms that can be used to help slow down the Hyperloop pod. In this section ideas to use multiple braking systems in conjunction with one another is also proposed, these conclusions were drawn after considering variable such as passenger safety, power efficiency and overall design.

Handbrake System

A Hand Braking system is the most classic form of braking a moving system. With the technology available today it is possible to introduce a button rather than a physical lever to be used for braking. One of the key benefits of having hand brake is for emergency purposes. Hand brakes are also mandatory for any transport systems which carry passengers to have the ability to manually intervene and override primary braking system. Introduction of such a handbrake system in the Hyperloop pod is important because of the speeds at which the pod is travelling. During the duration of flight there can be various scenarios that require the pod to be stopped such as a considerably seismic earthquake. Upon discussion it was concluded by the team that a pod halted inside the tube would be the safest scenario for passengers during any major seismic event taking the California terrain into consideration.

Eddy Current Braking System [ECBS]

The most optimal solution that was not only cost efficient but also required least maintenance is realized with the use of Eddy Current Braking System (ECBS) on board the Hyperloop pod. The brake consists of a magnetic yoke with electrical coils that are linearly placed to the rails and magnetized with alternating north and south poles. When the coils are put under current while the brake is not in motion, a symmetrical magnetic field is generated that includes the rail head and exerts a vertical magnetic force. When the magnet is moved along the rail it induces a non-stationary magnetic field in the rail head and generates electrical tension that causes eddy currents. These disturb the magnetic field in such a way that the magnetic force is diverted against the direction of travel. The horizontal component of this magnetic force is used as braking force. [1]

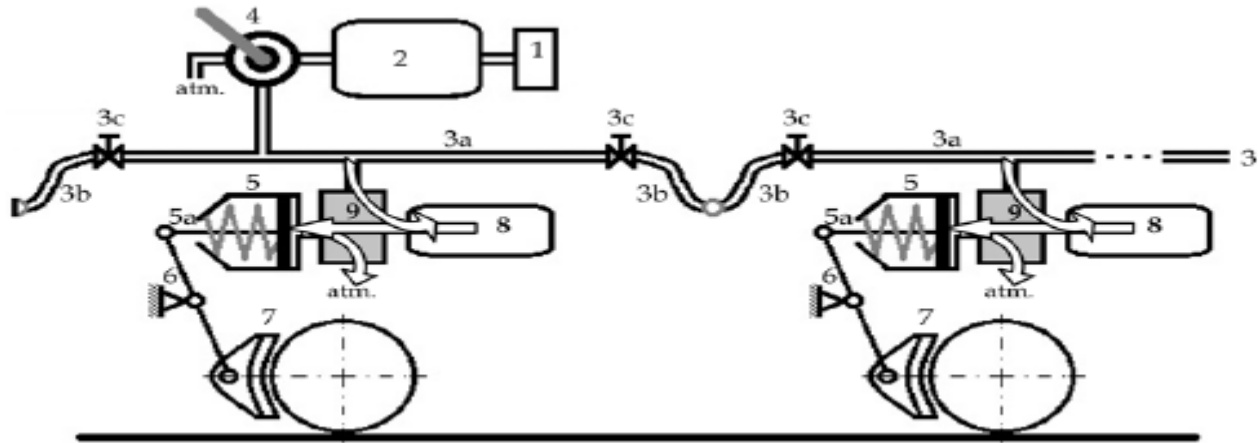


1: Eddy Current Effect - Cross Sectional View

Pneumatic Braking System

Pneumatic braking system applies air pressure to brake blocks or pads, with the varying pressure, the brake pads latch to a metal creating friction, allowing a moving mass to gradually slow down. Usage of compressed air is a viable solution to numerous situation when travelling at speeds regulated on commercial roads and highways. The braking pads and blocks used in pneumatic braking do not wear off easily as the speeds are controlled, for the Hyperloop pod, such a system may prove inefficient. However, pneumatic braking system may be used in conjunction with Eddy Current braking to ensure pod stops safely. Another disadvantage of using pneumatic braking system is the compressed air reservoirs stored on board the pod. Compressed air is most effective when used at 1 atmospheric pressure but in this system, the tube mimics a vacuum where pressure is estimated to be 0.02 psi.

The operations of a pneumatic braking system are shown below, where (1) refers to the brake paddle a driver uses. The compressed air is stored in a reservoir (9) once the brake paddle is pressed, compressed air is forced to exit the system where on it goes to pushing the dampener in (5). The force then exerts and the braking pad (7), grind against the wheels on the train, slowing it down.



2: Pneumatic Braking System

BRAKING SYSTEMS INTEGRATION

As it has been mentioned throughout the report of the speeds at which the pod will be travelling in the tube, it will be valid to make an assumption that the pod requires conjunction of multiple braking systems. This section provides a break-down of how above mentioned systems would interact with one another to ensure passenger safety is never compromised. Reader must consider there exists a primary and secondary braking mechanism, Eddy Current braking system and pneumatic braking system, respectively.

1) PRE-FLIGHT

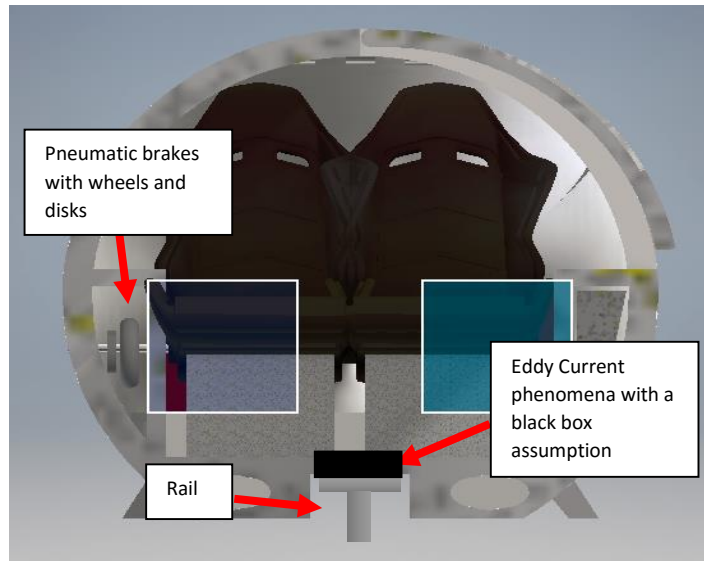
When the pod is in the staging area, has passengers onboard and is ready for the final signal, Nimbus will be using pneumatic braking system to hold the pod steady in place aligned with the rails. The wheels equipped on the side of the pod act like landing gears and can be deployed when pod's linear motion is not anything close to subsonic speeds.

2) TAKE OFF

Upon being cleared for take-off the pod will assume, it has its Linear Synchronous Motors ready to provide the thrust required. The landing gear provides sufficient support on either sides of the pod to maintain a stability avoiding loss of control. The landing gear can be controlled using pneumatic braking system. Although it has a few disadvantages to it when acting in a low-pressure environment feasible workarounds for this scenario can be sought. Using pneumatic braking mechanism the pod can be accelerated up to speeds of 200 mph – conclusion drawn upon the fact that cars on the road can reach those speeds without substantially damaging the brake pads/shoe.

3) IN FLIGHT

To conceptualize the in-flight scenario, there are numerous ways to help slow the pod down. One of the widely used methods in the High Speed Train System (HSTS) is Eddy Current (EC). Afore mentioned diagrams and explanation provide an insight on how EC works. The rail embedded in the concrete bed under the pod through the middle. With the use of EC the travelling pod can reduce its speed drastically. Any time the pod uses its braking system there is likelihood of loss of energy. This energy can be captured and used to produce further stronger EC. This is also referred to as regenerative braking.



Pod with Eddy Current and Pneumatic Braking System

4) LANDING

As the pod starts to approach a landing station, it will have to decelerate at a significant yet safe rate. This procedure will again use EC in conjunction with pneumatic braking system. EC is a primary braking system for the pod as it is the most reliable form of decelerating the pod from its top speed down to a speed that can employ the use of conventional braking methodology without jeopardizing the wear and tear of any rubber/brake pad.

ADDITIONAL SUGGESTIONS

The subsonic speed at which the pod is travelling at is a variable that design teams need to aim for, this speed can also be in a team's advantage to slow the pod down. If a concept like miniature intake valves on the pod body were to be introduced, it can catch air in the opposite direction, helping slow the pod down. These valves can function similar to that of flaps on an airplane. The position of the valves can be such that it pushes the overall weight downwards towards the track and that combined with a slightly low powered Eddy Current that can save energy at the same time.



2.2.2 Levitation



Figure 2.22 Shows a The Front View of Nimbus with it's Turbine Air Compressor

The Nimbus capsule features an electric axial flow compressor that produces 170 N of thrust, and 58 kW of output power. An axial flow compressor is a type of dynamic turbo compressor in which the acceleration of the gas stream in the meridional plane is performed in the direction parallel to the axis of rotation of the bladed wheel.

The air entering the axial compressor has a peak pressure of 0.099 kPa and a temperature of 292 K at a flow rate of 0.49 kg/s. The air exiting the Axial compressor, prior to entering the built-in intercooler system, has a pressure of 2.1 kPa and increases to a temperature of 857 K at a flow rate of 0.29 kg/s. The initial power consumption required for the axial compressor is a minimum of 276 kW. An assumption is made that there is a 30 - 40% efficiency loss due to high amount of power required to initiate the fan of the compressor. However,

although this can be energy intensive, an advantage of using an electric motor is the relatively high peak efficiency, and smaller frontal area for low pressure gas flow.

Electric Motor:

The electric motor operates at a range of 100 W up to 100 MW and consumes a total power of 6.6 kW during the nominal speed portion of flight.

Axial Compressor:

Air is compressed with a compression ratio of 30:1. The air travels via two narrow passageways that diverge into two tunnels near the bottom of the capsule to the tail cone. The compressed air then exits through the air bearings to create a viscous layer of air separating the outer wall of the capsule and the inner wall of the tube below the capsule. It is assumed that the capsule will levitate at a height of 10 mm with the help of 28 air bearings that must be custom designed to ensure that the thrust generated by the air bearings and compressor will be sufficient to support 15 tonnes of the estimated pod mass. Collectively, the air bearings must be custom designed due to the fact that no such air bearing exists in the market. To account for the increase in thermal energy, an on board water tank will be utilized to cool the air exiting the compressor.

An axial flow compressor is one in which the air flow enters the compressor in an axial direction, parallel with the axis of rotation, and exits from the electrically powered turbine, also in an axial direction. Axial flow compressors are frequently used in applications that involve gas turbines. However, the Nimbus requires that the compressor and all of its subsystems are electrically powered to avoid the circumstances in which gas accumulates and condenses within the internal tube environment. Gas turbines would cause high amounts of thermal energy which is undesirable in a low-pressure controlled environment in which the pod operates. Furthermore, the use of gas turbines would cause condensation of gas within the tube which could obstruct the proper functioning of other electrical systems and infrastructure within the tube. For the reasons stated above the Nimbus capsule's axial flow compressor will operate with an electric motor.

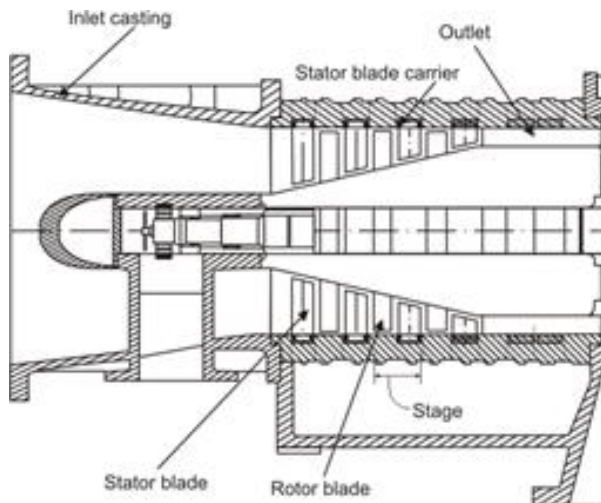


Figure 2.23 Shows a cross-sectional view of an axial compressor and its functioning parts

	Air Entering Axial Compressor	Air Exiting Axial Compressor
Pressure (kPa)	0.099 kPa	2.1 kPa
Temperature (K)	292 K	857 K
Flow Rate (kg/s)	0.49 kg/s	0.29 kg/s
Power (kW)	276 kW	52 kW



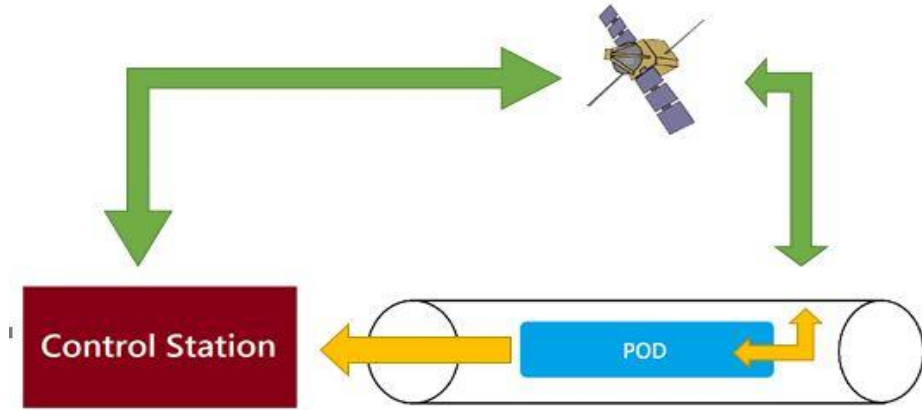
2.2.3 Navigation

As per initial proposal in Musk's Alpha document, the Hyperloop system ideally would be an autonomous self-powering system. This implies that individual capsules will be operated and guided by a pre-programmed course as determined by the location of the set track.

McMaster Hyperloop proposes the following systems in order to guide navigation throughout the Hyperloop.

Satellite Communications

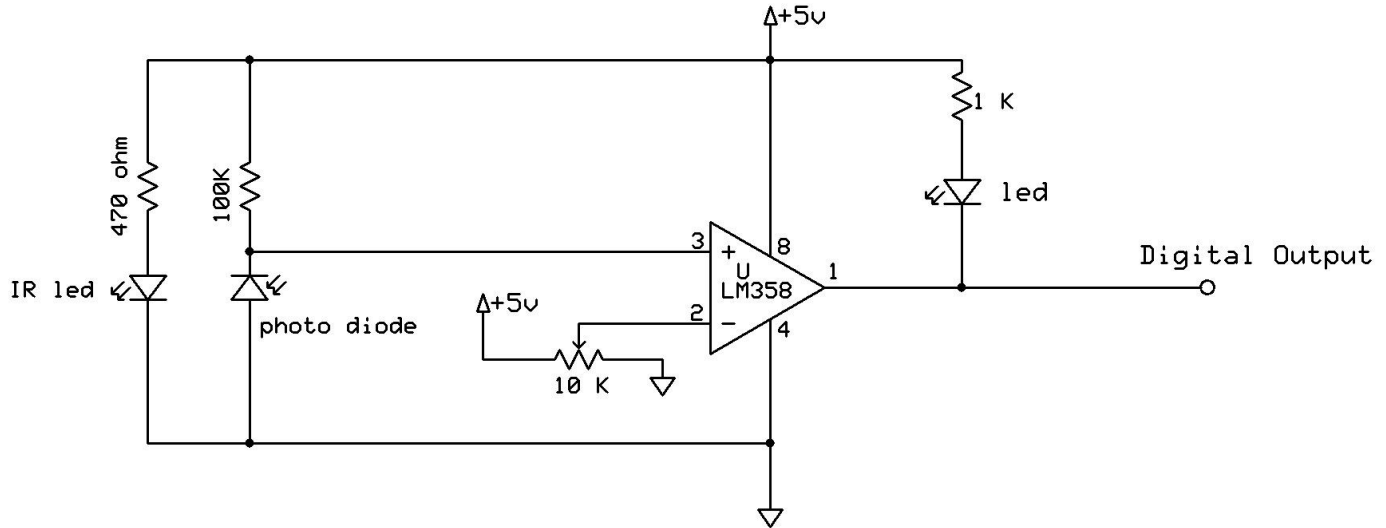
The pre-programmed trajectory of the Pod is monitored by the Control Station with the aid of Satellite Communications. An on Pod GPS system sends positional signals to a Satellite in space which then further relays the positional coordinates of the Pod in the Tube back to the Control Station. Figure 2.0 depicts a simple visual of the communications.



Proximity Sensor [IR-Photodiode Circuit]:

In the case that Satellite Communications fails for some reason, it is proposed that every 10 miles, the track be laid out with an IR-Photodiode System. Figure 2.0 depicts the simple circuit behind the system.

IR Module 1



[1] Figure 2.24 Shows the Proximity Sensor used for detection

This system sends an output every time the connection between the IR-Photodiode Circuit is broken. In this case the output would be a useful signal that the Pod has passed through that section of the Tube. Each Tube section is to be numbered, therefore if a sensor is not triggered and Satellite Communications is down, the Pod would go into appropriate mitigating procedures and the position of the Pod can be narrowed down to a 10 mile area vs. being unable to detect it in the entire track length of the tube.

As per implementation on the test track designed for the Texas A&M Design Weekend, the 2-inch wide reflective circumferential stripes will be placed periodically throughout the track that will aid the capsule in determining what action to perform based on the pattern observed by the optical sensor. This can be attained by using a polarized retro-reflective photoelectric sensor. The processed fluorescent tape pattern is then turned into an appropriate action from the drive system.



2.2.5 Sensor List & Location Map

Onboard Sensors

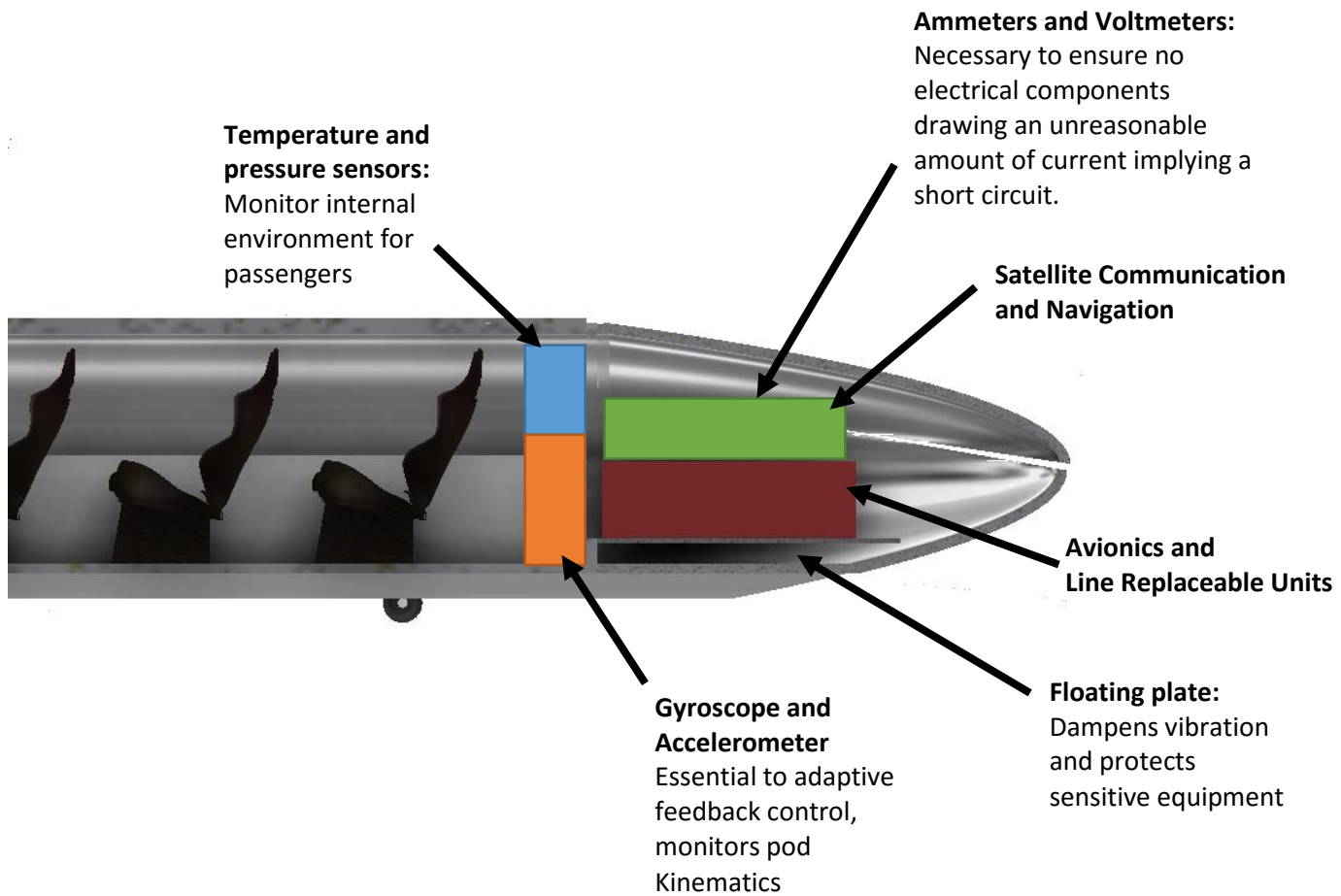


Figure 2.0



Front facing camera:
to inspect the track
and detect debris

Compressor motor:
to inspect the track
and detect debris

Seat Belt Lock detector:
ensures the passenger is
using their seatbelt.

LIDAR: verify camera
information and get
more precise distances
from the ground and
the track ahead

Seat Pressure Sensor:
detect if the seat is
vacant or being used.

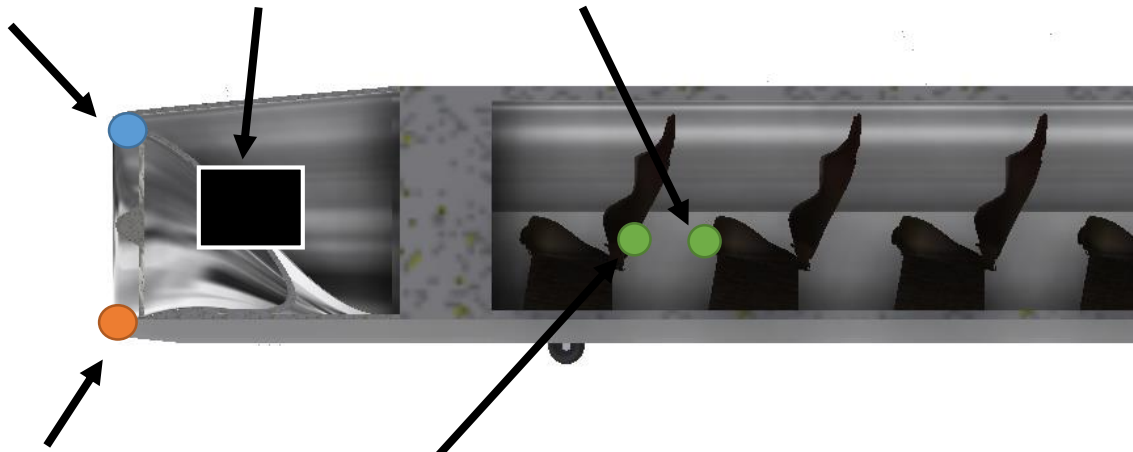


Figure 2.0

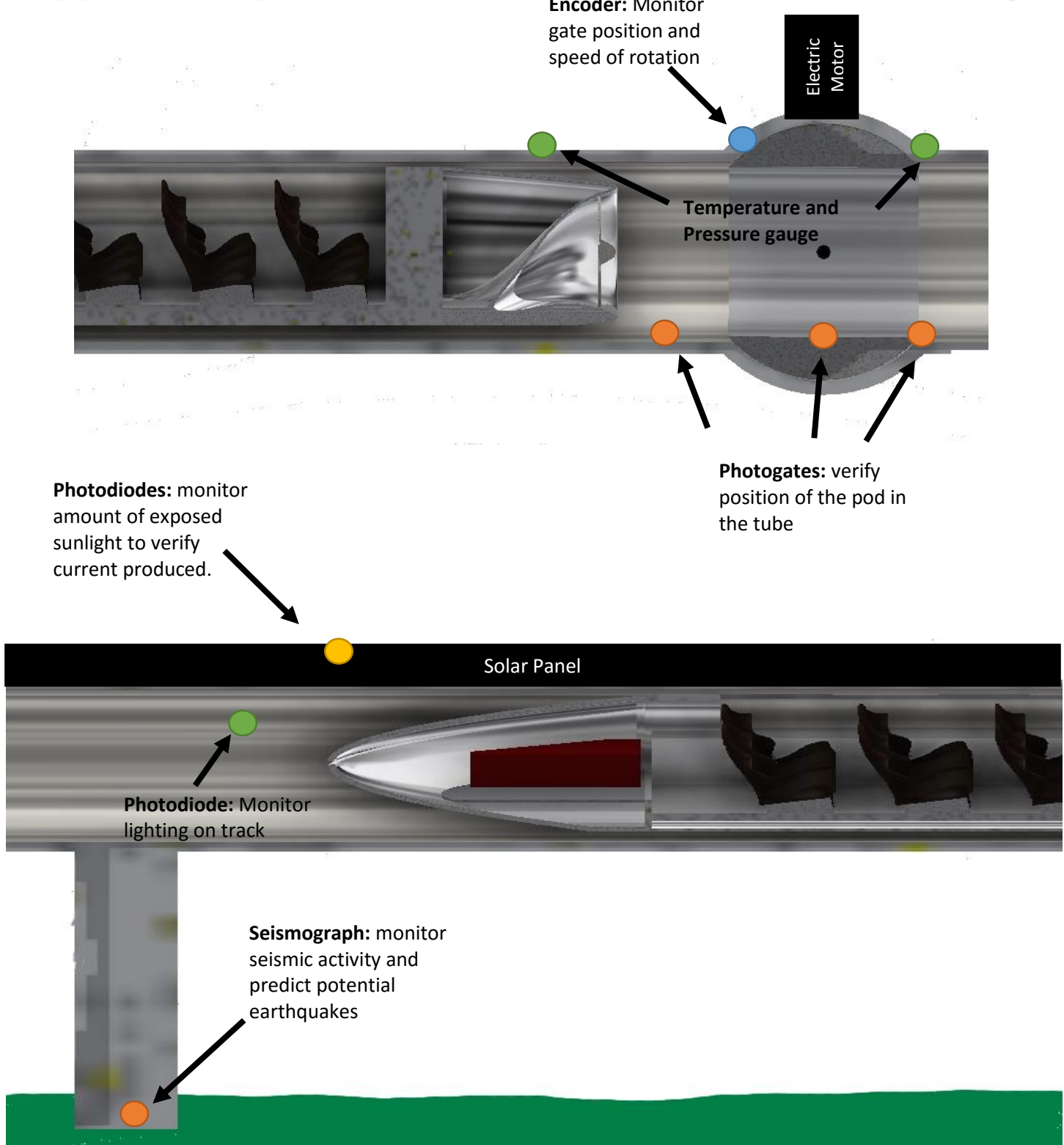


Figure 2.0

3 Performance

3.0 System Trajectory

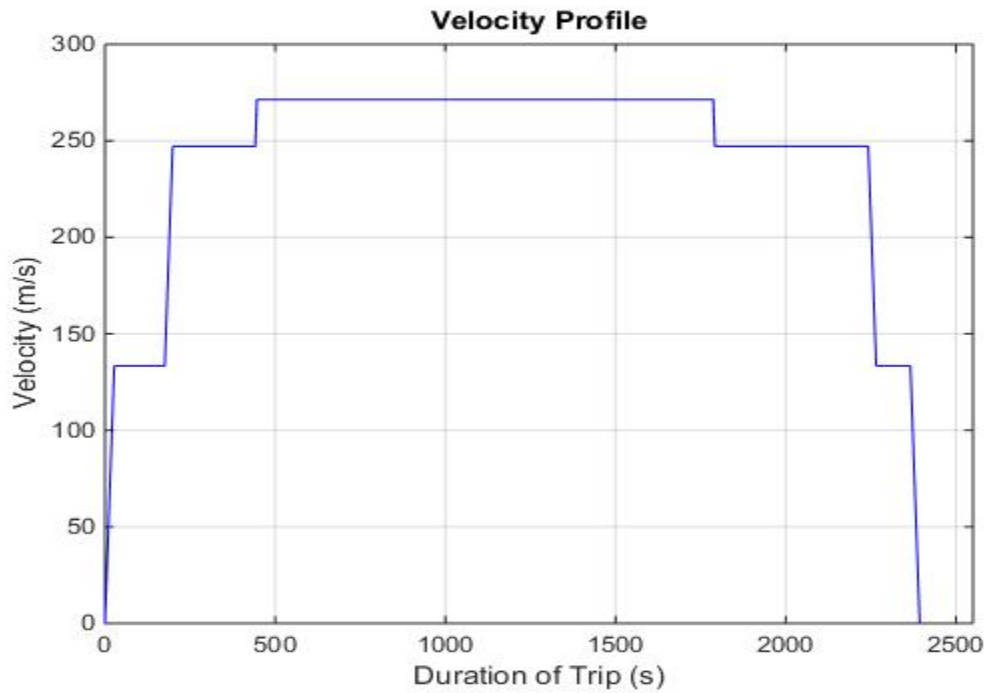
Note: This includes the required Initial Acceleration, Nominal Deceleration & End of Tube-Nominal Crash values

Time Interval to Accelerate (s)	Time Interval at Constant Speed (s) (Final Speed)	Initial-Final Speed (m/s)	Acceleration (m/s ²)	Total Distance (m)
27.2	148.4	0-400/3	0.5g	3629.2 +19786.7 =23415.9
23.2	242.6	400/3-2225/9	0.5g	4412.0 +59976.1 =64388.1
4.9	1340.5	2225/9-814/3	0.5g	1270.2 +363722.3 =364992.5
4.9	450.6	814/3-2225/9	-0.5g	1270.7 +111398.3 =112669.0
23.2	100.7	2225/9-400/3	-0.5g	4416.86 +13426.7 =17843.5
27.2	0	400/3-0	-0.5g	=1814.0

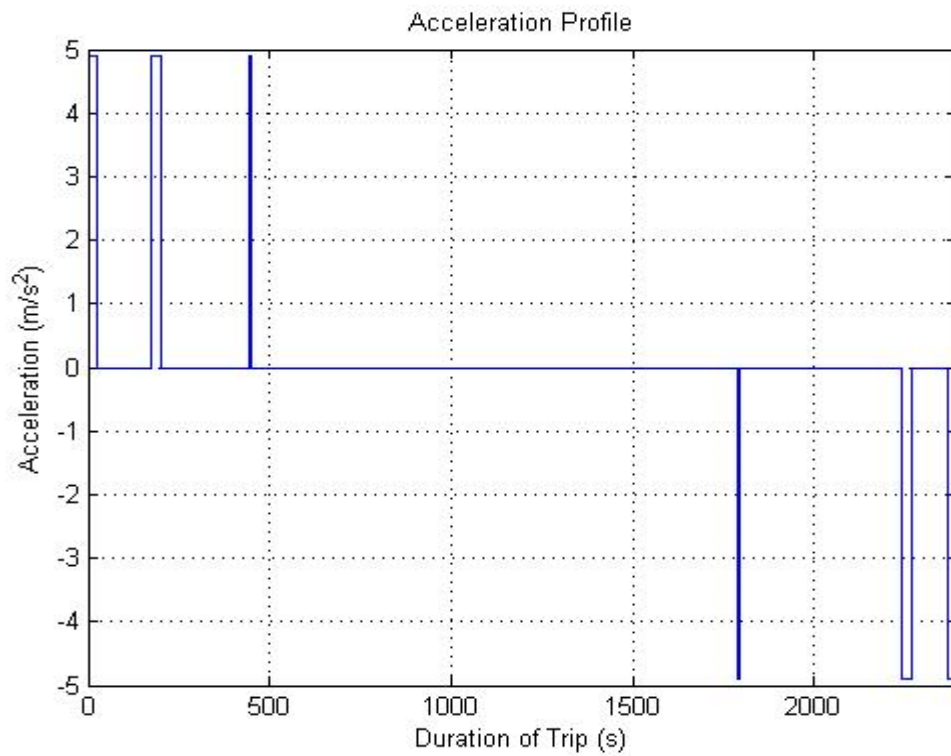
Figure: Summary of Predicted Pod Trajectory



3.1 Predictive Velocity Profile

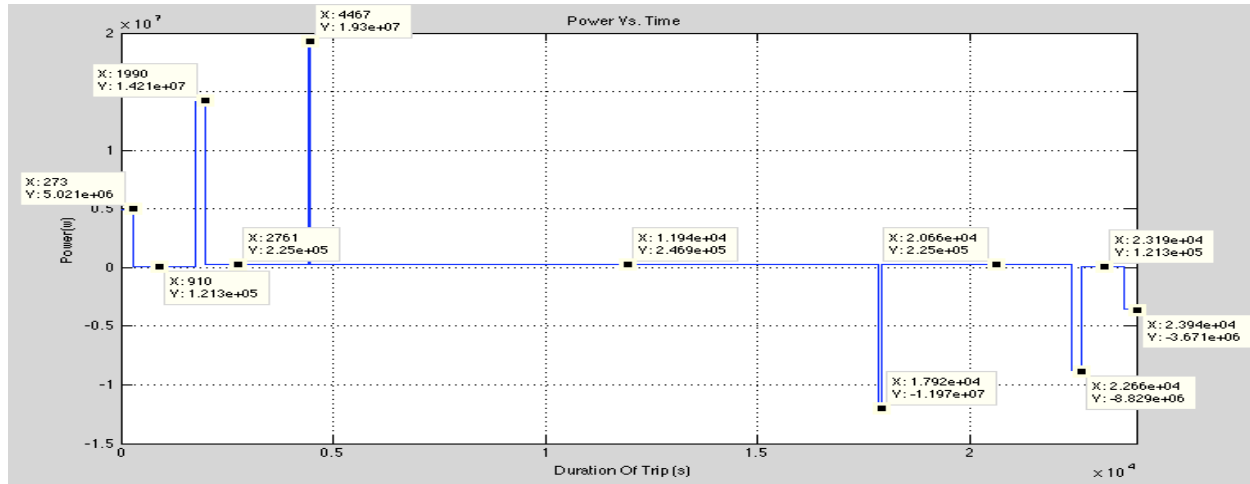


3.2 Predictive Acceleration Profile





3.3 Predictive Power Distribution Schematic



3.4 Predictive Power Profile

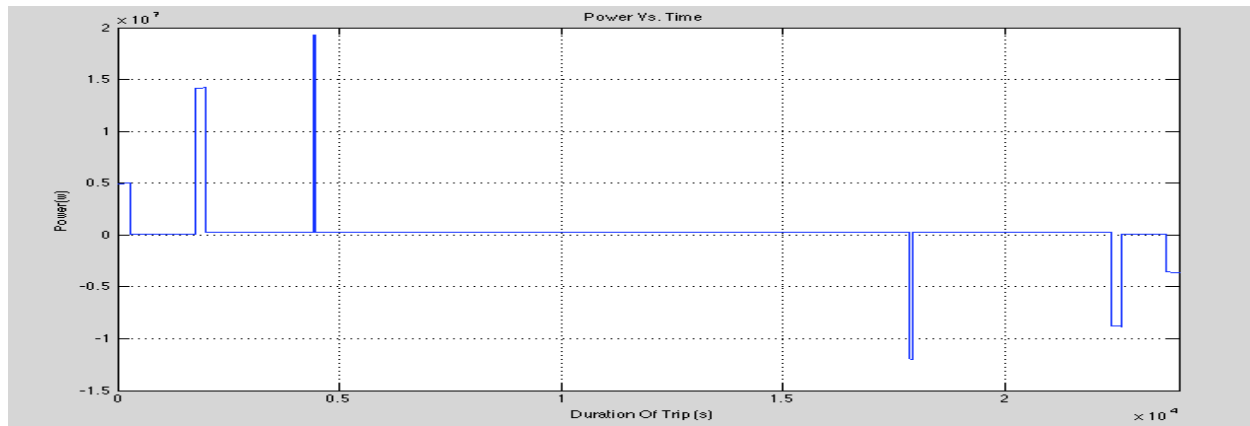


Figure: Power Vs. Time Graph

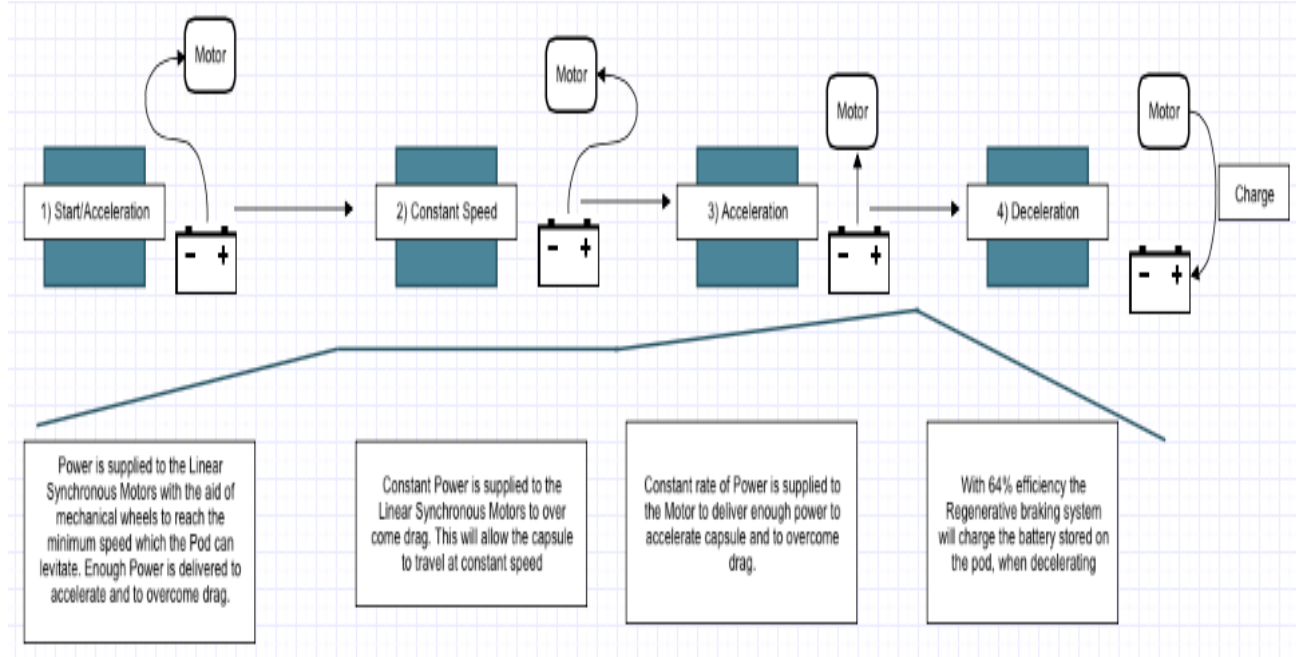
In the above graph, the variable 'y' denotes the value of the instantaneous power at each given period in time denoted by the axis of the dependant variable. The variable 'x' indicated in each label represents the time in seconds from the beginning of the trip.

In the **Figure** below, the distribution of energy is portrayed. In conjunction with the Power Vs. Time profile as seen in the **Figure** above, it is noted that during the acceleration process there are multiple large spikes in power consumption. With this in mind, it is advised to use ultracapacitors at these proposed locations due to their ability to discharge and recharge large sums of energy. The decision to use ultracapacitors over typical batteries is due to their long life expectancy and similar discharge capabilities. Also shown Below in **Fig** (Energy Flow Chart) is the regenerative braking our design uses during deceleration, it is noted that the efficiency is 64% similar to efficiency of tesla motors.

https://www.teslamotors.com/en_CA/blog/magic-tesla-roadster-regenerative-braking

3.5 Predictive Energy Schematic

Figure: Energy Flow-Chart



3.6 Predictive Energy Schematic

In the event of an unexpected power outage, there are contingency measures in place to counteract any problems and prevent potential damage.

For the rails, there will be a two stage energy storage system in place in which there is a main supply and backup supply. Using the solar panels placed atop the tunnel, the system will charge the backup battery first to ensure that there is always a fallback option in the event of emergency. In the event that neither system can provide power, a distress signal will be sent out to the capsule causing the system to slow down and come to a stop.

As for the capsule itself, in most general cases there will be a secondary onboard battery system which will provide enough power for the capsule to maintain both life support systems and levitation, and eventually bring the capsule down to a stop. Once the capsule has come to a stop, a rescue pod will be sent to retrieve the immobile capsule and bring it to the desired destination. To ensure that the backup system will work, it will be implemented as a single time use system that will be charged separately and will be replaced if in the event that it is required.

Process Step	Potential Failure Mode	Potential Failure Effect	SEV	Potential Causes	OCC	Current Process Controls	DET	RPN	Action Recommended
Capsule	Compressor loses power	-Crash -Catastrophic damage	10	-Insufficient power -Faulty wiring -Compressor damage	1	-Reserve power system	7	70	-Increase minimum threshold before reserve power system activates -Routine maintenance
	Navigation and control systems malfunction	-Potential crash -Ride instability	8	-Network communication error	4	-Subsystem reboot	2	64	-Periodic network checks
	Pressurization system malfunction	-Depressurization -Passenger discomfort	7	-Faulty wiring -Network miscommunication	2	-Oxygen masks -Subsystem reboot	2	28	-Routine maintenance
Rails	Linear stator motor loses power	-Severe loss in propulsion power	5	-Insufficient power -Motor malfunction	1	-Reserve power system	5	25	-Increase minimum threshold before reserve power system activates -Routine maintenance
	Insufficient power output	-Capsule arrival delayed	4	-Faulty wiring -Insufficient power -Motor malfunction	1	-System reboot	2	8	-Routine maintenance

Figure: FMEA - Electrical Systems

3.7 Payload Capability

Safety

7.1 Safety Requirements

7.2 Hazardous Systems and Operations

- Lithium-ion Cells
- Ultracapacitors
- Electronic devices
- Oxygen Tanks
- Coolant fluids
- Airbags
- Hydraulic Fluid
- Grease (motor oil, lubricant)
- Adhesives

<http://ehs.research.uiowa.edu/list-hazardous-materials-and-disposal-contacts>

7.3 FMEA

Process Step	Potential Failure Mode	Potential Failure Effect	S E V	Potential Causes	O C C	Current Process Controls	D E T	R P N	Action Recommended
Propulsion	Failure to maintain pressure of 0.02 psi in internal tube environment	Increase in drag and failure to reach nominal velocity	10	Breach in the tube structure	1	Pressure sensors feedback loop to main control	7	70	Activate air lock mechanism to isolate breached area Immediate replacement of the breached segment of the tube Routine tube maintenance
	Power outage	Pod ceases motion	8	Insufficient energy storage to supply power	4	Pod undergoes consistent pre-flight checks	2	64	Switch to secondary power grid to ensue motion Retire pod at the next

									terminal for maintenance Periodic battery checks
	Compressor Failure	Reduced internal pressure Increase in current draw Trouble maintaining pod's distance from the track	6	Broken or damaged compressor blades Compressor motor loosing efficiency, or damaged Obstructed air intake on Pod	Landing gears are partially deployed in anticipation for further pressure loss				Replace turbine blades If necessary replace compressor motor, Check for leaks or damages in main intake and manifold
	Levitation mechanism fails to support capsule	Pod drops to track height and decelerates	7	Payload capability exceeds that of recommended	2	Pressure sensors to maintain compression ratio	2	28	-Routine maintenance - examine proper functionality of air bearings
		Pod drops to track height and begins to decelerate	5	One of the air bearings fails to perform optimally	1	Pressure valve to control air volume that exits	5	25	Pre-flight checks to ensure the proper functionality of air bearings
	Failure to maintain pressure of 0.02 psi in internal tube environment	Increase in drag and failure to reach nominal velocity	10	Breach in the tube structure	1	Pressure sensors feedback loop to main control	7	70	Activate air lock mechanism to isolate breached area Immediate replacement of the breached segment of the tube Routine tube maintenance
	Power outage	Pod ceases motion	8	Insufficient energy storage to supply power	4	Pod undergoes consistent pre-flight checks	2	64	Switch to secondary power grid to ensue motion Retire pod at the next

								terminal for maintenance Periodic battery checks
	Compressor Failure	Reduced internal pressure Increase in current draw Trouble maintaining pod's distance from the track	6	Broken or damaged compressor blades Compressor motor loosing efficiency, or damaged Obstructed air intake on Pod	Landing gears are partially deployed in anticipation for further pressure loss			Replace turbine blades If necessary replace compressor motor, Check for leaks or damages in main intake and manifold
Levitation	Levitation mechanism fails to support capsule	Pod drops to track height and decelerates	7	Payload capability exceeds that of recommended	2	Pressure sensors to maintain compression ratio	2	Routine maintenance Examine proper functionality of air bearings
		Pod drops to track height and begins to decelerate	5	One of the air bearings fails to perform optimally	1	Pressure valve to control air volume that exits	5	Pre-flight checks to ensure the proper functionality of air bearings
Satellite Communication	Pod loses communication with Tube or Station	Failure to locate capsule in case of power outage or similar circumstance	4	Weather Communication Signal not found/recognized Increased data traffic causing network latency	1	Disconnect in SAT COM enables radio communication between tube and pod During total network isolation the pod comes to a safe stop at the nearest emergency exit.	2	Routine check for radio communication between the station, tube, and pod Communication failure leads to replacement of Satellite Communication Module. Establish contracts with multiple satellite communication networks to prevent signal loss.

Power-Capsule	Compressor loses power	-Crash -Catastrophic damage	10	-Insufficient power -Faulty wiring -Compressor damage	1	-Reserve power system	7	70	-Increase minimum threshold before reserve power system activates -Routine maintenance
	Navigation and control systems malfunction	-Potential crash -Ride instability	8	-Network communication error	4	-Subsystem reboot	2	64	-Periodic network checks
	Pressurization system malfunction	- Depressurization -Passenger discomfort	7	-Faulty wiring -Network miscommunication	2	-Oxygen masks -Subsystem reboot	2	28	-Routine maintenance
Power-Rail	Linear synchronous motor loses power	-Severe loss in propulsion power	5	-Insufficient power -Motor malfunction	1	-Reserve power system	5	25	-Increase minimum threshold before reserve power system activates -Routine maintenance
	Insufficient power output	-Capsule arrival delayed	4	-Faulty wiring -Insufficient power -Motor malfunction	1	-System reboot	2	8	-Routine maintenance
Braking/ Reduce the speed of the system	Braking mechanism reduces the speed of system too slowly	Train is not able to reach the speeds desired for conventional braking to kick in	8	Magnets not producing sufficient Eddy Current	Battery charge Magnet malfunction				Ensure braking system has sufficient batteries left after each ride Replace reusable batteries on timely service to ensure battery life is intact. Verify with control systems pre-flight

	Reduces speed too quickly	Abruptly disrupts the linear motion of the travelling pod	10	incorrect calculation in the feed-back loop				
	Eddy current causes the rail to heat up too much causing system failure	Eddy Current system may become inoperable if the rail is being heated up		Heat dissipation on the rail is not managed correctly	Temperature			Appropriate heatsink technology
	Feedback loop sends incorrect values required to ensure safe braking	Pod will not be able to halt in a controlled manner		Incorrect signal disruption, systems did not come online properly during pre-flight				Predefined threshold values updated during testing phase Ensure coding is correct based on the values received from rigorous testing phases
	Power supply to the Eddy Current system is not sufficient enough	Magnets will not be able to generate strong fields		Battery is being dissipated at a higher rate	Prior to flight, check the charge on batteries			
Structure - Capsule	Crack formation on pod windows	Crack propagation and window fracture due to stress from the pressure differential -pressure change in capsule		Higher than anticipated stress concentration	Periodic check for minor cracks on windows			-Fatigue testing -Increase factor of safety to anticipate for unexpected stresses
	Hull breach	-Decompression (potentially explosive)	8	-Unmaintained damage	3	-Oxygen masks for passengers	6 14 4	-Routine maintenance

		-Passenger discomfort						
Structure-Tube/Track	Tube breach	-Tube re-repressurization -Performance loss	8	-Earthquakes -Inclement weather	2	-Increase power to vacuum pumps -seismometers to detect and warn for potential	5	80 -Periodic pressure sensors
	Damaged support pillar	-Catastrophic damage	9	-Earthquakes -Vehicle collisions	1	-Emergency stop -Close track	9	81 -Routine checks
Avionics/Sensors	Internal and External Pressure Sensor malfunction or failure	Capsule fails to monitor pressure levels; cannot ensure safe levels False pressure warnings and false alarms triggered	8	-Power failure within pod -Failure of vacuum pump system to contain moisture or other elements		-Redundant sensor systems in order to keep operation -Deployment of compressor driven ram-air systems for essential sensors (e.g. pressure sensors)	9	-Evaluate if backup systems can provide enough situational awareness -In case of external pod sensor failure, use tube telemetry data -Run systems check at next terminal
	Internal and External 6-Axial Forces malfunction or failure	Pitch, yaw and roll data of the pod is compromised Situational and spatial awareness is lessened	7	-Primary power failure within pod -Faulty connections for displaying acquired data		-Changes inputs to Photo and IR sensors in order to determine spatial positions -Switches to pressure inputs to estimate forces on axes	7	-Reduce speed to reduce load on auxiliary sensors -Use proximity sensors to gauge pod orientation within tube
	Polarized Retro-reflective Photoelectric Sensor	Photoelectric sensor receives no data to output Proximity sensing to tube walls is compromised	9	-Retro-reflective tape has been damaged, now unreadable -Sensors have been misaligned from designed orientation to where they point		-Tube undergoes regular maintenance (daily during downtime) to check for functioning		-Reduce speed to lower risk of collision with the tube in case of control malfunction -If photoelectric sensor is being

					systems and damage -Sensor functionality check feeds back to pod as well as control centre for multiple monitoring location			used solely for guidance (other redundant systems offline), cease motion
Sensors	Internal and External Pressure Sensor malfunction or failure	Capsule fails to monitor pressure levels; cannot ensure safe levels False pressure warnings and false alarms triggered	8	-Power failure within pod -Failure of vacuum pump system to contain moisture or other elements	-Redundant sensor systems in order to keep operation -Deployment of compressor driven ram-air systems for essential sensors (e.g. pressure sensors)			-Evaluate if backup systems can provide enough situational awareness -In case of external pod sensor failure, use tube telemetry data -Run systems check at next terminal
	Internal and External 6-Axial Forces malfunction or failure	Pitch, yaw and roll data of the pod is compromised Situational and spatial awareness is lessened	7	-Primary power failure within pod -Faulty connections for displaying acquired data	-Changes inputs to Photo and IR sensors in order to determine spatial positions -Switches to pressure inputs to estimate forces on axes			-Reduce speed to reduce load on auxiliary sensors -Use proximity sensors to gauge pod orientation within tube
	Polarized Retro-reflective Photoelectric Sensor	Photoelectric sensor receives no data to output Proximity sensing to tube walls is compromised	9	-Retro-reflective tape has been damaged, now unreadable -Sensors have been misaligned from designed orientation to where they point	-Tube undergoes regular maintenance (daily during downtime) to check for functioning systems and damage -Sensor functionality			-Reduce speed to lower risk of collision with the tube in case of control malfunction -If photoelectric sensor is being used solely for guidance (other

						check feeds back to pod as well as control centre for multiple monitoring location			redundant systems offline), cease motion
--	--	--	--	--	--	--	--	--	--

Contingency: Power Outages

In the event of an unexpected power outage, there are contingency measures in place to counteract any problems and prevent potential damage.

For the rails, there will be a two stage energy storage system in place in which there is a main supply and backup supply. Using the solar panels placed atop the tunnel, the system will charge the backup battery first to ensure that there is always a fallback option in the event of emergency. In the event that neither system can provide power, a distress signal will be sent out to the capsule causing the system to slow down and come to a stop.

As for the capsule itself, in most general cases there will be a secondary onboard battery system which will provide enough power for the capsule to maintain both life support systems and levitation, and eventually bring the capsule down to a stop. Once the capsule has come to a stop, a rescue pod will be sent to retrieve the immobile capsule and bring it to the desired destination. To ensure that the backup system will work, it will be implemented as a single time use system that will be charged separately and will be replaced if in the event that it is required.

Process Step	Potential Failure Mode	Potential Failure Effect	SEV	Potential Causes	OCC	Current Process Controls	DET	RPN	Action Recommended
Capsule	Compressor loses power	-Crash -Catastrophic damage	10	-Insufficient power -Faulty wiring -Compressor damage	1	-Reserve power system	7	70	-Increase minimum threshold before reserve power system activates -Routine maintenance
	Navigation and control systems	-Potential crash -Ride instability	8	-Network communication error	4	-Subsystem reboot	2	64	-Periodic network checks

	malfunction								
	Pressurization system malfunction	- Depressurization - Passenger discomfort	7	-Faulty wiring -Network miscommunication	2	-Oxygen masks -Subsystem reboot	2	28	-Routine maintenance
Rails	Linear synchronous motor loses power	-Severe loss in propulsion power	5	-Insufficient power -Motor malfunction	1	-Reserve power system	5	25	-Increase minimum threshold before reserve power system activates -Routine maintenance
	Insufficient power output	-Capsule arrival delayed	4	-Faulty wiring -Insufficient power -Motor malfunction	1	-System reboot	2	8	-Routine maintenance

Energy Storage

Solar Panels:

Panels store 290MW of power. Assuming we use the same watt-to-kilogram ratio as the Tesla Roadster as seen in link below, the battery would have to weigh 2,396,695 kg. Therefore, using the known weight of a cell to be $(449.056/6831)$ kg, there would be 36,458,300 cells. Using the known dimensions of the 168A lithium-ion cell that is used, the total volume would be equal to $\pi \cdot (0.0186/2) \cdot 0.0652 \cdot (36458300) = 645.89 \sim 650 \text{ m}^3$

The capsule is estimated to require 325kW of power in order to power the onboard compressor and other various systems.

<https://my.teslamotors.com/roadster/technology/battery>

Li-ion 168A cells

18.6mm x 65.2mm \rightarrow 1 cell, diameter x length

990 lb \rightarrow 449.056 kg

6831 cells in 990lb battery \rightarrow $(449.056/6831)$ kg/cell

Pod

Batteries = 2700kg

6831 cells in 990lb battery -> (449.056/6831) kg/cell

60847.64484 -> 60848 cells

0.0186 m, r = 9.3e-3 m

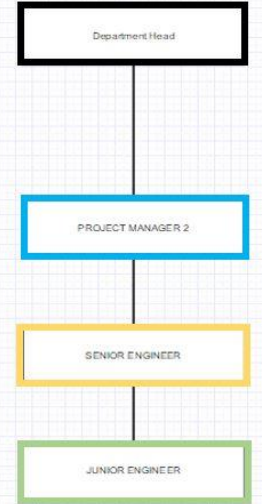
$\pi \cdot r^2 \cdot 0.0652 = 1.7716 \text{e-}5$

All cells -> 1.078 m³

8 Scalability to Operational Hyperloop

8.0 Economic Scale of Analysis

THOUSANDS OF CANADIAN DOLLAR UNLESS STATED OTHERWISE					
ECONOMICAL ANALYSIS					
SALARY	120.00	90.00	85.00	80.00	65.00
Drive Systems Engineering	1	1	1	1	3
Safety Engineering			1	1	3
Control Systems Engineering	1	1	1	1	3
Environmental	1	1	1	1	3
Development and Testing [H&S]		1	1	1	3
Information Technology	1	1	1	1	3
Communication/Infrastructure			1	1	3
					GRAND TOTAL
TOTAL EMPLOYEES	3	5	7	7	21
TOTAL SALARY PER DEPT ()	360.00	450.00	595.00	560.00	1365.00
					3330.00



		RESEARCH AND DEVELOPMENT						FUNCTIONAL TEST PHASE 1		FUNCTIONAL TEST PHASE 2		PRE-PRODUCTION
		2016	2017	2018	2019	2020	2021	2022	2023	2024	2025	
ESTIMATING \$5M/MILE TRACK +\$0.5M/MILE PHYSICAL TUBE	EMPLOYEE SALARY	3330.00	3396.60	3464.53	3533.82	3604.50	3676.59	3750.12	3825.12	3901.63		
P1-3 - THERE IS NO PASSENGERS P4-5 - THERE IS MAX OF 10 PASSENGERS	TUBE INFRASTRUCTURE				55000.00		275000.00		275000.00			
	POD PROTOTYPE BUILD COST ONLY	P1 - TEST 1		2000.00								
		P2 - TEST 2			2000.00							
		P3 - TEST 3				4000.00						
		P4 - PASSENGER					6000.00					
		P5 - PASSENGER						6000.00				
	MAINTENANCE	POD		500.00		1100.00		1600.00		2350.00		1500.00
		TRACK/TUBE		2000.00		20000.00		21000.00				24000.00
		EXPENSE TOTAL	3330.00	3396.60	5464.53	61033.82	5604.50	303776.59	32350.12	287175.12	29401.63	
	FUNDING FROM GOVT			50000.00			50000.00			10000.00		
	FUNDING FROM PRIVATE SECTOR		2000.00	10000.00	10000.00	30000.00	80000.00	50000.00	51000.00	300000.00	150000.00	
		FUNDING TOTAL	2000.00	10000.00	60000.00	30000.00	80000.00	100000.00	51000.00	310000.00	150000.00	
	PROFIT	-1330.00	6603.40	54535.47	-31033.82	74395.50	-203776.59	18649.88	22824.88	120598.37		

8.1 System Size

8.2 Cost

8.3 Estimated Mass of Full-Scale Model

8.4 Maintenance

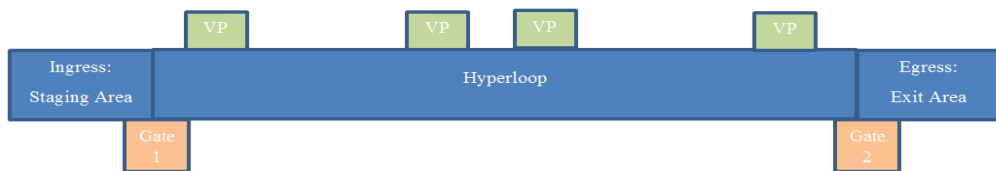
8.5 Pod Design

9 Additional Information for Intent to Build

11.0 Loading & Unloading Logistics

The Trip

As per Revision 2.0 of “SpaceX Hyperloop Pod Competition Rules and Requirements,” SpaceX proposes the following “Functional Diagram of the Test Track”:



McMaster Hyperloop has no major changes or modifications to that of the above proposed diagram. The text sections below outline the specifics of the entire Loading and Unloading Plan as per our vision and suggestions to the current proposed plan outlined by SpaceX.

Functional Tests

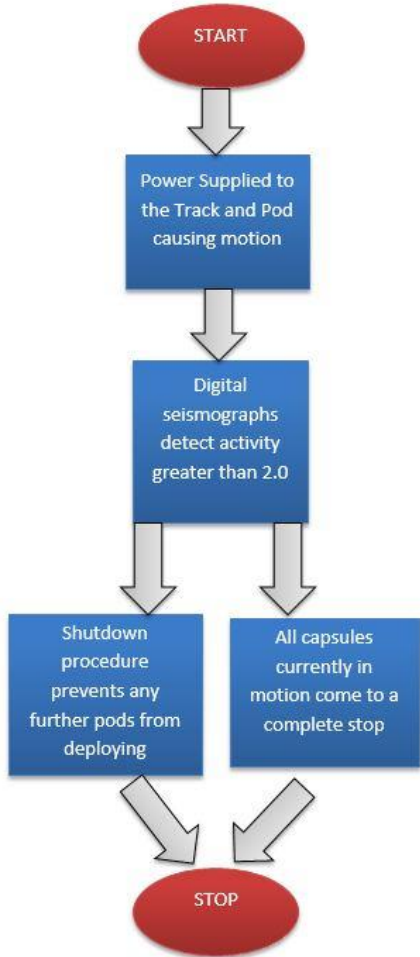
Similar to space shuttle launches, The Hyperloop requires ideal conditions in order to perform a nominal transport experience for its passengers. Unlike space shuttle launches (to our advantage), the conditions for Hyperloop can be created versus waiting for the correct conditions to occur based on predicable methods of the environment. In order to ensure said ideal conditions, McMaster Hyperloop proposes the following system classifications and their associated Functional Tests:

*Note Functional Tests are going to be described in the form of logical flow of statements outlining the process that the various LRUs and sensors encounter.

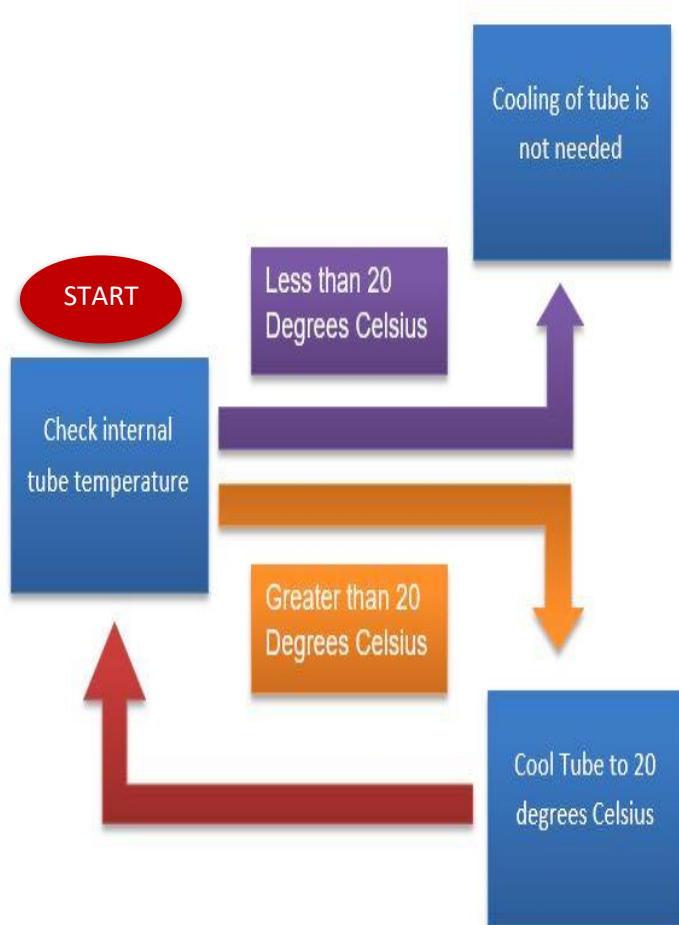
Tube Systems External

Internal Environmental Forecasting System Logic for Functional Testing

Earth Quakes

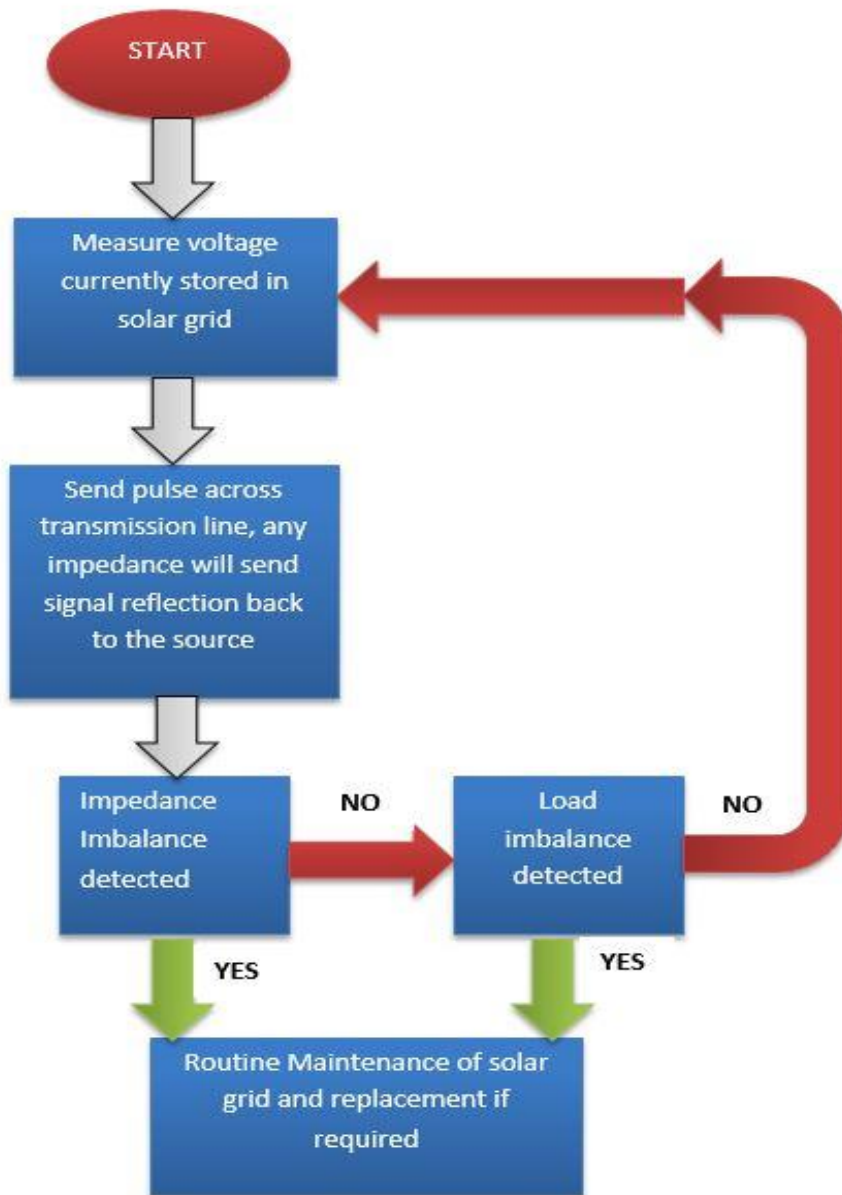


Temperature





Internal Solar Power System Logic for Functional Testing



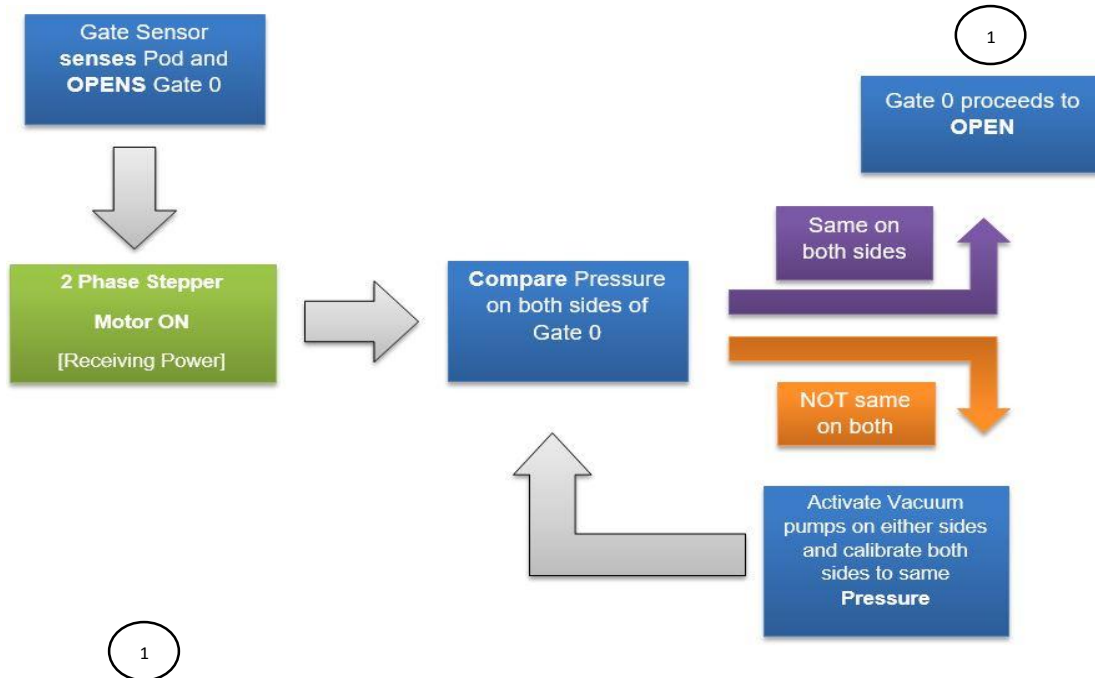
Signal Verification

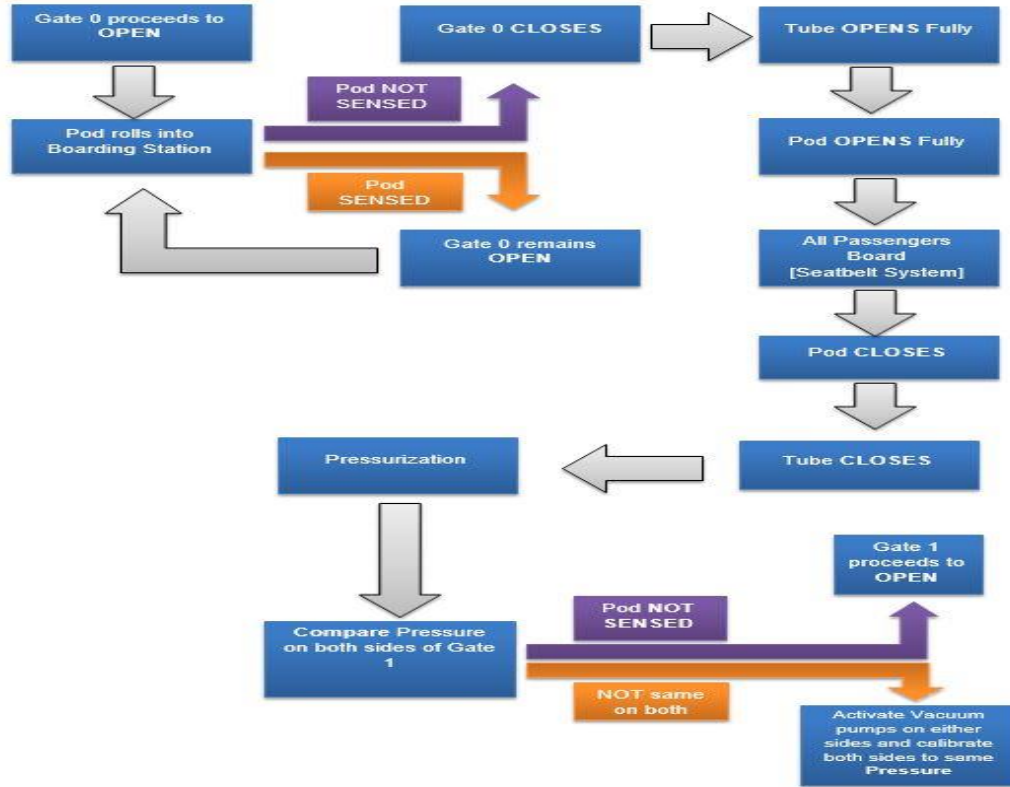
* See Pod Systems Internal

Tube Systems Internal

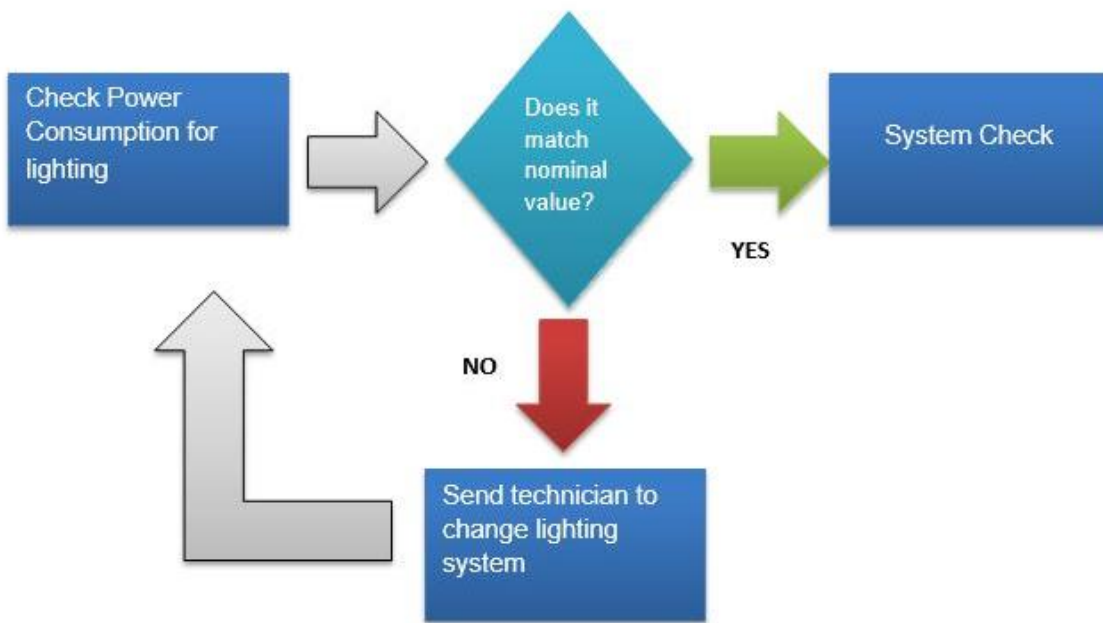
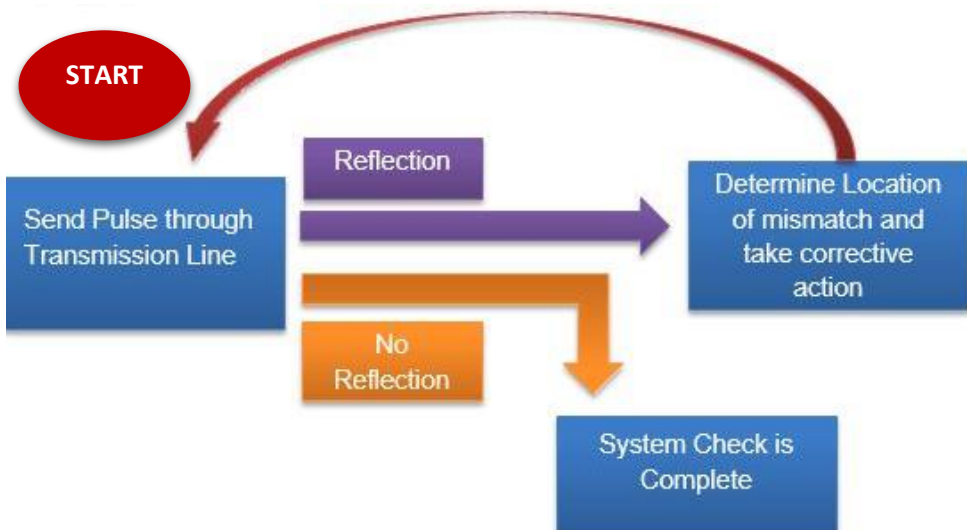
Environment

Internal Gate Logic for Functional Testing

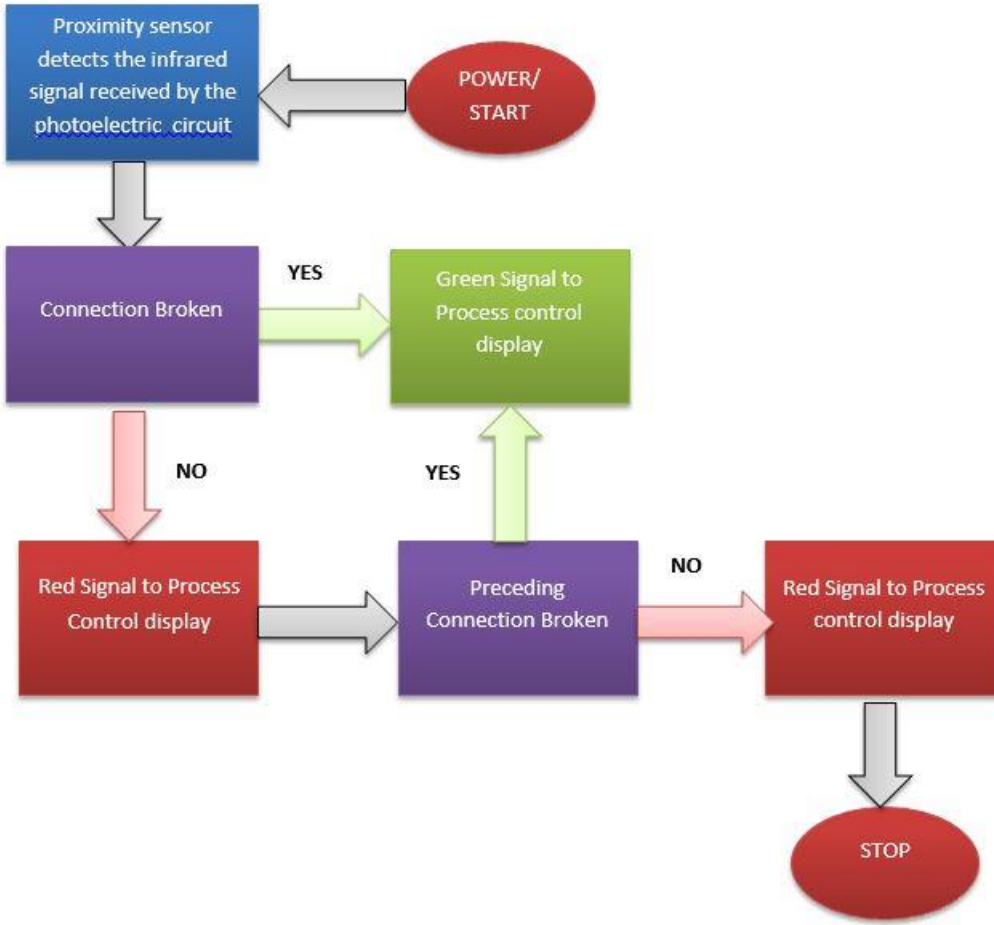




Internal Tube Lighting System Logic for Functional Testing



Internal Pod Sensing Logic for Functional Testing

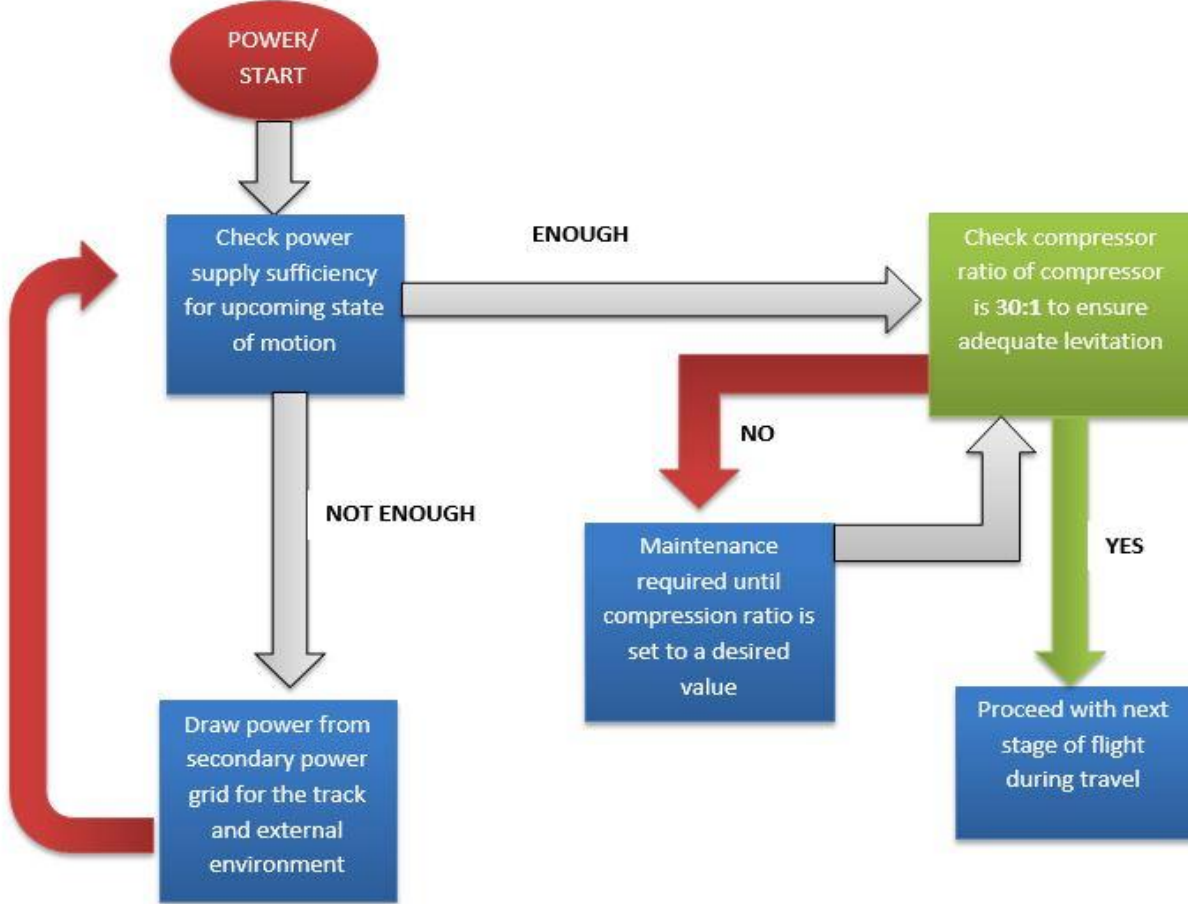


Signal Verification

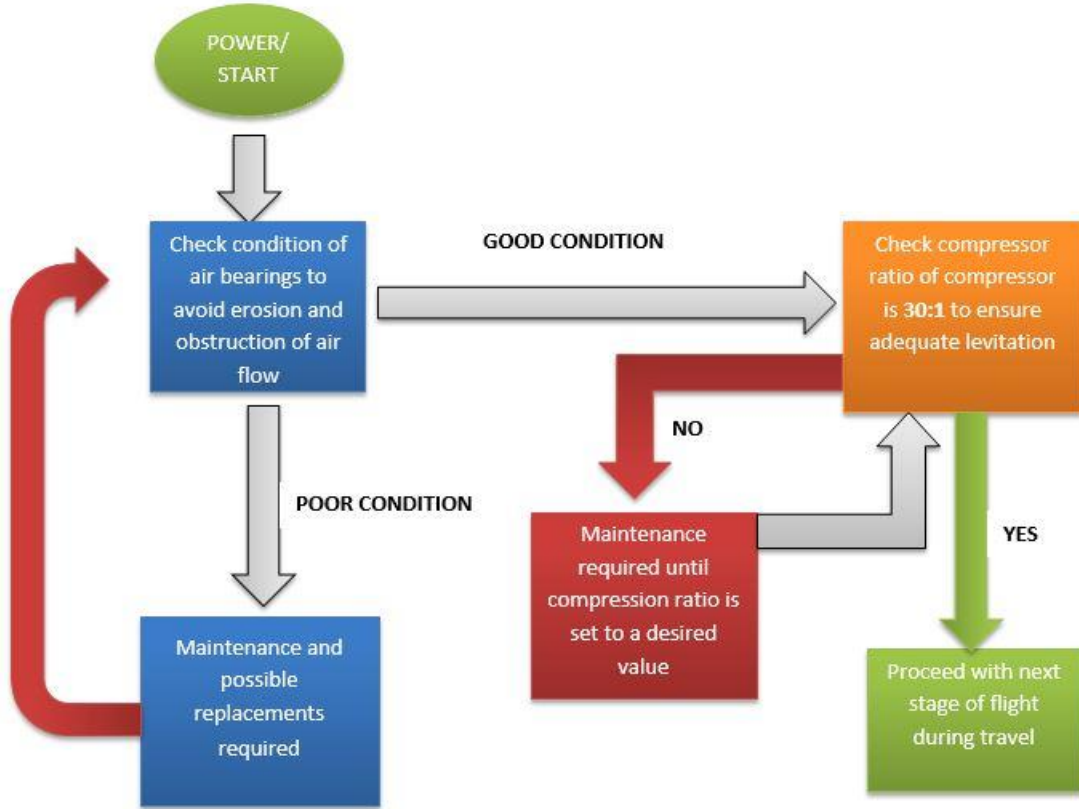
* See Pod Systems Internal

Pod Systems External

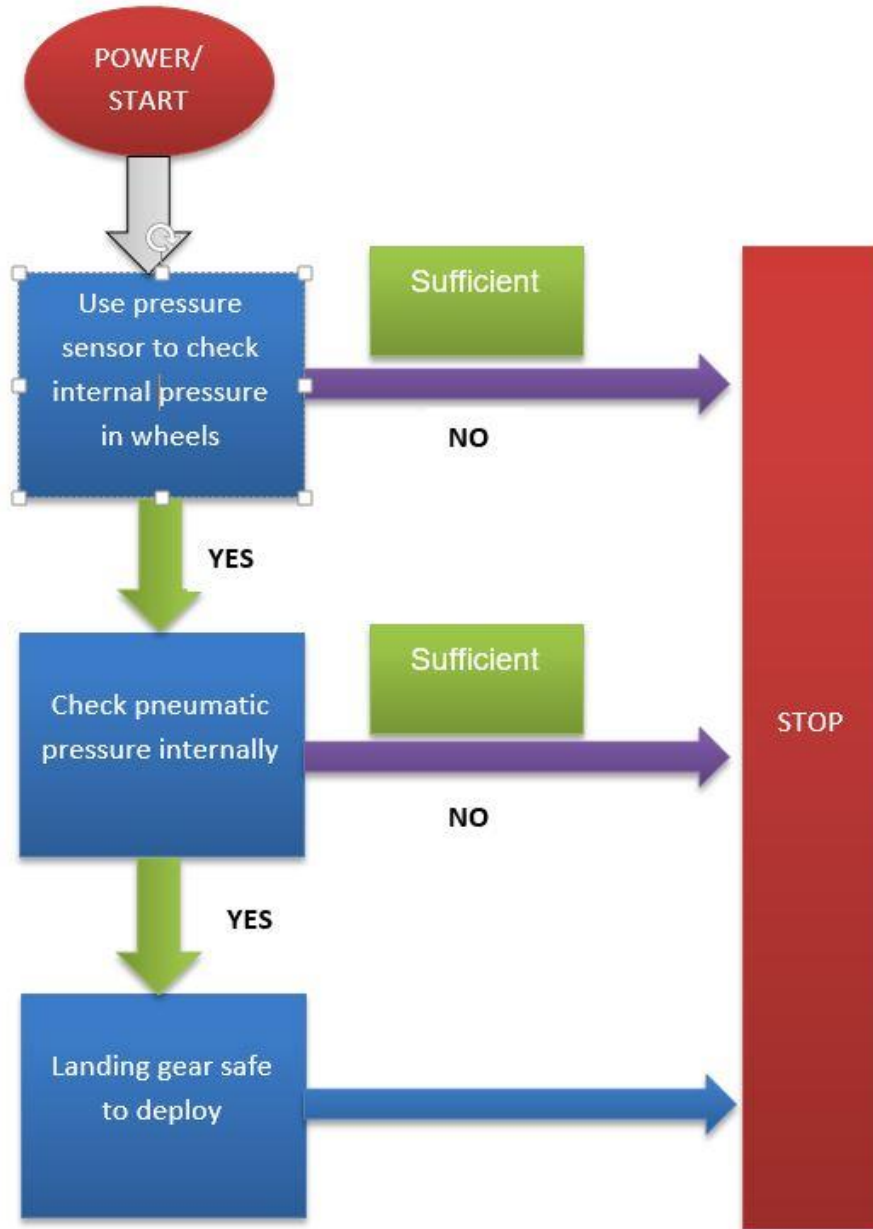
Internal Propulsion Logic for Functional Testing



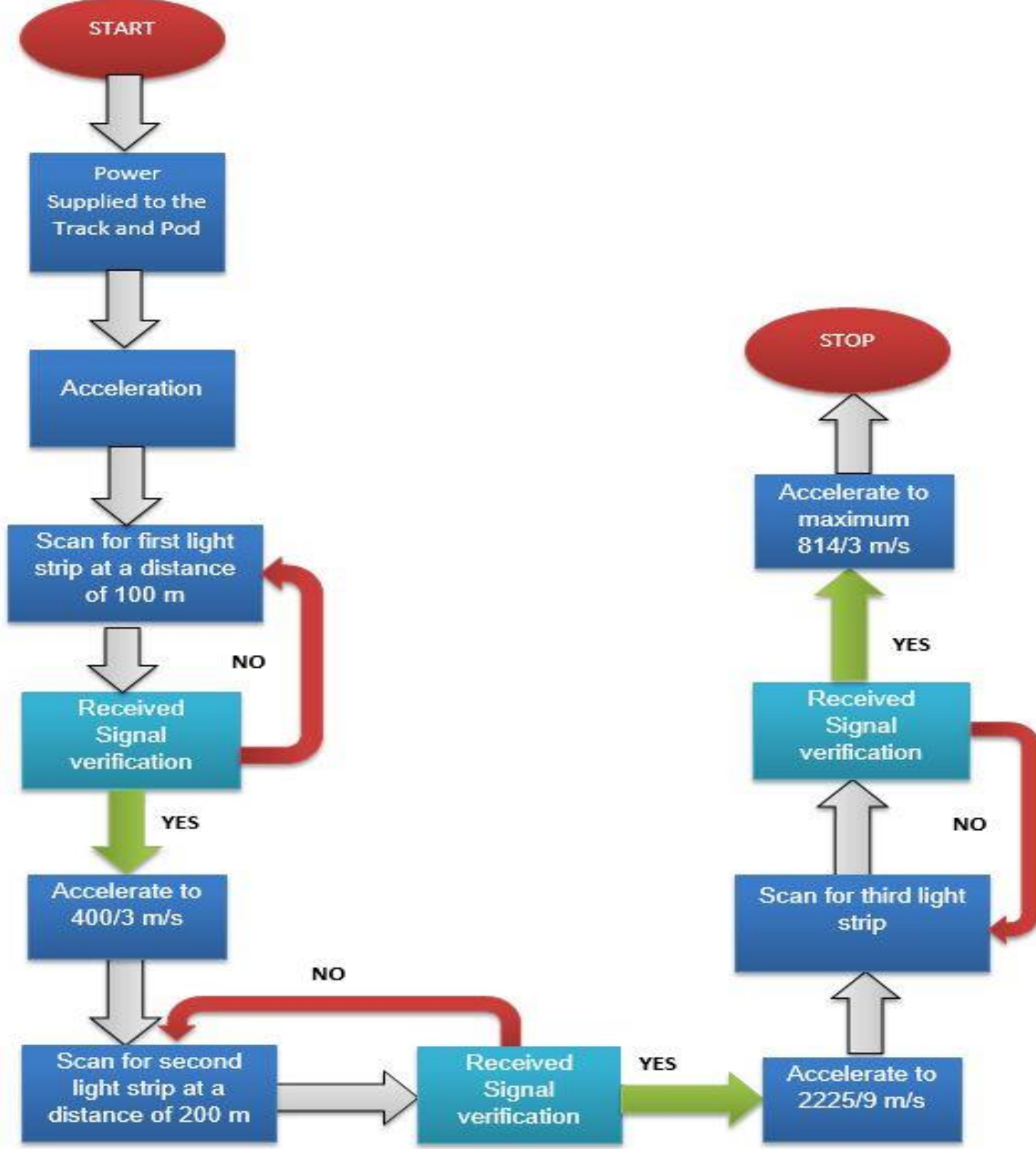
Internal Levitation Logic for Functional Testing



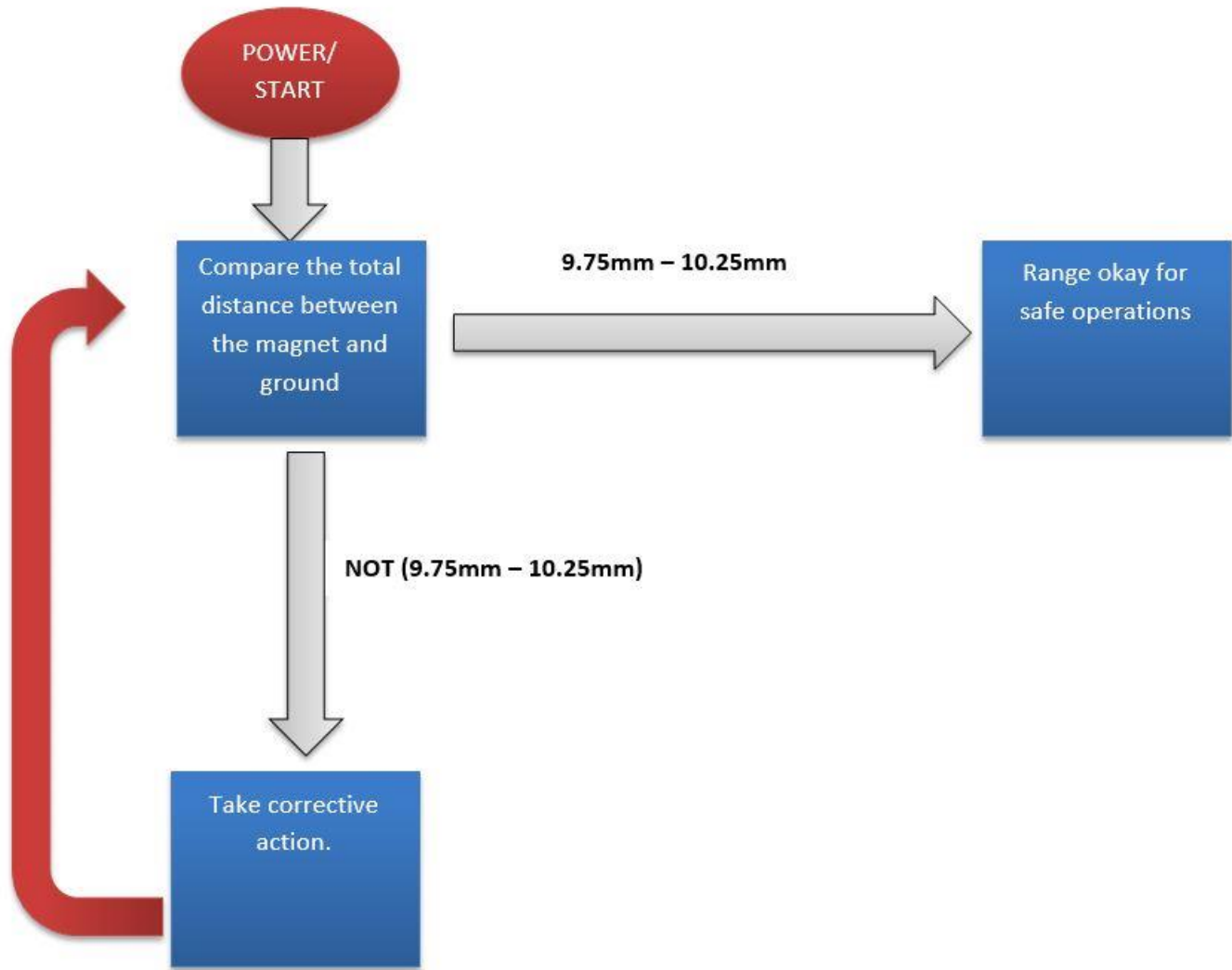
Internal Braking Logic for Functional Testing



Internal Navigation Logic for Functional Testing



Internal Dynamic Control Logic for Functional Testing



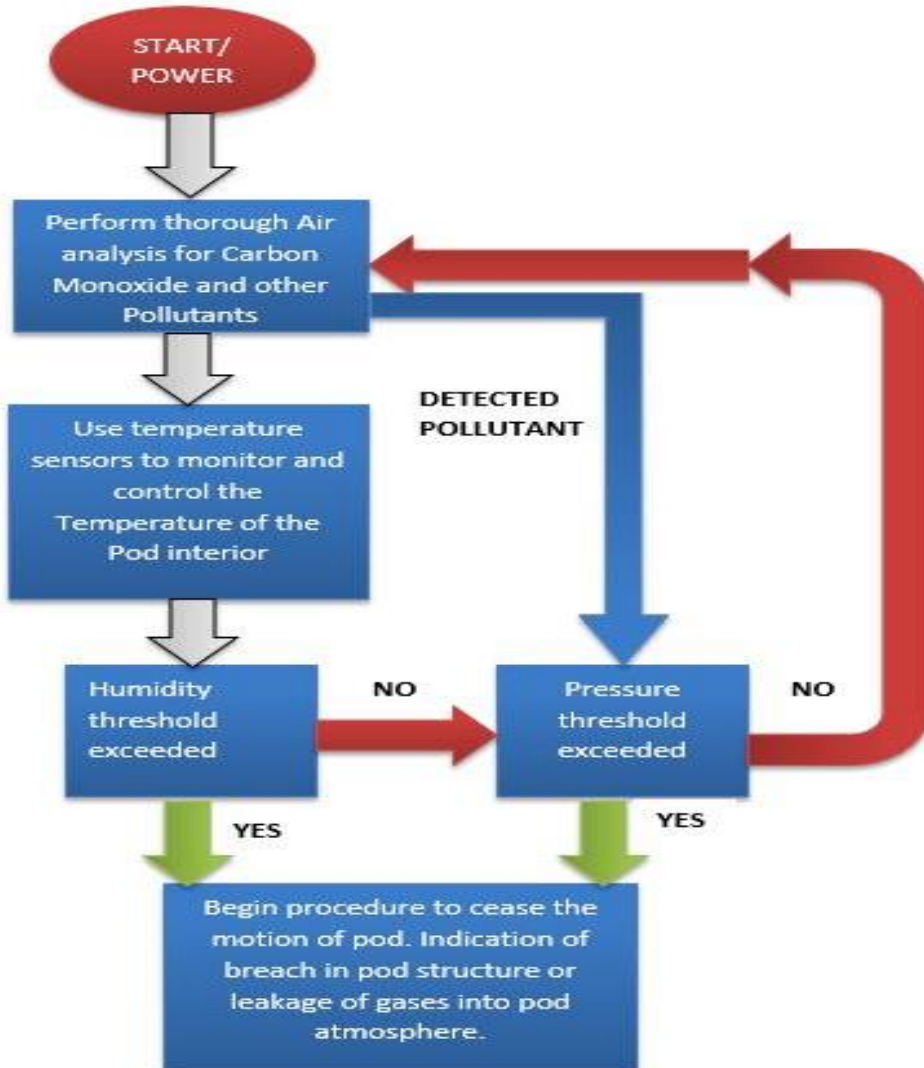
Signal Verification

* See Pod Systems Internal



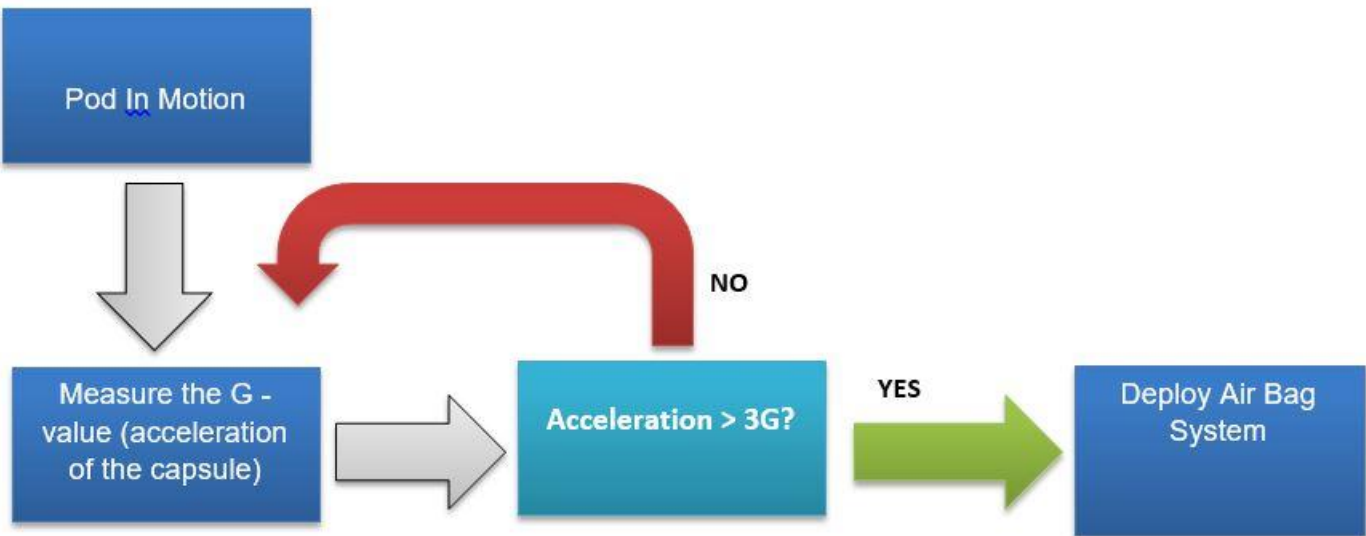
Pod Systems Internal

Environmental

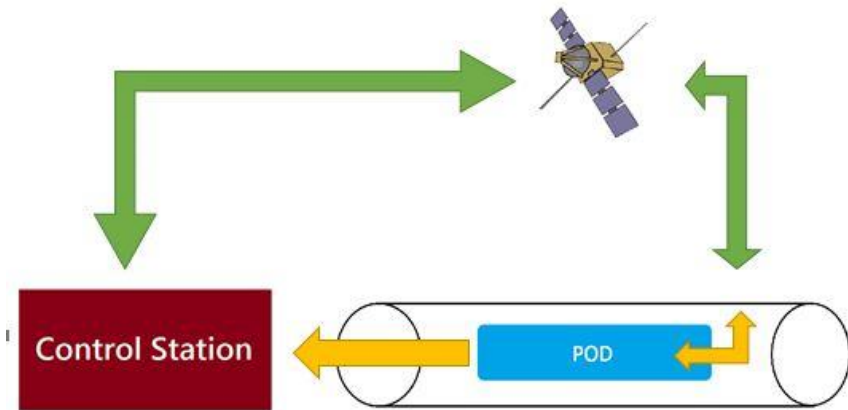


Seats

G-Force



Signal Verification



The above diagram outlines signal verification communication between all 4 recognized system groups. [Tube (Internal, External), Pod (Internal, External)]

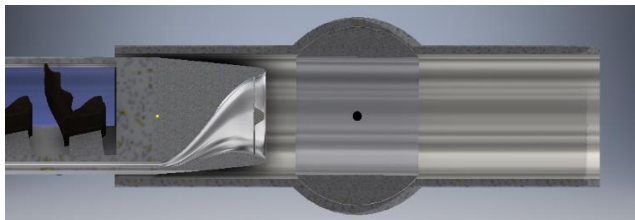
Phase I: Ingress; Staging Area

The Garage

This serves the same purpose as “hangar” for an airplane. It is the area in which multiple pods are stored and gets when not in transport mode. The internal pressure of The Garage is the same as the pressure external to the pod. This allows for Engineers and Technicians to easily access and service the Pod. Below is a visualization of the hangar and also how the Pod is proposed to move from The Garage to the Board Station.

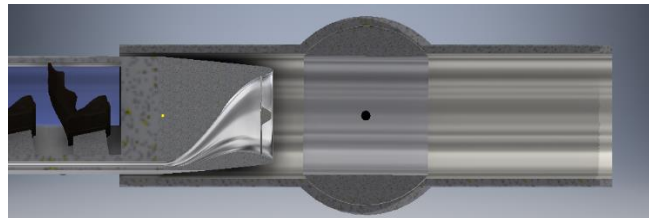
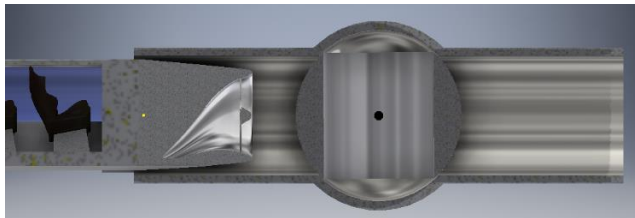
Gate 0 [Open]

Gate 0 serves the purpose of separating The Garage from Boarding Station. The purpose of Gates (as described earlier in “*Tube Systems Internal*”) is the same throughout the entire track; to ensure equal pressure on each side of the tube. Initially the pressure between Gate 1 and Board Station appear to be the same, however and as will be seen in further detail in “Pressurization”, once the passengers board the Pod, the tube closes and begins to pressurize down to Hyperloop conditions.



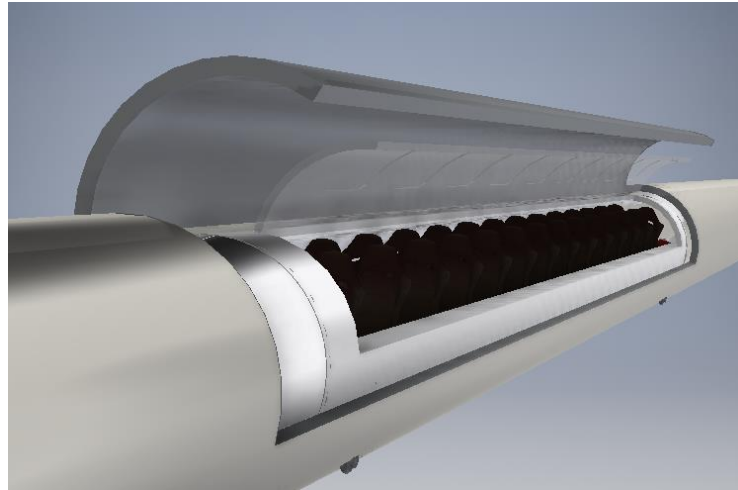
Gate 0 [Closed]

Once all Pre-Board Hyperloop Checklist criteria is met, the Pod rolls out into the Board Station in order to receive its passengers for the journey. Upon the Pod coming to a full stop, this signals that the Pod is fully in the Board station, Gate 0 proceeds to close in order to allow for the boarding of passengers to commence.



Board Station

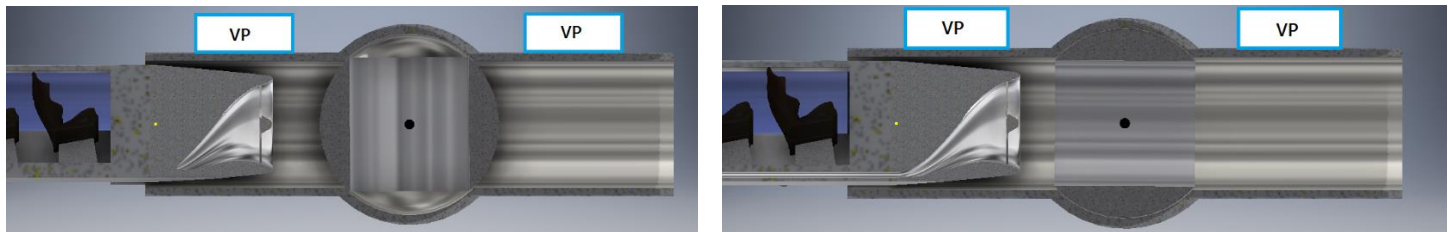
Upon the closing of Gate 0, the Pod doors begin to open. It needs to be mentioned that at this time the Tube itself is already opened prior to the Pod rolling in (similar to waiting underground for a subway to arrive). Once the Pod doors are fully opened, the passengers are given the go ahead to proceed to board the Pod. Upon the seating and strapping in of all passengers, the Pod doors proceed to close.



The full closing of the Pod doors now signals the Tube to start closing as well. Once the tube is fully closed both Pod and Tube enter the Pressurization phase of Pre-Hyperloop Checklist.

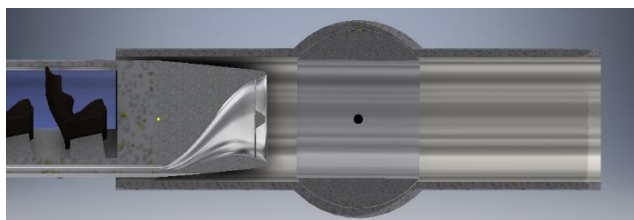
Pressurization

The beginning of creating Hyperloop conditions truly begins at this final phase of the Pre-Hyperloop Checklist. The tube (via Vacuum Pump) begins to drop in pressure until the pressure on either side of Gate 1 are equal. It is crucial that the pressure on both sides are equal. When Gate 1 turns, it slowly introduces the opening which the Pod goes through, since the pressure is already equal, the Pod can move in the conditions same to that of Hyperloop.



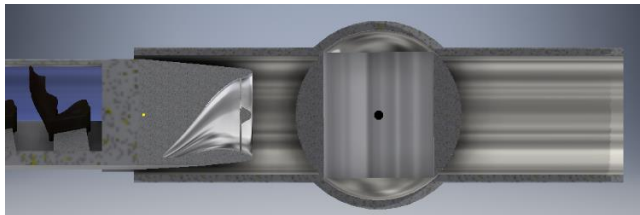
Gate 1 [Open]

Once there is equal pressure on both sides of Gate 1 [between Boarding Station & Hyperloop], this now signals Gate 1 to open in order to allow the Pod to roll out into the Hyperloop portion of the Tube.



Gate 1 [Closed]

The Pod rolls out until completely passed Gate 1. Once the Pod is completely passed Gate 1, Gate1 proceeds to close and the internal Ready to Launch Check List commences.



Ready to Launch Check List

As per outlined above, all Functional Tests must be passed in order for the Pod to commit to launch. To re-cap the list of test, the following check list is providing.

- Environmental Forecasting
- Solar Power
- Structural Stability
- Signal Verification

Tube Systems Internal

- Environment
- Gates
- Lighting
- 2 - Way Communications
- Signal Verification

Pod Systems External

- Propulsion
- Levitation
- Braking
- Navigation
- Vibrations
- Gyrometer
- 2 - Way Communications
- Dynamic Control
- Signal Verification

Pod Systems Internal

- Environment [Air Analysis, Temp, Pressure, Humidity]
- Seats
- G-Force
- 2 - Way Communications
- Signal Verification

Ready to Remove Check List

Whenever the Pod comes to a complete stop, the following criteria must be met from an internal logic stand point and should be physically seen from the movement of the pod. Complete stops are seen in the following areas of The Trip and can be considered removals in their own way or form (removal of pod from one section to another, removal of passengers or removal of pod from garage):

Garage to Gate 0

Gate 0 to Gate 1

Gate 1 to Hyperloop

Hyperloop to Gate 2

Gate 2 to Gate 3

Gate 3 to Garage

Additional: Removal of Pod from Garage

11.1 Stored Pod Energy

Batteries: the on board batteries will be providing power to the all electrical devices on the pod. This includes but may not restrict: compressor, motors running compressor, low powered electronics, any sort of user interface, cooling/heating system, and a pressure system to maintain on board pressure. The pod will be holding

Pressurized Tanks: Since, this mode of transportation is in an isolated environment there is need to mimic outside environment, for example, air tanks and water tanks are stored to provide circulated cooled air to passengers.

11.2 List of Hazardous Materials

Hazardous Material	Hazardous Class
Lithium-ion Cells	Explosive, Flammable solid
Ultracapacitors	Explosive, Flammable Solid
Electronic devices	Explosive
Oxygen Tanks	Compressed gas (Flammable gas)
Coolant fluids	Combustible Liquid, Flammable Liquid
Airbags	-
Grease (motor oil, lubricant)	Flammable Liquid
Adhesives	Poison

11.3 Preliminary Bill of Materials

Material	Cost (Dollars)
168A Lithium Ion Cell Batteries	145,500
Aluminum 6061 T6	270000
Lexan Polycarbonate	1036

[1] http://www.greencarreports.com/news/1084682_what-goes-into-a-tesla-model-s-battery--and-what-it-may-cost

These are the costs of the materials that are known and were retrieved publicly with no consultation from private companies. The pod requires extensive customization with the components of the pod.

<https://www.infosys.com/engineering-services/white-papers/Documents/carbon-composites-cost-effective.pdf>

11.4 Safety Features

Risk	Mitigation of Risk
Preventing Complete Power Loss Pod	Back up Power on Board
Pod robustness to a tube breach resulting in rapid pressurization	Stop the Pod
Single point of failures within the Pod	Refer to function test of Internal pod system and further cross reference with FEMA Analysis
Recovery plan if Pod becomes immovable within tube	Start Back up generators, reduce power consumption to increase time required to come up with solution
Implementation of the Pod-Stop command	Override Command on board to implement braking

11.5 Component & System Test Program

SpaceX outlines that

11.6 Vacuum Compatibility Analysis

Vacuum Analysis

When analyzing a vacuum, it is important to take into consideration the outgassing constant of each of the materials that will be in contact with the vacuum system. As it can be seen the following materials are reasonable to be used in the vacuum system, since these were approved by LIGO (Laser Interferometer Gravitation Wave Observatory).

<https://dcc.ligo.org/public/0003/E960050/013/E960050-v13%20Vacuum%20Compatible%20Materials%20List.pdf>

Material	Outgassing Constant (Torr L/ sec cm ²)
Aluminum	1.6×10^{-10}
Lexan Polycarbonate	1×10^{-7}
Stainless Steel	1.1×10^{-8}

http://vacuumcursus.nl/casussen/Vacuum_Systems_UHV.pdf (for lexan)

http://home.fnal.gov/~mlwong/outgas_rev.htm (for the rest)



10 Contact Information

11 Faculty Sponsors

12 Appendices

A) Sources

2.1.2 Materials

- [1] Nacelle manufacturers optimize hand layup and consider closed molding methods : CompositesWorld. (n.d.). Retrieved January 20, 2016, from <http://www.compositesworld.com/articles/nacelle-manufacturers-optimize-hand-layup-and-consider-closed-molding-methods>
- [2] (n.d.). Retrieved January 20, 2016, from <http://www.vacuumlab.com/articles/vaclab36.pdf>
- [3] LIGO Document E960050-v13. (n.d.). Retrieved January 20, 2016, from <https://dcc.ligo.org/E960050/public>
- [4] CiteSeerX — Document Not Found. (n.d.). Retrieved January 20, 2016, from <http://citeseerx.ist.psu.edu/viewdoc/download?doi=10.1.1.470.107&rep=rep1&type=pdf>
- [5] Comparison of carbon fiber vs steel manufacturing costs. (n.d.). Retrieved January 20, 2016, from http://www.rmi.org/RFGraph-carbonfiber_vs_steel_manufacturing
- [6] Nacelle manufacturers optimize hand layup and consider closed molding methods : CompositesWorld. (n.d.). Retrieved January 20, 2016, from <http://www.compositesworld.com/articles/nacelle-manufacturers-optimize-hand-layup-and-consider-closed-molding-methods>
- [7] (n.d.). Retrieved January 20, 2016, from <http://www.certainteed.com/resources/30-29-120.pdf>
- [8] LEXAN™ Solid Sheet. (n.d.). Retrieved January 20, 2016, from <http://sfs.sabic.eu/product/lexan-solid-sheet/>
- [9] Gases - Specific Heats and Individual Gas Constants. (n.d.). Retrieved January 20, 2016, from http://www.engineeringtoolbox.com/specific-heat-capacity-gases-d_159.html
- [10] (n.d.). Retrieved January 20, 2016, from http://www.chem.zju.edu.cn/~lihaoran/kejian/5_60_l06_s05.pdf

2.1.3 Aerodynamic Coefficients

- [1] "SpaceX Hyperloop Test-Track Specification", Space Exploration Technologies Corp., Hawthorne, CA, Tech. Revision 4.0, Jan. 8, 2016

- [2] *Drag Coefficient - The Engineering ToolBox* [Online]. Available: http://www.engineeringtoolbox.com/drag-coefficient-d_627.html
- [3] E.W. Perkins *et al.*, "Investigation of the Drag of Various Axially Symmetric Nose Shapes of Fineness Ratio 3 for Mach Numbers From 1.24 to 7.4", NACA, Moffett Field, CA, Report 1386, Jan. 01, 1958
- [4] *Drag of Cylinders & Cones* [Online]. Available: <http://www.aerospaceweb.org/question/aerodynamics/q0231.shtml>
- [5] C.E. Jobe, "Prediction of Aerodynamic Drag", Flight Dyn. Lab., Air Force Wright Aeronautical Labs., Wright-Patterson AFB, OH, AFWAL-TM-84-203 Jul. 1984
- [6] A. Kantrowitz. and C. Donaldson, "Preliminary Investigation of Supersonic Diffusers", Langley Memorial Aeronautical Laboratory, Langley Field, VA, ACR L5D20, May 1945
- [7] J.C. Chin *et al*, "Open-Source conceptual Sizing models for the Hyperloop Passenger Pod", NASA Glenn Research Center, Cleveland, OH, AIAA 2015-1587, Jan. 2015
- [8] *Air - Specific Heat at Constant Temperature and Various Pressures - The Engineering ToolBox* [Online]. Available: http://www.engineeringtoolbox.com/air-specific-heat-various-pressures-d_1535.html
- [9] *Flow types caused by viscous effects* [Online]. Available: <http://aerostudents.com/files/aerodynamicsA/viscousEffects.pdf>
- [10] *General Thrust Equation* [Online]. Available: <https://www.grc.nasa.gov/www/k-12/airplane/thrsteq.html>

2.1.4 Power Source & Consumptions

- [1] (n.d.). Retrieved January 20, 2016, from http://www.spacex.com/sites/spacex/files/hyperloop_alpha.pdf
- [2] (n.d.). Retrieved January 20, 2016, from http://web.archive.org/web/20130603055918/http://www.panasonic.com/industrial/includes/pdf/Panasonic_LiIon_CGR18650DA.pdf
- [3] Battery. (2011, January 26). Retrieved January 20, 2016, from <https://my.teslamotors.com/roadster/technology/battery>
- [4] [\(n.d.\). Retrieved January 20, 2016, from http://www.spacex.com/sites/spacex/files/hyperloop_alpha.pdf](http://www.spacex.com/sites/spacex/files/hyperloop_alpha.pdf)

2.1.5 Thermal Profile

[1] Gases - Specific Heats and Individual Gas Constants. (n.d.). Retrieved January 20, 2016, from http://www.engineeringtoolbox.com/specific-heat-capacity-gases-d_159.html

[2] (n.d.). Retrieved January 20, 2016, from http://www.chem.zju.edu.cn/~lihaoran/kejian/5_60_l06_s05.pdf

2.2.0 Propulsion

[1] (n.d.). Retrieved January 20, 2016, from <http://jfgieras.com/lsm-chapter 1.pdf>

[2] Linear Motor Basics. (n.d.). Retrieved January 20, 2016, from <http://www.productionmachining.com/articles/linear-motor-basics>

2.2.1 Braking

IMAGE 1& 2:

Cătălin Cruceanu (2012). Train Braking, Reliability and Safety in Railway, Dr. Xavier Perpinia (Ed.), ISBN: 978-953-51-0451-3, InTech, Available from: <http://www.intechopen.com/books/reliability-and-safety-inrailway/braking-systems-for-railway-vehicles>

[1] rail temperature rise characteristics caused by linear eddy current brake of high-speed

2.2.2 Levitation

[1] <http://www3.epa.gov/gasstar/documents/installelectriccompressors.pdf>

[2] Compressors/drivers | IPIECA. (n.d.). Retrieved January 20, 2016, from <http://www.ipieca.org/energyefficiency/solutions/60291>

[3] <https://www.netl.doe.gov/File%20Library/Research/Coal/energy%20systems/turbines/handbook/2-0.pdf>

[4] http://www.nrcan.gc.ca/sites/oee.nrcan.gc.ca/files/pdf/commercial/password/downloads/EMS_14_compressors_and_turbines.pdf

2.2.3 Navigation

[1] IR-Photo Diode Sensor. (2013). Retrieved January 20, 2016, from <https://forelectronics.wordpress.com/2013/05/17/ir-photo-diode-sensor/>

[2] PRK 53/6.22,5000 - Polarized retro-reflective photoelectric sensor. (n.d.). Retrieved January 20, 2016, from http://www.leuze.com/en/deutschland/produkte/schaltende_sensoren/optische_sensoren/lichtschrangen_lichttaster_kubisch/baureihe_53/reflexions_lichtschrangen_30/prk_1_53_4/selector.php?supplier_aid=50121898

B) MATLab Code

2.1.5 Thermal Profile

```
% Thermal Profile (Modified from Velocity Time Graph by Hossein Rejali)
```

```
%Name: Andy Chu
```

```
a=4.9
Vf=0;
%.....Accelerate to 400/3 (m/s).....
t=0:0.1:27.21;
v=a.*t+Vf
Vf=400/3;
t_f=27.21

T_P = 293*(1+((0.00118)*v.^2)/200).^0.2891;

%plot(t,v,'b')
plot(t,T_P,'r')
hold on
%.....Constant at 400/3 (m/s).....
t=t_f:0.1:(t_f+148.40);
v=linspace(400/3,400/3,length(t))
t_f=t_f+148.40;
v_f=400/3;

T_P = 293*(1+((0.00118)*v.^2)/200).^0.2891;

%plot(t,v,'b')
plot(t,T_P,'r')
hold on;
%.....Accelerate to 2225/9 (m/s).....
t=0:0.1:23.24;
v=a.*t+Vf;
t=t+t_f;
Vf=2225/9;
```

```
t_f=t_f+23.24;
```

```
T_P = 293*(1+((0.00118)*v.^2)/200).^0.2891;
```

```
%plot(t,v,'b')
plot(t,T_P,'r')
hold on
%.....Constant at 2225/9 (m/s).....
t=t_f:0.1:(t_f+242.61);
v=linspace(2225/9,2225/9,length(t));
t_f=t_f+242.61;
v_f=2225/9
```

```
T_P = 293*(1+((0.00118)*v.^2)/200).^0.2891;
```

```
%plot(t,v,'b')
plot(t,T_P,'r')
hold on;
%.....Accelerate to 814/3 (m/s).....
t=0:0.1:4.9;
v=(a).*t+Vf;
t=t+t_f;
Vf=814/3;
t_f=t_f+4.9;
```

```
T_P = 293*(1+((0.00118)*v.^2)/200).^0.2891;
```

```
%plot(t,v,'b')
plot(t,T_P,'r')
hold on
%.....Constant at 814/3 (m/s).....
t=t_f:0.1:(t_f+1340.5);
v=linspace(814/3,814/3,length(t));
t_f=t_f+1340.5;
v_f=814/3;
T_P = 293*(1+((0.00118)*v.^2)/200).^0.2891;
%plot(t,v,'b')
plot(t,T_P,'r')
hold on;
%.....Decelerate to 2225/9 (m/s).....
t=0:0.1:4.9;
v=-(a).*t+Vf;
t=t+t_f;
Vf=2225/9;
t_f=t_f+4.9;
```

$$T_P = 293 * (1 + ((0.00118) * v.^2) / 200).^0.2891;$$

```
%plot(t,v,'b')
plot(t,T_P,'r')
hold on
%.....Constant at 2225/9 (m/s).....
t=t_f:0.1:(t_f+450.59);
v=linspace(2225/9,2225/9,length(t));
t_f=t_f+450.59;
v_f=2225/9
T_P = 293 * (1 + ((0.00118) * v.^2) / 200).^0.2891;

%plot(t,v,'b')
plot(t,T_P,'r')
hold on
%.....Decelerate to 400/3 (m/s).....
t=0:0.1:23.24;
v=-a.*t+Vf;
t=t+t_f;
Vf=400/3;
t_f=t_f+23.24;

T_P = 293 * (1 + ((0.00118) * v.^2) / 200).^0.2891;

%plot(t,v,'b')
plot(t,T_P,'r')
hold on
%.....Constant at 400/3 (m/s).....
t=t_f:0.1:(t_f+100.67);
v=linspace(400/3,400/3,length(t));
t_f=t_f+100.67;
v_f=400/3

T_P = 293 * (1 + ((0.00118) * v.^2) / 200).^0.2891;

%plot(t,v,'b')
plot(t,T_P,'r')
hold on
%.....Decelerate to 400/3 (m/s).....
t=0:0.1:27.21;
v=-a.*t+Vf;
t=t+t_f;
Vf=0;
t_f=t_f+27.21;
```

$$T_P = 293 * (1 + ((0.00118) * v.^2) / 200).^0.2891;$$

```
%plot(t,v,'b')
plot(t,T_P,'r')
hold on
%.....
grid on;
xlabel('Duration of Trip (s)')
%ylabel('Velocity (m/s)')
ylabel('Temperature (K)')
%title('Velocity Profile')
title('Thermal Profile')
xlim([0 2550])
```

Velocity Profile

% Velocity Time Graph

%Name:Hossein Rejali

```

a=4.9
Vf=0;
%.....Accelerate to 400/3 (m/s).....
t=0:0.1:27.21;
v=a.*t+Vf
Vf=400/3;
t_f=27.21
plot(t,v,'b')
hold on
%.....Constant at 400/3 (m/s).....
t=t_f:0.1:(t_f+148.40);
v=linspace(400/3,400/3,length(t))
t_f=t_f+148.40;
v_f=400/3;
plot(t,v,'b')
hold on;
%.....Accelerate to 2225/9 (m/s).....
t=0:0.1:23.24;
v=a.*t+Vf;
t=t+t_f;
Vf=2225/9;
t_f=t_f+23.24;
plot(t,v,'b')
hold on
%.....Constant at 2225/9 (m/s).....
t=t_f:0.1:(t_f+242.61);
v=linspace(2225/9,2225/9,length(t));
t_f=t_f+242.61;
v_f=2225/9
plot(t,v,'b')
hold on;
%.....Accelerate to 814/3 (m/s).....
t=0:0.1:4.9;
v=(a).*t+Vf;
t=t+t_f;
Vf=814/3;
t_f=t_f+4.9;
plot(t,v,'b')
hold on

%.....Constant at 814/3 (m/s).....

```

```
t=t_f:0.1:(t_f+1340.5);
v=linspace(814/3,814/3,length(t));
t_f=t_f+1340.5;
v_f=814/3;
plot(t,v,'b')
hold on;
%.....Decelerate to 2225/9 (m/s).....
t=0:0.1:4.9;
v=-a.*t+Vf;
t=t+t_f;
Vf=2225/9;
t_f=t_f+4.9;
plot(t,v,'b')
hold on
%.....Constant at 2225/9 (m/s).....
t=t_f:0.1:(t_f+450.59);
v=linspace(2225/9,2225/9,length(t));
t_f=t_f+450.59;
v_f=2225/9
plot(t,v,'b')
hold on
%.....Decelerate to 400/3 (m/s).....
t=0:0.1:23.24;
v=-a.*t+Vf;
t=t+t_f;
Vf=400/3;
t_f=t_f+23.24;
plot(t,v,'b')
hold on
%.....Constant at 400/3 (m/s).....
t=t_f:0.1:(t_f+100.67);
v=linspace(400/3,400/3,length(t));
t_f=t_f+100.67;
v_f=400/3
plot(t,v,'b')
hold on
%.....Decelerate to 400/3 (m/s).....
t=0:0.1:27.21;
v=-a.*t+Vf;
t=t+t_f;
Vf=0;
t_f=t_f+27.21;
plot(t,v,'b')
hold on
%
```

```
grid on;  
xlabel('Duration of Trip (s)')  
ylabel('Velocity (m/s)')  
title('Velocity Profile')  
xlim([0 2550])
```

Acceleration Profile

% Acceleration Time Graph

%Name:Hossein Rejali

```
a=linspace(0,0,23943);
t_t=linspace(0,0,23943);
Vf=0;
i=1;
```

%.....Accelerate to 400/3 (m/s).....

```
for t=0:0.1:27.2
    t_t(i)=t;
    a(i)=4.9;
    i=i+1;
end
t_t(1)=0;
t_f=27.2+0.1;
```

%.....Constant at 400/3 (m/s).....

```
for t=t_f:0.1:t_f+148.4
    t_t(i)=t;
    a(i)=0;
    i=i+1;
end
t_f=t_f+148.4+0.1;
```

%.....Accelerate to 2225/9 (m/s).....

```
for t=t_f:0.1:(23.2+t_f)
    t_t(i)=t;
    a(i)=4.9;
    i=i+1;
end
t_f=t_f+23.24+0.1;
```

%.....Constant at 2225/9 (m/s).....

```
for t=t_f:0.1:(t_f+242.61);
    t_t(i)=t;
    a(i)=0;
    i=i+1;
```

```

end
t_f=t_f+242.61+0.1;

%.....Accelerate to 814/3 (m/s).....
for t=t_f:0.1:(4.9+t_f);
    t_t(i)=t;
    a(i)=4.9;
    i=i+1;
end
t_f=t_f+4.9+0.1;
%.....constant at 814/3 (m/s).....
for t=t_f:0.1:(1340.5+t_f);
    t_t(i)=t;
    a(i)=0;
    i=i+1;
end
t_f=t_f+1340.5+0.1;
%.....Decelerate to 2225/3.....
for t=t_f:0.1:(4.9+t_f)
    t_t(i)=t;
    a(i)=-4.9;
    i=i+1;
end
t_f=t_f+4.9+0.1;

%.....constant at 2225/3 (m/s).....
for t=t_f:0.1:t_f+450.5
    t_t(i)=t;
    a(i)=0;
    i=i+1;
end
t_f=t_f+450.5+0.1;

%.....Decelerate to 400/3 (m/s).....
for t=t_f:0.1:(23.3+t_f);
    t_t(i)=t;
    a(i)=-4.9;
    i=i+1;
end
t_f=t_f+23.3+0.1;

%.....Constant at 400/3 (m/s).....
for t=t_f:0.1:(100.6+t_f);
    t_t(i)=t;
    a(i)=0;

```

```
i=i+1;  
end  
t_f=t_f+100.6+0.1;  
%.....Decelerate to 0 (m/s).....  
for t=t_f:0.1:(27.2+t_f);  
    t_t(i)=t;  
    a(i)=-4.9;  
    i=i+1;  
end  
%.....  
plot(t_t,a);  
grid on;  
xlabel('Duration of Trip (s)')  
ylabel('Acceleration (m/s^2)')  
title('Acceleration Profile')  
xlim([0 2393]);
```